



Kent Academic Repository

Singh, Yogendra Kumar (1977) *Some constraints on scattering amplitudes in low energy region*. Doctor of Philosophy (PhD) thesis, University of Kent.

Downloaded from

<https://kar.kent.ac.uk/94656/> The University of Kent's Academic Repository KAR

The version of record is available from

This document version

UNSPECIFIED

DOI for this version

Licence for this version

CC BY-NC-ND (Attribution-NonCommercial-NoDerivatives)

Additional information

This thesis has been digitised by EThOS, the British Library digitisation service, for purposes of preservation and dissemination. It was uploaded to KAR on 25 April 2022 in order to hold its content and record within University of Kent systems. It is available Open Access using a Creative Commons Attribution, Non-commercial, No Derivatives (<https://creativecommons.org/licenses/by-nc-nd/4.0/>) licence so that the thesis and its author, can benefit from opportunities for increased readership and citation. This was done in line with University of Kent policies (<https://www.kent.ac.uk/is/strategy/docs/Kent%20Open%20Access%20policy.pdf>). If you ...

Versions of research works

Versions of Record

If this version is the version of record, it is the same as the published version available on the publisher's web site. Cite as the published version.

Author Accepted Manuscripts

If this document is identified as the Author Accepted Manuscript it is the version after peer review but before type setting, copy editing or publisher branding. Cite as Surname, Initial. (Year) 'Title of article'. To be published in *Title of Journal*, Volume and issue numbers [peer-reviewed accepted version]. Available at: DOI or URL (Accessed: date).

Enquiries

If you have questions about this document contact ResearchSupport@kent.ac.uk. Please include the URL of the record in KAR. If you believe that your, or a third party's rights have been compromised through this document please see our [Take Down policy](https://www.kent.ac.uk/guides/kar-the-kent-academic-repository#policies) (available from <https://www.kent.ac.uk/guides/kar-the-kent-academic-repository#policies>).

SOME CONSTRAINTS ON $\pi\pi$ SCATTERING AMPLITUDES
IN LOW ENERGY REGION

BY

YOGENDRA KUMAR SINGH, M.Sc.(Patna),D.I.C.

A thesis submitted to University of Kent at Canterbury,
for the degree of Ph.D.

MATHEMATICAL INSTITUTE

JANUARY 1977



F_77503

BKL Microfilm

No. D 20971/77

ABSTRACT.

There is still great need for more theoretical input in the form of information and constraints, derived from basic principles, on the main features of physical scattering amplitudes of $\pi\pi$ interactions in the low energy region. We derive new constraints on scattering lengths and test the consistency of the experimental data in the inelastic region with crossing, analyticity and positivity leading to an amplitude of $\pi\pi$ interaction. To extract the scattering amplitude from the cross section and other experimentally observable quantities such as polarisations we perform phase shift analysis. Above the inelastic threshold the unitarity puts constraints on a scattering amplitude in the form of an inequality, and consequently, there exists a continuum of different amplitudes corresponding to the same observables. The continuum ambiguity is serious, even in ideal phase shift analysis with perfect data. In order to remove the continuum ambiguity, we need theoretical input of a dynamical nature. And we need data of high accuracy, as numerical analytic continuation is always involved. However, the scattering amplitude is a complex number and the differential cross section is real, it is not obvious that the information exists to fix an amplitude. In fact, there is as yet no way reliable, in practice, of finding the complex amplitude from the real cross section and other measurements in the inelastic region.

In the first part of this work, we derive rigorous phenomenological new upper bounds on the s-wave $\pi\pi$ scattering lengths. On defining a central family of S, P, D and F phase shifts with associated errors in the energy range $0.45\text{Gev} \leq E_{c.m.} \leq 1.9\text{ Gev}$, we use maximal amount of available data as directly as possible. Also, proper care is taken of the consistency of the chosen phenomenology with principles of unitarity, analyticity and crossing. We have derived some new upper bounds on the $\pi\pi$

(ii)

s-wave scattering lengths from $\Pi^0\Pi^0 \rightarrow \Pi^0\Pi^0$ and $\Pi^+\Pi^0 \rightarrow \Pi^+\Pi^0$ data in the elastic region ($0.45 \text{ GeV} \leq \text{Ec.m.} \leq 0.95 \text{ GeV}$) and in the broad energy region ($0.45 \text{ GeV} \leq \text{Ec.m.} \leq 1.9 \text{ GeV}$). The results show appreciable improvement over Bonnier's Bounds [18]. We have compared our results with results of BFP[30] model, satisfying the low energy s wave phenomenology. Our method is model independent and is capable of producing new class of upper bounds on s-wave scattering lengths and their linear combinations from central family of phase shifts with associated errors in the low energy region.

In the second part of this work, we have derived new sum-rule inequality on $\Pi^+\Pi^- \rightarrow \Pi^+\Pi^-$ scattering amplitudes in the inelastic region from analyticity and positivity of these amplitudes. They connect the real and imaginary parts of the amplitude in the region where they are calculated from phase shift analysis, and do not require knowledge of these quantities at low energies or in the high energy region. The experimental inelastic region $s_1^{\leq} s_2^{\leq} s_3$ is mapped onto the unit circle in the v -plane, while remaining parts of the physical cuts in this circle. To write the sum-rule inequality, we multiply the amplitude by a polynomial $P(v)$ which has zeros at $v=0$ and $v=\infty$, the point which corresponds to infinity in the complex s -plane. It is arranged such that $\text{Im}F(v)P(v)$ has a constant positive sign on the cuts in the v -plane corresponding to the cuts in the s -plane. As the phase shifts are known in the inelastic region this information can be used in the sum-rule. The data from Estabrooks and Martin solutions A, B, C, D [81] and Froggatt & Petersen [68, 68a] are used to test the sum-rule inequality. Furthermore, the EM-solutions have been rotated

by Common [82] in a special way, the rotated data are also used to test the sum-rule inequality. The local minimisation programs from NAG-routines are used to find the minima with respect to zeros of $P(v)$.

Violations of our sum-rule inequality would either indicate the experimental data being at fault or something wrong with our basic properties of the scattering amplitude.

EM's figure give the impression of very smooth Argand diagrams, but actual solutions are noisy. On plotting Argand diagrams of FP's data, we get smoother curves which agree with results of the published papers [68, 68a].

There are clear violations of our sum-rule inequality in case of EM's solutions A, B, C, D and their rotated data. However, they are of the order of one to two standard deviations (in most of the cases) i.e. the order of errors involved in the experimental data. Hence, we can not rule out EM-solutions completely on the basis of violations of our sum-rule inequality. In case of FP-data, our analysis shows much smoother behaviour and there is less violation of our sum-rule inequality and we can not rule out their solutions either. It shows that as one would expect the smoother data is more consistent with analyticity properties of the scattering amplitude.

The references are expressed in square brackets with capital surname of scientific workers.

TABLE OF CONTENTS.

<u>C H A P T E R I: General Introduction.</u>	Page No.
1.0 General Introduction to $\pi\pi$ Interactions	1
1.1 Mathematical Framework of scattering Theory	5
1.2 Kinematics	8
1.3 Analyticity, Unitarity and Positivity	11
1.4 Crossing Symmetry	15
1.5 Rigorous Constraints in Unphysical Region	17
1.6 Low Energy models based on Roy's Equations	22
1.7 Bounds on Scattering Lengths and Amplitudes	27
1.8 Lopez and Mennessier Bounds	30
1.9 Experimental Results	31
<u>C H A P T E R II: Phase-shifts Analysis of $\pi\pi$ Scattering.</u>	
2.0 Introduction	36
2.1 Problem of Ambiguities	37
2.2 The Modulus and The Phase of The scattering Amplitudes	40
2.3 Phase shifts in Elastic Region	41
2.4 Phase-Shift Solutions in Inelastic Region	45
2.5 Analysis of Martin and Estabrooks	50
2.6 Analysis of Froggatt and Petersen	56
<u>P A R T O N E.</u>	
<u>C H A P T E R III: New Bounds on S-wave $\pi\pi$ scattering</u> <u>Lengths.</u>	
3.0 Introduction	59
3.1 Bonnier's Bounds On the $\pi\pi$ s-wave Scattering Lengths	61
3.2 Introduction	61
3.3 Notations and Sum-rule Inequality	62
3.4 Bounds On The scattering Lengths	65
3.5 Phenomenological Input	67

Chapter III (continued)	Page No.
3.6 Conclusions and Remarks	68
3.7 New Upper Bounds on the $\Pi \Pi$ S-wave Scattering lengths	69
3.8 Introduction	69
3.9 Notation and Normalization	70
3.10 Sum-rule Inequalities	71
3.11 Zero of the amplitude	73
3.12 Domain of Analyticity of the Function	76
3.14 Numerical Calculations	80
3.15 Upper Bounds In the Elastic Region	84
3.16 Upper Bounds in the Broad Energy Region	90
3.17 Discussion of Results:	95
(A) Elastic Region ($0.45 \text{ Gev} \leq E_{c.m.} \leq 0.95 \text{ Gev}$)	96
$\Pi^0 + \Pi^0 \rightarrow \Pi^0 + \Pi^0$	
$\Pi^+ + \Pi^0 \rightarrow \Pi^+ + \Pi^0$	
(B) The Broad Energy Region ($0.45 \text{ Gev} \leq E_{c.m.} \leq 1.9 \text{ Gev}$)	97
$\Pi^0 + \Pi^0 \rightarrow \Pi^0 + \Pi^0$	
$\Pi^+ + \Pi^0 \rightarrow \Pi^+ + \Pi^0$	
3.18 Conclusions	99

P A R T T W O.

C H A P T E R IV: Sum-Rules and Phase-Shift Solutions of $\Pi \Pi$ Scattering in The Inelastic Region.

4.0 Introduction	102
4.1 Description of sum-rule Inequalities	104
4.2 Introduction	107
4.3 Derivation of sum-rule Inequalities	109
4.4 Convergence of S	111
4.5 Numerical Results	112
(A) Rotated Data	112
(B) EM's Unrotated Data	114
(C) FP's Data	114

Chapter IV(Continued)	Page No.
4.6 Discussion of Results	151
4.7 Conclusions	153

A P P E N D I X

1. Convergence of S	154
2. Table Captions	157
3. Figure Captions	159
4. Acknowledgements	167
5. References	168

CHAPTER I.1.0 GENERAL INTRODUCTION TO $\pi\pi$ INTERACTIONS.

The hadron world is complex and we lack a dynamical theory that could allow us to understand and calculate its properties. Confronted with such a reality we try to construct models: they are limited theoretical descriptions of limited sectors of physical phenomena. Although, as yet, there is no established fundamental theory of hadrons much progress has been made towards understanding their properties and interactions. Many principles have emerged which seem likely to be necessary ingredients or consequences of any complete theory. This can be regarded as a limited objective. Eventually we hope to obtain a theory that embraces both hadrons and leptons and which treats all the types of interaction in a unified way.

The basic idea in such a model dynamical formulation is that forces of interaction are due to the exchange of particles. Each particle produces a force of interaction between some pair of particles. This force may be attractive or repulsive and in situations where this is strongly attractive these two particles can form a bound state or a resonance: a bound state of two particles has mass less than the sum of the masses of the particles so that it can not decay back into two constituents and a resonance has a mass greater than the sum of the masses and so it can decay.

To resolve the first order model, coming from non-relativistic considerations of pion-nucleon scattering, Mandelstam introduced double dispersion relations and oriented the whole idea towards analyticity properties, unitarity and crossing. On this line we have tremendous efforts to understand low and medium energy $\pi\pi$ interactions.

The famous Veneziano models have been successful in producing model amplitudes that accommodated ---with certain limitations---: (A) the low energy amplitudes, (B) natural spin parity mesons in exchange degenerate SU3 nonet patterns in reasonable agreement with experiment. It has also provided us with the predictions: (A) relations between masses and coupling of particles with different arbitrary spin at the parent level, (B) existence of daughter states, (c) specific behaviours of low partial waves in exotic channels. The model, however, lacks unitarity.

The dispersion theory and related ones like Roy equations have clarified interaction below 0.9 Gev energies but the main problems associated with analyticity and the need for considering other $\pi\pi$ channels at higher energies remain in the inelastic region.

The Chew-Low-Goebel suggestion of pion-exchange between the incoming meson and the target nucleon laid the solid basis for experimental meson-meson studies. In fact, the meson-meson amplitude can be factored out in the meson-two-meson transition amplitude off a nucleon, which is only possible for the OPE reaction cross-section. The statistics of available data has made it easier to achieve the goal of a model independent pole extrapolation at expense of some necessary assumptions on the production mechanism: dominance of OPE, neglect of off-shell corrections, etc. are the points of greatest criticism. All inferences from data to elastic scattering proceed via some form of extrapolation either explicitly or implicitly. The implicit methods habitually understate the errors or fail to state the assumptions by which errors are reduced. Despite the greatest difficulties, elastic phase shifts are available with believable errors associated with them and various ambiguities have been resolved.

Attempts to construct interaction Hamiltonian, which one can apply in a field-theoretical framework to calculate strong interaction processes have been almost entirely unsuccessful. The reason for this failure, presumably, being the strength of strong interactions which makes it meaningless to treat the interaction part of the Hamiltonian as a perturbation. So, this does not seem to be a good model for $\pi\pi$ interactions. Most of the progress in $\pi\pi$ interaction theory has been based on S-matrix models using rather general properties of scattering amplitudes. In the first chapter, we review the present status of $\pi\pi$ scattering (in light of our work): (a) S-matrix and its mathematical framework, (b) Kinematics, (c) analyticity-unitarity-positivity, (d) rigorous constraints in unphysical region, (e) models based on Roy's equations, (f) results of model calculations of low energy $\pi\pi$ amplitudes (g) bounds on $\pi\pi$ scattering lengths.

To extract the $\pi\pi$ scattering amplitude from the experimentally observable quantities such as cross-sections and polarisations, we perform phase shift analysis. Unitarity determines the unobservable angle-dependent complex phase of the scattering amplitude with only a few alternative solutions for elastic scattering. And above the inelastic threshold the unitarity constraint on a scattering amplitude is only an inequality and a continuum of different amplitudes correspond to exactly the same observables. Practically, these differences are very important. Extra theoretical input of a dynamical nature can remove the continuum ambiguity but, because numerical analytic continuation is always involved, data of high accuracy is required. Thus unique answers can only be found by introducing further model-dependent assumptions. In the second chapter, we have reviewed some aspects of the principles of phase shift analysis and ambiguities of $\pi\pi$ interactions.

There is still a great need for more theoretical input in the form of information and constraints, derived from basic principles, based on main features of a scattering amplitude of $\Pi\Pi$ interactions. In the third chapter, we derive rigorous phenomenological new upper bounds on the s-wave $\Pi\Pi$ scattering lengths from $\Pi^0\Pi^0 \rightarrow \Pi^0\Pi^0$ and $\Pi^+\Pi^0 \rightarrow \Pi^+\Pi^0$ in the elastic region ($0.45\text{Gev} \leq \text{E.c.m.} \leq 0.95\text{Gev}$) and in the broad energy region ($0.45\text{Gev} \leq \text{E.c.m.} \leq 1.9\text{Gev}$); while taking care of the consistency of the chosen phenomenology of low energy $\Pi\Pi$ scattering with general principles of unitarity, analyticity and crossing.

In the fourth chapter, we derive new constraints in the form of sum-rule inequalities, to test the consistency of experimental data in the inelastic region with crossing, analyticity and positivity leading to an amplitude of $\Pi^+\Pi^- \rightarrow \Pi^+\Pi^-$ interaction.

1.1 Mathematical Framework of Scattering Theory.

As scattering process due to strong interactions may be described in terms of initial and final states of non interacting particles. Because of the short range of strong interactions the ingoing particles may be assumed to be non-interacting a sufficient time before the collision and similarly the outgoing particles will be non-interacting a sufficient time after the scattering. If we form the Hilbert space H of all possible vectors representing any number of non-interacting particles and if $|i\rangle$ and $|f\rangle$ are any two normalized vectors of H , then a typical scattering amplitude is the amplitude for an initial state $|i\rangle$ of n_i non-interacting particles to be found, after scattering has taken place, as the final state $|f\rangle$ containing n_f non-interacting particles. We write this amplitude as $\langle f|S|i\rangle$. The set of all such amplitudes for all the normalized vectors $|i\rangle, |f\rangle$ of H may be regarded as the matrix elements of an operator S which is then fully defined by these matrix elements. S may be called the scattering operator and its matrix elements can be written as

$$\langle f|S|i\rangle \equiv S_{fi} \quad (1.1.1)$$

The set of all these scattering amplitudes, that is the matrix defined by the operator S , is called the S -matrix.

The conservation of probability requires that the S -matrix is unitary:

$$\sum_n S_{fn}^\dagger S_{ni} = \delta_{fi} \quad (1.1.2)$$

(6)

It is convenient to separate off the amplitude associated with no interaction, and work in terms of a T-matrix defined by

$$S = I + iT \quad (1.1.3)$$

Studies of the S-matrix with the strong interactions use theoretically based relations between S-matrix elements. These relations are from rather basic properties, in particular analyticity, unitarity and the invariance properties such as Lorentz invariance, time reversal, etc. The analyticity properties of the S-matrix are thought to be connected with causality. The unitarity comes from the conservation of probability. An important group of relations between scattering amplitudes which are deduced from the analytic properties of the S-matrix are those known as dispersion relations.

Theoretical investigations of strong interactions using the S-matrix fall into two categories. The first of these uses relations involving S-matrix elements to correlate experimental data. By inserting experimental data on one side of such an equation deductions can often be made about the results of some other experiments. Or we can use these relations to check on the consistency of these results of different experiments. The other type of calculation involving the S-matrix is based on the philosophy that the S-matrix is in fact fully determined by rather general properties. It amounts to postulating a dynamical S-matrix theory in which all the elements of the S-matrix could be calculated in terms of little or no input data. In such a s-matrix theory the dynamical postulate of quantum mechanics

(7)

involving the Hamiltonian has been replaced by a dynamical postulate about the S-matrix. Now, since we have a complete set of states $|n\rangle$ we can always make them orthogonal, in particular the momentum states are orthogonal. Then the total number of events of all types, including no scattering at all as a final event, is from the completeness

$$\sum_n \langle f_i | n \rangle \langle n | f_i \rangle = \langle f_i | f_i \rangle \quad (1.1.4)$$

But the total number of final events is, from the conservation of probability or the fact that each initial state will give rise to just one final event, just the total number of particles in the beam; so

$$\langle f_i | f_i \rangle = \langle i | i \rangle \quad (1.1.5)$$

Then from (1.1.4) and (1.1.5)

$$\langle i | S^\dagger S | i \rangle = \langle i | i \rangle \quad (1.1.6)$$

As it is true for all $|i\rangle$, we can write it as an operator equation i.e. the unitarity of the S-matrix:

$$S^\dagger S = I \quad (1.1.7)$$

In terms of the T-matrix the unitarity relation becomes

$$T - T^\dagger = iT^\dagger T \quad (1.1.8)$$

$$\text{or } \text{Im} T_{fi} = \frac{1}{2} \sum_n T_{fn}^\dagger T_{ni} \quad (1.1.8a)$$

1.2 KINEMATICS.

We consider the two-body process $\Pi+\Pi\rightarrow\Pi+\Pi$ and introduce (Fig.1) the four ingoing four-momenta q_1, q_2, q_3, q_4 with $q_i=(E_i, \underline{q}_i)$, ($i=1,2,3,4$) and the metric $q_i^2=E_i^2-\underline{q}_i^2=m_i^2$. The three relativistically invariant quantities s, t, u (Mandelstam variables) are defined as:

$$s=(q_1+q_2)^2=(q_3+q_4)^2 \quad (1.2.1a)$$

$$t=(q_1+q_3)^2=(q_2+q_4)^2 \quad (1.2.1b)$$

$$u=(q_1+q_4)^2=(q_2+q_3)^2 \quad (1.2.1c)$$

In the case of $\Pi\Pi$ scattering, the relation between these three variables is

$$s+t+u=4m_{\Pi}^2=4, \quad (1.2.1d)$$

where $m_{\Pi}=1$ is the pion mass. The three related channels are

$$\text{S-channel: } \Pi+\Pi\rightarrow\Pi+\Pi \quad (1.2.2a)$$

$$\text{t-channel: } \bar{\Pi}+\Pi\rightarrow\bar{\Pi}+\Pi \quad (1.2.2b)$$

$$\text{u-channel: } \bar{\Pi}+\Pi\rightarrow\bar{\Pi}+\Pi \quad (1.2.2c)$$

In the c.m. frame, the total 3-momentum of the ingoing particles and hence also the outgoing pair of particles is zero (Fig.2). This frame of reference is the most suitable for a theoretical analysis of any kind of scattering process since in this frame we do not have to separate off a part of the total 4-momentum corresponding to the overall motion of the system, which is irrelevant to the interaction itself.

Relation between the q_i and the physical four-momenta p_i in the s-channel is

$$q_1=p_1 \quad (1.2.3a)$$

$$q_2=p_2 \quad (1.2.3b)$$

$$q_3=-p_3 \quad (1.2.3c)$$

$$q_4=-p_4 \quad (1.2.3d)$$

For the simple case of equal masses $m_i=m_{\Pi}$:

$$s = w_s^2 = 4(p_s^2 + m_{II}^2) \geq 4m_{II}^2 \quad (1.2.4a)$$

$$t = -2p_s^2(1 - \cos\theta_s) \leq 0 \quad (1.2.4b)$$

$$u = -2p_s^2(1 + \cos\theta_s) \leq 0 \quad (1.2.4c)$$

$$\cos\theta_s = 1 + t/2p_s^2, \quad (1.2.4d)$$

where w_s, p_s and θ_s are total energy, momentum and scattering angle in the c.m.s (respectively) for the s-channel reaction.

The range of values of variables s, t, u which corresponds to a physically possible process is called the physical region for that channel or process. As there are only two independent variables the physical regions can be easily depicted on a two dimensional plot with these two variables as coordinates. To display the symmetry between the s, t, u channels, we draw the $s=0, t=0, u=0$ axes so that they form an equilateral triangle of heights

$$s+t+u = 2(m_{II}^2 + m_{II}^2) \quad (1.2.4e)$$

For equal mass elastic scattering, the physical regions in the s-channel are given by equations (1.2.4a, b, c). And this case has boundary curve decomposing into three straight lines (Fig. 3)

In the t-channel, for equal masses, we have

$$q_1 = p_1 \quad (1.2.5a)$$

$$q_2 = -p_2 \quad (1.2.5b)$$

$$q_3 = p_3 \quad (1.2.5c)$$

$$q_4 = -p_4 \quad (1.2.5d)$$

And the physical region for s, t, u in the t-channel is given by (Fig. 3):

$$s = -2p_t^2(1 - \cos\theta_t) \leq 0 \quad (1.2.6a)$$

$$t = w_t^2 = 4(p_t^2 + m_{II}^2) \geq 4m_{II}^2 \quad (1.2.6b)$$

$$u = -2p_t^2(1 + \cos\theta_t) \leq 0 \quad (1.2.6c)$$

$$\cos\theta_t = 1 + s/2p_t^2, \quad (1.2.6d)$$

where w_t, p_t and θ_t are total energy, momentum and scattering angle

in the cms respectively for the t-channel reaction.

In the u-channel for equal masses, we have

$$q_1 = p_1 \quad (1.2.7a)$$

$$q_2 = -p_2 \quad (1.2.7b)$$

$$q_3 = -p_3 \quad (1.2.7c)$$

$$q_4 = p_4 \quad (1.2.7d)$$

and the physical region for s, t, u in the u-channel are given by (Fig. 3):

$$s = -2p_u^2(1 + \cos\theta_u) \leq 0 \quad (1.2.8a)$$

$$t = -2p_u^2(1 - \cos\theta_u) \leq 0 \quad (1.2.8b)$$

$$u = w_u^2 = 4(p_u^2 + m_{II}^2) \geq 4m_{II}^2 \quad (1.2.8c)$$

$$\cos\theta_u = 1 + t/2p_u^2, \quad (1.2.8d)$$

where w_u, p_u, θ_u are total energy, momentum and scattering angle in the cms respectively for the u-channel reaction.

The physical regions for s, t, u in the three channels are displayed in the Mandelstam diagram by figure 3 (shaded areas).

The three physical regions do not overlap.

We can eliminate u by the relation $s+t+u=4m_{II}^2$:

$$\text{s-channel: } s \geq 4m_{II}^2 \quad (1.2.9a)$$

$$t = -2p_s^2(1 - \cos\theta_s) = -2(s/4 - m_{II}^2)(1 - \cos\theta_s) \quad (1.2.9b)$$

$$t_{\max.} = 0 \quad \text{for } \cos\theta_s = 1 \quad (1.2.9c)$$

$$t_{\min.} = -s + 4m_{II}^2 \quad \text{for } \cos\theta_s = -1 \quad (1.2.9d)$$

$$\text{t-channel: } t \geq 4m_{II}^2 \quad (1.2.9e)$$

$$s = -2(t/4 - m_{II}^2)(1 - \cos\theta_t) \quad (1.2.9f)$$

$$s_{\max.} = 0 \quad (1.2.9g)$$

$$s_{\min.} = -t + 4m_{II}^2 \quad (1.2.9h)$$

$$\text{u-channel: } s \leq 0 \quad (1.2.9i)$$

$$t \leq 0 \quad (1.2.9j)$$

The physical regions are shown in figure 4.

1.3 ANALYTICITY, UNITARITY AND POSITIVITY.

The $\pi\pi$ scattering amplitude for fixed physical t within a finite interval $-t_0 < t \leq 0$ is the boundary value of an analytic function of s :

$$F_{\pi\pi+\pi\pi}(s, t) = \lim_{\epsilon \rightarrow 0} F(s+i\epsilon, t) \quad (1.3.1)$$

$F(s, t)$ is an analytic function in the complex s -plane with right cut ($s \text{ real} > s_0 = 4m_{\pi}^2$) and a left-hand cut $-t-s > s'_0$.

And along the left-hand cut, we have

$$\lim_{\epsilon \rightarrow 0} F(s-i\epsilon, t) = F_{\pi\pi+\bar{\pi}\bar{\pi} \rightarrow \pi\pi+\bar{\pi}\bar{\pi}}, \quad (1.3.2)$$

where (E.C.M.)² of the reaction $\pi\pi+\bar{\pi}\bar{\pi} \rightarrow \pi\pi+\bar{\pi}\bar{\pi}$ is given by $u = (4m_{\pi}^2) - s - t$.

The discontinuities of F across the cuts are given by the absorptive parts in the s -channel and the u -channel respectively.

$$A_s(s, t) = 1/2i [F(s+i\epsilon, t) - F(s-i\epsilon, t)] \quad (1.3.3)$$

Further, if the scattering amplitude is polynomially bounded, which is true in Lehmann-Symanzik-Zimmermann formalism:

$$F(s, t, u) = \frac{s^N}{\pi} \int_{s_0}^{\infty} \frac{A_s(s', t) ds'}{s'^N (s' - s)} + \frac{u^N}{\pi} \int_{u_0}^{\infty} \frac{A_u(u', t) du'}{u'^N (u' - u)} + \text{polynomial in } s \text{ and } u, \quad (1.3.4)$$

for t fixed, $-t_0 \leq t \leq 0$.

For s physical and $\cos\theta_s$ outside the interval $-1 < \cos\theta_s < 1$, Lehmann[1] has proved that $F(s, \cos\theta_s)$ is analytic inside an ellipse in the $\cos\theta_s$ -plane with foci $\cos\theta_s = \pm 1$, which means that inside this ellipse its Legendre polynomial expansion converges uniformly and absolutely.

The pion-pion scattering amplitude has the following extended analyticity domain [16a]:

$$\{s, t, u \mid s+t+u=4m_{\pi}^2; t \in \mathcal{D}, s \neq \alpha^2 + 4m_{\pi}^2, u \neq \beta^2 + 4m_{\pi}^2; \alpha, \beta \text{ real}\}, \quad (1.3.5)$$

where the domain $t \in \mathcal{D}$ contains in particular

$$|t| < 4m_{\pi}^2 \text{ and } -28m_{\pi}^2 \leq t \leq 0.$$

We can expand the scattering amplitude for equal mass and spin zero particles ($\Pi \Pi \rightarrow \Pi \Pi$) in the s-channel into partial waves at fixed physical energies:

$$F^I(s, t) = \sum_{l=0}^{\infty} (2l+1) f_l^I(s) P_l(\cos\theta_s) \quad (1.3.6)$$

$$f_l^I(s) = (\eta_l^I(s) e^{2i\delta_l^I(s)} - 1) / 2i \rho(s), \quad (1.3.7)$$

below the inelastic threshold $\eta_l^I(s)=1$, and so

$$f_l^I(s) = \sin\delta_l^I(s) e^{2i\delta_l^I(s)} / \rho(s) \quad (1.3.8)$$

$$\rho(s) = ((s-4)/s)^{\frac{1}{2}} \quad (1.3.9)$$

The partial wave amplitudes, $f_l^I(s)$, for orbital angular momentum l and isospin I are related to the real phase shift $\delta_l^I(s)$ and elasticity coefficient $\eta_l^I(s)$ ($0 \leq \eta_l^I(s) \leq 1$) by equation (1.3.7).

Scattering lengths a_l^I are defined as

$$a_l^I = \lim_{s \rightarrow 4^+} f_l^I(s) / 2k^{2l} \quad (1.3.10)$$

$$k^2 = \frac{1}{4}(s-4) \quad (1.3.11)$$

$$\text{and } a_l^I = f_l^I(4) = F^I(4, 0, 0) \quad \text{for } l=0 \text{ and } 2 \quad (1.3.12)$$

The optical theorem becomes

$$\text{Im } F^I(s, 0) = (s(s-4))^{\frac{1}{2}} \cdot \sigma_{\text{total}}^I / 16\pi \quad (1.3.13)$$

The partial wave can be projected into the form [1a]:

$$f_l^I(s) = \frac{1}{2} \int_{-1}^1 F(s, t', u') P_l(\cos\theta_s) d(\cos\theta_s) \quad (1.3.14)$$

There are two possible sources of singularity in $f_l^I(s)$.

The first one occurs when $F(s, t', u')$ has singularities in the s-plane whose positions are independent of the values of t' or u' . Secondly, we get possible source of singularities in $f_l^I(s)$ at values of s for which, as $\cos\theta_s$ moves along its path of integration -1 to +1, one of the variables t' or u' might take a value for which $F(s, t', u')$ is singular.

The discontinuity in $f_1(s)$ across right-hand cut is simply $2i \text{Im } f_1(s)$, where

$$\text{Im } f_1(s) = \frac{1}{2} \int_{-1}^1 A_s(s, t'(\cos\theta_s)) d(\cos\theta_s) P_l(\cos\theta_s) \quad (1.3.15)$$

So, $f_1(s)$ has a right-hand branch cut together with possible poles on the positive real axis and these singularities correspond directly to the s-channel singularity in $F(s, t', u')$. Also, $f_1(s)$ is singular along the negative real axis from $s=0$ to $s=-\infty$. These singularities are branch point singularities (at each point along the negative axis) coming from the second source mentioned above.

The linear aspect or the positivity property of the unitarity condition gives results:

(a) the positivity property,

$$\text{Im } f_1(s) \geq |f_1(s)|^2 > 0 \quad (1.3.16)$$

(b) the boundedness aspect

$$1 \geq \text{Im } f_1(s) \geq |f_1(s)|^2 > 0 \quad (1.3.17)$$

In the elastic region, we have

$$|f_1(s)|^2 = \text{Im } f_1(s) \quad (1.3.18)$$

Some immediate consequences of the positivity property can be expressed in the following way [16a] :

(i) The imaginary -or the absorptive-part of the scattering amplitude in the forward direction is a sum of the positive terms and hence it is positive:

$$\text{Im } F(s+i\epsilon, \cos\theta_s=1) \equiv A_s(s, \cos\theta_s=1) > 0 \quad (1.3.19)$$

(ii) From the expansion of the scattering amplitude into partial waves at fixed physical energies, we have extremely important relations:

$$\left. \left(\frac{d}{d\cos\theta_s} \right)^n A_s(s, \cos\theta_s) \right|_{\cos\theta_s=1} > 0, \quad (n=0, 1, \dots) \quad (1.3.20)$$

and

$$\left(\frac{d}{d \cos \theta_s} \right)^n A_s(s, \cos \theta_s) \Big|_{\cos \theta_s = 1} \geq \left(\frac{d}{d \cos \theta_s} \right)^n A_s(s, \cos \theta_s) \Big|_{-1 < \cos \theta_s < 1}, \quad (1.3.21)$$

for $n=0, 1, \dots$

$$\left(\frac{d}{dt} \right)^n A_s(s, t) \Big|_{t=0} \geq 0, \quad \text{for } n=0, 1, \dots \quad (1.3.22)$$

$$\left(\frac{d}{dt} \right)^n A_s(s, t) \Big|_{t=0} \geq \left(\frac{d}{dt} \right)^n A_s(s, t) \Big|_{-4k^2 < t < 0}, \quad \text{for } n=0, 1, \dots \quad (1.3.23)$$

The constraints (i) and (ii) put linear constraints on the scattering amplitude.

1.4 CROSSING SYMMETRY.

The amplitudes describing each of the three related channels for $\Pi \Pi$ elastic scattering are represented by one and the same set of analytic functions. The three related channels are:

$$s\text{-channel: } \Pi + \Pi \rightarrow \Pi + \Pi \quad (1.4.1a)$$

$$t\text{-channel: } \bar{\Pi} + \Pi \rightarrow \Pi + \bar{\Pi} \quad (1.4.1b)$$

$$u\text{-channel: } \bar{\Pi} + \Pi \rightarrow \bar{\Pi} + \Pi, \quad (1.4.1c)$$

The pion is its own antiparticle and we write $\bar{\Pi}$ only to indicate which pions have been crossed. In terms of these amplitudes we have for instance

$$F_{\Pi^0 \Pi^0 \rightarrow \Pi^0 \Pi^0}(s, t, u) = 1/3 \cdot (F^0(s, t, u) + 2F^2(s, t, u)) \quad (1.4.2a)$$

$$F_{\Pi^+ \Pi^0 \rightarrow \Pi^+ \Pi^0}(s, t, u) = 1/2 (F^1(s, t, u) + F^2(s, t, u)) \quad (1.4.2b)$$

$$F_{\Pi^+ \Pi^- \rightarrow \Pi^+ \Pi^-}(s, t, u) = 1/3 \cdot (2F^0(s, t, u) + 3F^1(s, t, u) + F^2(s, t, u)), \quad (1.4.2c)$$

where $F^I(s, t, u)$ is the total amplitude for the s-channel isospin I. This crossing symmetry can be expressed in terms of

$$F^I(s, t, u) = \sum_I C_{II, (s \leftrightarrow t)} F^{I'}(t, s, u) \quad (1.4.3a)$$

$$= \sum_I C_{II, (s \leftrightarrow u)} F^{I'}(u, t, s) \quad (1.4.3b)$$

$$= \sum_I C_{II, (t \leftrightarrow u)} F^{I'}(s, u, t) \quad (1.4.3c)$$

where crossing matrices are

$$C_{II, (s \leftrightarrow t)} = 1/6 \cdot \begin{pmatrix} 2 & 6 & 10 \\ 2 & 3 & -5 \\ 2 & -3 & 1 \end{pmatrix} \quad (1.4.4a)$$

$$C_{II, (s \leftrightarrow u)} = 1/6 \cdot \begin{pmatrix} 2 & -6 & 10 \\ -2 & 3 & 5 \\ 2 & 3 & 1 \end{pmatrix} \quad (1.4.4b)$$

$$C_{II, (t \leftrightarrow u)} = \begin{pmatrix} 1 & 0 & 0 \\ 0 & -1 & 0 \\ 0 & 0 & 1 \end{pmatrix} \quad (1.4.4c)$$

The crossing property of $\Pi\Pi$ scattering amplitudes plays a fundamental role and it has the features of relating all partial wave amplitudes to one another. In certain cases, it can be used directly to infer some structures of these partial-wave amplitudes. Using the $s \leftrightarrow u$ crossing properties of the $\Pi^0\Pi^0 \rightarrow \Pi^0\Pi^0$ amplitude, we can write a twice subtracted fixed t dispersion relation for $4 > t > -28$ in the form

$$F(s, t, u) = g(t) + \frac{1}{\Pi} \int_4^{\infty} \frac{ds'}{s'^2} \left(\frac{s^2}{s' - s} + \frac{u^2}{s' - u} \right) A(s', t), \quad (1.4.5)$$

where $g(t)$ is a constant in s and only contributes to the $l=0$, partial-wave in the t -channel.

1.5 RIGOROUS CONSTRAINTS IN UNPHYSICAL REGION.

The search for the properties of the partial wave amplitudes on the unphysical interval $0 \leq s \leq 4$ is justified by the hope that it may lead to limitations on the low energy behaviour of the phase shift problem of pion-pion interactions. Balchandran and Nuyts[2] discovered implications of crossing alone, and later on Roskies [3] and others[4] established their practical usefulness. Martin et al.[5] initiated a new approach incorporating also analyticity and unitary properties. We get sets of inequalities for partial waves in the unphysical region. GMN[6] have shown that knowledge of the $l=1$ p-wave and of some high-energy parameters practically limits the possible s-waves in a very restricted domain.

Wanders[7] and Roskies[8] have obtained crossing constraints for higher waves, excluding s- and p-wave amplitudes on physical partial waves. On the other hand, Roy[9] has discovered $\pi\pi$ equations with the properties of (i) expressing each partial wave amplitude in the physical region (including s and p waves) as an integral over physical absorptive parts, and (ii) being well-defined up to 1100 Mev, giving us direct consistency tests for experimental data. BGN[10] have shown how the Chew-Mandelstam equation can be obtained as a first approximation. Lovelace[11] proved that the Chew-Mandelstam equations have no solutions if the p-wave absorptive part does not vanish, and therefore in order to construct s- and p-wave $\pi\pi$ amplitudes which satisfy unitarity and crossing, we have to incorporate some informations about higher waves and asymptotic contributions. The Martin inequalities and sum rules are well suited for this.

Wanders [12] has introduced the constraints in the unphysical region in the following way:

Introducing

$$T^I(s, t, u) = \lim_{\epsilon \rightarrow 0^+} F^I(s+i\epsilon, t, u-i\epsilon), \quad (1.5.1)$$

we have

$$\int_{\Delta} ds du T^I(s, t, u) Q(s, t, u) = 0, \quad (1.5.2)$$

where Δ is the triangle $\{s, t, u | s \geq 0, t \geq 0, u \geq 0\}$ and the polynomial

$Q(s, t, u)$ is antisymmetric if $I=0, 2$ and symmetric if $I=1$ in s, t, u under $s \leftrightarrow u$ crossing.

Expanding $Q(s, t, u)$ in the Legendre polynomials: $P_1(z)$ ($z=1+2t/(s-4)$)

$Q(s, t, u) = \sum_{l=0}^N q_l(s) P_l(z)$, we get (1.5.2) in the form

$$\begin{aligned} & \sum_{l=0}^N \int_0^4 ds (4-s) q_l(s) \int_{-1}^{+1} dz T^I(s, t, u) P_l(z) \\ & = \sum_{l=0}^N \sum_{I'} C_{II'}^{(s+u)} \int_0^4 ds (4-s) q_l(s) f_1^{I'}(s) = 0 \end{aligned} \quad (1.5.3)$$

As $q_l(s)$ are polynomials in s , (1.5.3) is a linear relation between moments of a finite number of partial waves over the unphysical interval $[0, 4]$. There are two (and only two) conditions involving s waves only, and three (and only three) conditions involving both s and p waves only:

$$\int_0^4 ds (4-s) (3s-4) (f_0^0(s) + 2f_0^2(s)) = 0 \quad (1.5.4a)$$

$$\int_0^4 ds (4-s) (2f_0^0(s) - 5f_0^2(s)) = 0 \quad (1.5.4b)$$

$$\int_0^4 ds (4-s) s (2f_0^0(s) - 5f_0^2(s)) = -3 \int_0^4 ds (4-s)^2 f_1^1(s) \quad (1.5.4c)$$

$$\int_0^4 ds (4-s)^2 s (2f_0^0(s) - 5f_0^2(s)) = -3 \int_0^4 ds (4-s)^2 3f_1^1(s) \quad (1.5.4d)$$

$$\int_0^4 ds (4-s)^3 s (2f_0^0(s) - 5f_0^2(s)) = -3 \int_0^4 ds (4-s)^2 s (3s-4) f_1^1(s) \quad (1.5.4e)$$

Balchandran and Nuyts [2] have shown that it is convenient to expand

$f_1^I(s)$ in Jacobi polynomials $P_n^{(2l+1, 0)}(\frac{1}{2}s-1)$:

$$f_1^I(s) = \sum_{n=0}^{\infty} f_{1;n}^I P_n^{(2l+1, 0)}(\frac{1}{2}s-1) \quad (1.5.5)$$

And this series converges for $0 < s < 4$. The crossing conditions relate the coefficients $f_{1,n}^I$ with constant $(1+n)$:

$$f_{1,n}^I = \sum_{l'=0}^{1+n} \sum_{I'} B_{1,1'}^{n, I, I'} f_{1,1+n-I'}^{I'} \quad (1.5.6)$$

Martin[5] started the investigations of the constraints imposed by positivity and crossing symmetry on the S and P waves in the interval $[0, 4]$, his coworkers followed his method[13].

Wanders[12] has derived the following inequalities:

$$T(s_0, t_0, u_0) > T_0(t_0) + 3T_1(t_0) \left(1 - \frac{2s_0}{4-t_0}\right) \quad (1.5.7a)$$

$$T(s_0, t_0, u_0) < T_0(s_0) + 3T_1(s_0) \left(1 - \frac{2t_0}{4-s_0}\right), \quad (1.5.7b)$$

where (s_0, t_0, u_0) are points of the triangle Δ .

Furthermore, the inequalities comparing the values of S and P waves (or their first order derivative) at two points s_0 and t_0 of the interval $[0, 4]$ are:

$$f_0^{00}(0) > f_0^{00}(3.155) \quad (1.5.8a)$$

$$f_0^{00}(0.2134) > f_0^{00}(2.9863) \quad (1.5.8b)$$

$$1.844f_1^I(0.2937) + 3.765f_1^I(2.4226) < f_0^O(0.2937) - f_0^O(2.4226) - f_0^O(0.2937) + f_0^O(2.4226) \quad (1.5.8c)$$

$$0.6146f_1^I(0.2937) + 2.510f_1^I(2.4226) > f_0^O(2.4226) - f_0^O(0.2937) + \frac{2}{3}f_0^O(0.2937), \quad (1.5.8d)$$

where $f_1^{00}(s) = \frac{1}{3}f_1^O(s) + \frac{2}{3}f_1^I(s)$ are the $\pi^0\pi^0 \rightarrow \pi\pi$ amplitudes.

$$1.494f_2^{00}(0.537) - 1.623f_2^{00}(2.363) < f_0^O(0.537) - f_0^O(2.363) < 1.510f_2^{00}(0.537) - 1.622f_2^{00}(2.363) \quad (1.5.8e)$$

These inequalities lead to the conclusion that $f_0^O(0.537)$

is equal to $f_0^{00}(2.363)$, up to D-wave corrections.

Thirdly, we have inequalities relating the derivatives of S and P-wave amplitudes:

$$\frac{d}{ds} f_0^{00}(s) < 0 \text{ for } 0 \leq s \leq 1.127 \quad (1.5.9a)$$

$$\frac{d}{ds} f_0^{00}(s) > 0 \text{ for } 1.7 \leq s \leq 4 \quad (1.5.9b)$$

$$\frac{d^2}{ds^2} f_0^{00}(s) > 0 \text{ for } 0 \leq s \leq 1.7, \quad (1.5.9c)$$

showing that $f_0^{00}(s)$ has a unique minimum in the interval $[0, 4]$

located between $s=1.127$ and $s=1.7$.

$$f_0^{00}(3.155) < f_0^{00}(0) < f_0^{00}(4) \quad (1.5.10a)$$

$$f_0^{00}(2.9863) < f_0^{00}(0.2134) < f_0^{00}(3.205) \quad (1.5.10b)$$

From these inequalities, we get a fairly good idea of the shape of $\Pi^0 \Pi^0$ s-wave in the interval $[0, 4]$. However, it is difficult to judge which inequalities are the most constraining and which ones are redundant. Both Roskies' and Martin's inequalities are very useful ways of building up phenomenological models, but they hold in the unphysical region $0 \leq s \leq 4$.

Common and Pidcock [14] have used crossing and positivity of the scattering amplitude to (i) improve the constraints on the derivative of the d wave previously obtained by one of the authors, and (ii) to derive an infinite set of inequalities between the values of the d-wave at three points in the unphysical region. They checked these inequalities against a number of models, and some qualitative conclusions have been drawn. By using more restrictive crossing inequalities they have been able to derive constraints on $f_2(s)$ in the whole interval $[0, 4]$.

Their general effect is to ensure that $f_2(s)$ is a smooth function of s in this interval, and although it can have a maximum for $s \leq 1.47$, it cannot become too small as $s \rightarrow 0$.

Common, Hodgkinson and Pidcock [15] have investigated constraints on the derivative of the G -wave $f_4^{00}(s)$ for $\pi\pi^0 \rightarrow \pi^0\pi^0$ using crossing sum rules which follow from quadruply subtracted dispersion relations. In particular, they have shown that

$$\frac{df_4(s)}{ds} \leq 0 \quad \text{for } 4 \geq s \geq 1.488. \quad (1.5.11)$$

1.6 LOW ENERGY MODELS BASED ON ROY'S EQUATIONS

In constructing low energy models, one intends to present the complete set of amplitudes consistent with recent high statistics pion-pion experiments and with the theoretical constraints of analyticity, crossing and unitarity. Then the implications of these results and future experiments, which would remove the final ambiguities in the low energy $\pi\pi$ amplitude, are considered. The experimental πN information is much more accurate and abundant, while theoretical constraints on $\pi\pi \rightarrow \pi\pi$, which is a closed system under crossing, are more stringent. Our basic starting point consists in the rigorous equations, expressing the crossing property directly on physical partial wave amplitudes, derived by Roy [24]. Roy's equations, which are non-diagonal but linear, give relationships between the real and imaginary parts of the partial wave amplitudes, provide us with a check that the phase-shifts deduced from the data are consistent with crossing and analyticity properties [25] — at least within the limited energy region in which they are valid. The smaller the errors on the data the more restrictive are Roy's equations — therein lies their power to discriminate between different phase-shift solutions and analyses.

Several groups of workers like FP [26], BG [27], GB [28], PP [29], BGN [10] have analysed the situation and the results may be considered qualitatively similar. In future, it is absolutely necessary to supplement crossing and unitarity with very precise dynamical properties — and not just a few low energy parameters in order to specify the $\pi\pi$ amplitude.

We write the dispersion relation for $\pi^0\pi^0 \rightarrow \pi^0\pi^0$ in the form:

$$F^{00}(s, t, u) = a_0^{00} + \frac{t(t-4)}{\pi} \int_4^{\infty} \frac{dx}{x(x-4)} A^{00}(x, 0) \left[\frac{1}{x-t} + \frac{1}{x+t-4} \right] \\ + \frac{1}{\pi} \int_4^{\infty} dx A^{00}(x, t) \left[\frac{1}{x-s} + \frac{1}{x-u} - \frac{1}{x} - \frac{1}{x+t-4} \right], \quad (1.6.1)$$

where a_0^{00} is the s-wave scattering length, the absorptive part can be expanded in partial waves:

$$A^{00}(x, t) = \sum_{\ell=0}^{\infty} (2\ell+1) \text{Im} f_{\ell}^{00}(x) P_{\ell} \left(1 + \frac{2t}{x-4} \right), \quad 4 \geq t \geq -28 \quad (1.6.2)$$

Using $t \leftrightarrow u$ symmetry in the direct channel and projecting $F^{00}(s, t, u)$ onto partial waves, we have [10]

$$f_{\ell}^{00}(s) = \frac{1}{2} \int_{-1}^1 F^{00}(s, t, u) P_{\ell}(z) dz = \int_0^1 F^{00}(s, t, u) P_{\ell}(z) dz \\ = \frac{2}{s-4} \int_{\frac{4-s}{2}}^0 F^{00}(s, t, u) P_{\ell} \left(1 + \frac{2t}{s-4} \right) dt, \quad (1.6.3)$$

We obtain a set of relations for partial wave amplitudes on using equations (1.6.1) and (1.6.2):

$$f_{\ell}^{00}(s) = a_0^{00} \delta_{\ell 0} + \sum_{\ell'} (2\ell'+1) \int_4^{\infty} ds' K_{\ell}^{\ell'}(s, x) \text{Im} f_{\ell'}^{00}(x), \quad (1.6.4)$$

where $\delta_{\ell 0}$ is the kronecker delta and the kernels $K_{\ell}^{\ell'}(s, x)$ can be deduced from the above equations, provided ℓ' converges in the range $-4 \leq s \leq 60$.

Roy has argued that if the absorptive parts $\text{Im} f_{\ell}(s)$ are known in the inelastic region $s \geq 16$, the elastic unitarity relation

$$\text{Im} f_{\ell}(s) = p(s) \left[(\text{Re} f_{\ell}(s))^2 + (\text{Im} f_{\ell}(s))^2 \right] \quad (1.6.5)$$

provides a system of non-linear singular equations defining $\text{Im} f_{\ell}(s)$, and hence the amplitude in the elastic region.

In case of charged pions, the equations have the form [30]:

$$f_{\mathbb{L}}^I(s) = \left[\begin{pmatrix} a_0^0 \\ 0 \\ a_0^2 \end{pmatrix} d_{\mathbb{L}0} + \frac{1}{3}(2a_0^0 - 5a_0^2)(s-4)/4 \cdot \begin{pmatrix} d_{\mathbb{L}0} \\ 1/6 d_{\mathbb{L}1} \\ -1/2 d_{\mathbb{L}0} \end{pmatrix} \right] + \sum_{I'=0}^2 \sum_{\mathbb{L}'=0}^1 \int_4^{\infty} K_{\mathbb{L},I}^{\mathbb{L}',I'}(s,x) \text{Im} f_{\mathbb{L}}^{I'}(x) dx + \mathbb{O}_{\mathbb{L}}^I(s), \quad (1.6.6)$$

where a_0^0 and a_0^2 are the s-wave scattering lengths for $I=0,2$; $\mathbb{O}_{\mathbb{L}}^I(s)$ is a well defined sum of higher wave contributions ($\mathbb{L}' \geq 2$):

$$\mathbb{O}_{\mathbb{L}}^I(s) = \sum_{I'=0}^2 \sum_{\mathbb{L}'=2}^{\infty} \int_4^{\infty} K_{\mathbb{L},I}^{\mathbb{L}',I'}(s,x) \text{Im} f_{\mathbb{L}}^{I'}(x) dx \quad (1.6.7)$$

The kernels are given by BGN [10]. The first term in (1.6.6) is a polynomial subtraction term, satisfying all crossing constraints. The second term is an integral over s and p waves, satisfying all Martin inequalities and Roskies relations for all $\text{Im} f_{\mathbb{L}}^{I'}$, $\mathbb{L}'=I'=0,1$ provided they are positive.

Introducing some cut off parameter N, we split the x integral into two parts:

$$f_{\mathbb{L}}^I(s) = \text{S.T.} + \sum_{I'=0}^2 \sum_{\mathbb{L}'=0}^1 \int_4^N K_{\mathbb{L},I}^{\mathbb{L}',I'}(s,x) \text{Im} f_{\mathbb{L}}^{I'}(x) dx + d_{\mathbb{L}}^I(s), \quad (1.6.8)$$

where S.T. is the first order polynomial subtraction term in (1.6.6) and $d_{\mathbb{L}}^I(s)$ is called a driving term:

$$d_{\mathbb{L}}^I(s) = d_1^{\mathbb{L}I}(s) + d_2^{\mathbb{L}I}(s) \quad (1.6.9)$$

The first term in (1.6.9) is the contribution of all waves for $x > N$, whereas the second term $d_2^{\mathbb{L}I}(s)$ is the contribution of higher waves $\mathbb{L}' \geq 2$ for $x < N$:

$$d_1^{\mathbb{L}I}(s) = \sum_{I'=0}^2 \sum_{\mathbb{L}'=0}^1 \int_N^{\infty} K_{\mathbb{L},I}^{\mathbb{L}',I'}(s,x) \text{Im} f_{\mathbb{L}}^{I'}(x) dx \quad (1.6.10)$$

$$d_2^{\mathbb{L}I}(s) = \sum_{I'=0}^2 \sum_{\mathbb{L}'=2}^{\infty} \int_4^N K_{\mathbb{L},I}^{\mathbb{L}',I'}(s,x) \text{Im} f_{\mathbb{L}}^{I'}(x) dx \quad (1.6.11)$$

We choose for N an energy squared above which a Regge representation of the amplitude is convenient.

On computing the Regge contribution in the dispersion relation (1.6.1) and projecting the result on partial waves, the driving term for the amplitude is

$$d_l^I(s) = \frac{1}{2} \int_{-1}^1 dz P_l(z) \frac{1}{\Gamma} \int_N^{\infty} dx \left[a(x,t) A^{00}(x,0) + b(x,t,s) A^{00}(x,t) \right], \quad (1.6.12)$$

where one can read off $a(x,t)$ and $b(x,t,s)$ from equation (1.6.1)

In S and P-waves, the resulting driving terms can be approximately parameterized between threshold and N by

$$d_l^I(s) = (s-4) \sum_{n=1}^3 d_{l,n} (s-4)^{n-1}, \quad (1.6.13)$$

where $d_{l,n}$ are coefficients.

Once we know the driving terms $d_l^I(s)$, equation (1.6.8) becomes a system of non linear singular integral equations for the amplitude in the region $4 \leq s \leq N$ when put together with the unitarity condition

$$\text{Im} f_l^I(s) = p(s) |f_l^I(s)|^2 + \frac{1 - (\eta_l^I(s))^2}{4p(s)} \quad (1.6.14)$$

After determining S and P-wave amplitude, higher partial waves are computed directly by equation (1.6.8):

$$f_l^I(s) = \sum_{I'=0}^2 \sum_{l'=0}^l \int_4^N K_{ll'}^I(s,x) \text{Im} f_{l'}^{I'}(x) dx + \frac{(s-4)^l}{\Gamma} \int_4^N dx \frac{\text{Im} f_l^I(x)}{(x-4)^l (x-s)} + \tilde{d}_l^I(s), \quad l \geq 2, \quad (1.6.15)$$

where the driving term contribution is redefined in order to extract the direct channel right hand cut contribution.

In the region $4 \leq s \leq 60$, unitarity is a very weak constraint on these waves, we define the phase shift by the approximate relation:

$$\tan \delta_1^I(s) = ((s-4)/s)^{\frac{1}{2}} \text{Re } f_1^I(s) \quad (1.6.16)$$

The crossing constraints, which relate the d and higher waves, together with positivity imply that the size of the d-wave (in some defined average sense) controls the size of the imaginary parts of the higher waves. These constraints imply that as far as the s and p waves are concerned Roy's equations embody the full content of this limited $s \leftrightarrow t$ crossing provided the so called 'driving terms' satisfy these subsidiary crossing conditions.

1.7 BOUNDS ON SCATTERING LENGTHS AND AMPLITUDES

In addition to the asymptotic bounds, rigorous limits on the pion-pion amplitude have been obtained by Martin [16] for finite values of the argument:

$$\left| F\left(\frac{4}{3}, \frac{4}{3}, \frac{4}{3}\right) \right| < 100 \quad (1.7.1)$$

Using the axiomatic analyticity and unitarity we can show that in the region $s < 4$, $t < 4$ and $u < 4$ the $\pi\pi$ scattering amplitude cannot be arbitrarily large. The upper and lower limits have the merit to exist.

At a fixed t , $-t_0 \leq t \leq 4$, a dispersion relation for a scattering amplitude, which is symmetric in s and u , is

$$F(s, t) = g(t) + \frac{s^2}{\pi} \int_4^\infty \frac{A_s(s', t) ds'}{s'^2 (s' - s)^2} + \frac{u^2}{\pi} \int_4^\infty \frac{A_u(u', t) du'}{u'^2 (u' - u)^2} \quad (1.7.2)$$

Introducing the variable $z = (s - 2 + t/2)^2$, the right and left cuts may be folded to give [16a]:

$$F(s, t) = G(z, t) = g(t) + \frac{z}{\pi} \int_{(2+t/2)^2}^\infty \frac{\text{Im} G(z', t) dz'}{z'^2 (z' - z)^2} \quad (1.7.3)$$

This function, $G(z, t)$, becomes a Herglotz function [16b] if it is regular in $\text{Im} z > 0$ and $\frac{\text{Im} G}{\text{Im} z} > 0$ for $\text{Im} z > 0$

$$(1.7.3A)$$

Now, from (1.7.3) we have

$$\left(\frac{d}{dt}\right)^n G(z, t) > 0 \quad \text{for } z \text{ real} < (2+t/2)^2 \text{ and } 0 \leq t \leq 4 \quad (1.7.4a)$$

$$\left(\frac{d}{ds}\right)^n F(s, t) > 0 \quad \text{for fixed } t, \quad 2-t/2 \leq s \leq 4 \quad (1.7.4b)$$

From crossing symmetry, we have

$$\left(\frac{d}{dt}\right)^n F(s, t) > 0, \quad \text{for fixed } s \text{ and } 2-s/2 \leq t \leq 4 \quad (1.7.5a)$$

$$\left(\frac{d}{dt}\right)^n F(4-u-t, t, u) > 0, \quad \text{for fixed } u \text{ and } 2-u/2 \leq t \leq 4 \quad (1.7.5b)$$

(28)

Jin and Martin [17] have shown that inside the triangle $s < 4, t < 4$ and $u < 4$, the point $s=t=u=4/3$ is an absolute minimum of $F(s,t,u)$. As we know that atleast two out of the three variables s,t,u are positive, one can take s,t positive. For $s > t > u$, we have two distinguished cases:

(A) if $t > 4/3$ i.e. $s > 4/3$,

$$F(s,t,u) = F(s,t,u) - F(s, \frac{4}{3}, \frac{8}{3}-s) + F(s, \frac{4}{3}, \frac{8}{3}-s) - F(\frac{4}{3}, \frac{4}{3}, \frac{4}{3}) + F(\frac{4}{3}, \frac{4}{3}, \frac{4}{3}) \quad (1.7.6)$$

The first two terms on the right-hand side, taken together, are positive on the basis of (1.7.5a), and the third and the fourth terms together are positive on the basis of (1.7.4b). Consequently, we have

$$F(s,t,u) > F(4/3, 4/3, 4/3). \quad (1.7.7)$$

(B) if $t < 4/3$ i.e. $u < 4/3$,

$$F(s,t,u) = F(s,t,u) - F(8/3-t, t, 4/3) + F(8/3-t, t, 4/3) - F(4/3, 4/3, 4/3) + F(4/3, 4/3, 4/3)$$

The first four terms taken together are positive, we have

$$F(s,t,u) > F(4/3, 4/3, 4/3) \quad (1.7.8)$$

This result is true in all parts of the triangle. Also, $F(s,t,u)$ increases along any straight line originating from the symmetry point inside the triangle.

Using partial-wave expansions, Lukaszuk and Martin [17] have found a function $\phi(|F(s, \cos \theta_s)|, s, t)$ such that

$$A_s(s, t) \geq \phi(|F(s, \cos \theta_s)|, s, z) \text{ for } -k \cos \theta_s < 1, t > 0. \quad (1.7.9a)$$

$$|F(2, 2, 0)| < 37 \quad (1.7.9b)$$

$$-100 < F(4/3, 4/3, 4/3) < 16 \quad (1.7.9c)$$

The $\Pi^\circ \Pi^\circ$ scattering length has the lower bound

$$a_{\Pi^\circ \Pi^\circ} > -23m_{\Pi}^{-1} \quad (1.7.10)$$

Ignoring subtractions, we have much better absolute bounds:

$$0 \leq F(4/3, 4/3, 4/3) < F(2, 2, 0) < 3.6 \quad (1.7.11)$$

Bonnier and Vinh Mau [17] have improved the bound to

$$a_{\pi^0 \pi^0} > -2.5 m_{\pi}^{-1} \quad (1.1.12)$$

Bonnier[18] has developed a new approach to derive rigorous phenomenological bounds for the s-wave scattering lengths. A new class of upper bounds on s-wave scattering lengths appear and the lower bounds are improved. The best result at present given by Bonnier is (in units of the pion mass):

$$a_0^{00} > -3.3. \quad (1.1.13)$$

We discuss Bonnier's bounds in chapter III, in detail, since our method is a new development over his.

1.8 LOPEZ AND MENNESSIER BOUNDS.

Lopez [19] has developed a new method for finding a new lower bound on the $\Pi^{\circ}\Pi^{\circ}$ S-wave scattering length in terms of the D-wave scattering length. The main ingredients of the method are the Roy exact partial wave equations and an extensive use of unitarity in the physical region. For a value of $a_2^{00} = 7.3 \times 10^{-4}$, he gets the bound $a_0^{00} \gg -0.33$. This is an improvement over the earlier results by Common and De Witt, $a_0^{00} > -1.16$; Dita, $a_0^{00} > -0.71$; Furmansky, $a_0^{00} > -0.56$ and Grassberger, $a_0^{00} > -0.42$ [20].

As the basic idea is to use Roy's equations as a way of imposing analyticity and crossing constraints, the method is in principle applicable to other waves by using the corresponding Roy's equation. The result for an "Experimental" value $a_2^0 = 1.6 \times 10^{-3}$ is $a_1^{(1)} \geq -0.23$ [19a]

Furthermore, Bonnier, Lopez and Mennessier have used axiomatic properties [21] to derive new absolute bounds on the $\Pi^{\circ}\Pi^{\circ}$ amplitude in the Mandelstam triangle. In particular, if the amplitude is so normalized that its value at threshold is the scattering length, the value at the symmetry point, which is considered as a measure of the $\Pi\Pi$ coupling, is shown to lie between -13.5 and 2.75:

$$-13.5 < F(4/3, 4/3, 4/3) < 2.75$$

$$-4.85 < F(2, 0, 2) < 2.9. \quad (1.8.1)$$

Lopez and Mennessier [22] have improved substantially the precedent absolute lower bounds on the $\Pi^{\circ}\Pi^{\circ}$ S-wave scattering length. The main feature in their derivation is the exploitation of the known structure of the partial wave left hand cut discontinuity, explicitly exhibited by Roy equations. Their final result is

$$a_0^{00} > -1.75. \quad (1.8.2)$$

1.9 EXPERIMENTAL RESULTS.

The picture of the nucleon which is implied by Yukawa model is of a particle continually emitting and reabsorbing pions, so that it is effectively surrounded by a pion cloud. If we consider the various inter-nucleon forces in terms of the exchange of the Yukawa quanta, pions, we obtain the following results (fig. 6). For proton-proton and neutron-neutron scattering exchange of a neutral pion is required, unless exchange of two-charged mesons is allowed. For neutron-proton scattering, however, we may have exchange of both neutral and charged pions. The equality of the n-n, n-p and p-p forces indicates that all are due to the same type of exchange, so that we must suppose that neutral, as well as charged, mesons should exist. This extension of the original Yukawa proposal was made in 1938 by Kemmer.

The Yukawa picture would suggest that it should be possible to produce pions in nucleon-nucleon collisions if the bombarding energy is high enough. We may picture the incident nucleon interacting with a pion in the "cloud" and actually knocking it free (fig. 7).

The pion has spin-parity 0^- and is called pseudo-scalar particle. There exist three π -mesons which are almost identical except for their charges. Thus we write $2I_{\pi} + 1 = 3$, so that isotopic spin $I_{\pi} = 1$ and we assign:

$$(I_{\pi}^-)_3 = -1, (I_{\pi}^0)_3 = 0, (I_{\pi}^+)_3 = +1.$$

The extraction of $\pi\pi$ elastic phase shifts from experimental information differs from the other low energy process in the sense that there is no direct data and one has to rely on indirect evidence based on the following special features, as reviewed by Morgan and Pisut [25a]:

(a) The pion is the lightest hadron therefore dipion systems often feature among reaction products

(b) One pion exchange (OPE) is pervasive, which leads to the possibility of extrapolation to the pion-pole (Chew Low) from the analysis of peripheral dipion production in $\pi N \rightarrow \pi\pi N$ and also in $\pi N \rightarrow \pi\pi\Delta$, $\pi d \rightarrow \pi N \pi\pi$.

(c) The structure of $\pi\pi$ elastic scattering is especially simple. In fact up to 1 GeV, $\pi\pi$ scattering appears to be describable by the five phase shifts (notation δ_1^I) and inelasticities (notation η_1^I):

$$\delta_0^0, \delta_0^2, \delta_1^1, \delta_2^0, \delta_2^2$$

$$\eta_0^0, \eta_0^2, \eta_1^1, \eta_2^0, \eta_2^2.$$

A few partial waves are excited, $\pi\pi \rightarrow 3\pi$ because of G parity and $\pi\pi \rightarrow 4\pi$ does not set in until high energies.

(d) $\pi\pi$ scattering is a crossing-symmetry in a relevant way.

We can classify reactions yielding information on the $\pi\pi$ system into those in which just two pions appear.

K_{e_4} decay: $e^+e^- \rightarrow \pi^+\pi^-$, $K_S^0 \rightarrow 2\pi$, $\pi N \rightarrow \pi N$ (extrapolated to the t-channel), $\pi N \rightarrow \pi\pi N$ with the OPE term successfully isolated. There are some reactions in which three or more pions appear or two pions appear in company with another hadron:

$$\eta, K_L^0, K^\pm, N\bar{N} \rightarrow 3\pi, \pi N \rightarrow \pi\pi N \text{ with OPE term not isolated.}$$

BFP [32a] have used the crossing conditions on physical region $\Pi\Pi$ partial wave amplitudes to study the implications of the existence of the ρ . They have shown that the mere existence of the ρ does not constrain appreciably the s wave scattering lengths and that no correlation from crossing between the ρ and the $I=0$ ξ resonance can be established without further physical assumptions. They have been able to draw the following conclusions:

- (a) The uniqueness claim, made by GMN and BG, is a failure.
- (b) Their findings are somewhat similar to those of Morgan and Shaw [33], barring a few differences.
- (c) Their findings are also similar to those of Piguet and Wanders' results with the unphysical region constraints.
- (d) They find the absence of any crossing correlation between the ρ and ξ resonances. In particular, crossing does not constrain the striking features of low energy $\Pi\Pi$ s and p waves.

On making further investigation of $\Pi\Pi$ phenomenology below 1100 Mev, BFP [32b] have incorporated the following information:

- (a) For the p wave we fix the mass and width of the rho meson $M_\rho = 765\text{Mev}$, $\Gamma_\rho = 135\text{Mev}$, but allow the scattering length a_1^1 to be arbitrary.
- (b) The isoscalar s wave phase shift d_0^0 in the mass range $500 < M_{\Pi\Pi} < 900$ Mev must lie in the between-down or between-up bands [34].
- (c) The $I=2$ s wave phase shift d_0^2 has a rather smooth behaviour with a value at the rho mass in the range $d_0^2(M_\rho) = -15^\circ \pm 5^\circ$

(d) Inelasticity due to $4\pi\pi$ production below 1Gev is negligible, but there is a strong cusp or S^* effect causing d_0^0 to accelerate rapidly through 180° and a sharp onset of inelasticity, at the $K\bar{K}$ threshold.

Commenting on $\pi\pi$ dynamics, BBSFP [35] have made concluding remarks:

(i) that once a given set of data is chosen for d_0^0 and once a_0^0 is fixed the $\pi\pi$ amplitudes below 900 Mev are determined practically uniquely. And a very strong correlation is put by crossing symmetry between the various partial wave amplitudes.

(ii) In order to reduce the remaining ambiguities, the direct procedure would require (A) an accurate Ke_4 experiment with known small systematic errors and (B) a reliable determination of d_0^0 .

(iii) Owing to the correlations, several other pieces of information constitute direct counter checks to any assignment for a_0^0 (and $d_0^0(m_p)$).

(iv) As the s-wave scattering lengths are concerned, it is not at all established at present that Weinberg's predictions, $a_0^0 \sim 0.16$ and $a_0^2 \sim -0.045$, are supported by experiment.

(v) If a_0^0 and a_0^2 turn to be noticeably different from Weinberg's values, either the structure of $SU(2) \times SU(2)$ breaking or the PCAC smoothness assumption will have to be considered.

(vi) The exact values of a_0^0 and a_0^2 are of little importance for the $\pi\pi$ amplitude as we depart from the threshold region, since we can produce phases with different scattering lengths but which are very close above, say, 500 Mev.

At present the most accurate and detailed information on $\pi\pi$ scattering above 1 Gev comes from the 17 Gev/c CERN-Munich experiment on $\pi^-p \rightarrow \pi^+\pi^-n$ [36]. However, there are several ambiguities involved in obtaining the $\pi\pi$ scattering amplitude from the data. Broadly speaking, there are 3 different classes of ambiguities in reconstructing the amplitude from experiment [26]:

- (a) it pertains to production amplitudes neither containing the one pion exchange signal nor affecting it in the observables,
- (b) it pertains to production amplitudes describing (or affecting) off-shell $\pi\pi$ scattering,
- (c) the third class of ambiguities contain those one would have if experiments on a real pion target (rather than a virtual one) could be carried out— an ordinary scattering experiment only measures the absolute magnitude of the amplitude.

In the second chapter, we discuss these ambiguities in detail.

CHAPTER II: PHASE-SHIFT ANALYSIS OF $\pi\pi$ SCATTERING.2.0. INTRODUCTION.

The scattering amplitude is the most important object at the interface between theory and experiment. Theories are supposed to predict scattering amplitudes, while experiment gives some informations about observables like the scattering cross section and other quantities such as polarisations. Phase-shift analysis is the extraction of the scattering amplitude from scattering cross section and other experimentally observable quantities. In the case of energy dependent elastic scattering, unitarity gives us the un-observable angle-dependent complex phase of the scattering amplitude with a few choice of solutions. On the contrary, above the inelastic threshold the unitarity puts constraint on a scattering amplitude in the form of only an inequality, and consequently, there exists a continuum of different amplitudes corresponding to the same observables. The continuum ambiguity is serious, even in ideal phase shift analysis with perfect data.

2.1. PROBLEM OF AMBIGUITIES.

In the elastic region unitarity directly relates real and imaginary parts of the amplitude for each partial wave, but in the inelastic region it only provides an inequality constraint between them, demanding each partial-wave amplitude to lie inside or on its unitarity circle.

The basic continuum ambiguity is defined in the following way. At fixed energy

$$\tilde{F}(z) = e^{i\phi(z)} F(z), \phi(z) \text{ real}, -1 < z < 1, \quad (2.1.1)$$

gives the same cross section as given by $F(z)$ for any such function $\phi(z)$. This continuum ambiguity is serious. This phase factor has nothing to do with the unobservable phase of wave functions in quantum mechanics where,

$$\Psi(x) = e^{ik \cdot x} + F(\theta) \frac{e^{ikr}}{r}, \quad r \rightarrow \infty, \quad (2.1.2)$$

but the phase of the scattering amplitude is the relative phase of the incident and scattered waves. The phase function $\phi(z)$ [26a] is restricted by the normal theoretical assumptions of phase shift analysis, namely:

(L) Lorentz invariance: it restricts the kinematical variables to two, e.g., energy \sqrt{s} and θ_S or $z = \cos \theta_S$.

(U) Unitarity: $f_1(s)$ is on a unit circle in the elastic region and inside it in the inelastic region; it is this weakening of the unitarity constraint to an inequality that gives the continuum ambiguity.

(R) Finite range: for large angular momentum

$$f_1(s) \sim O(e^{-1/kR}), \quad l \rightarrow \infty, \quad (2.1.3)$$

where R is the range of the longest force.

The theoretical assumption of finite range is extended to general analytic structure in z : there is a cut plane of analyticity in z with z_0 and \bar{z}_0 corresponding to the lightest

t-channel and u-channel exchange respectively (Eq.5):

$$Z_0 = 1 + \frac{1}{2k^2 R^2} \quad (2.1.4)$$

The unitarity restriction has to be explored numerically on the line of a few general remarks:

(i) An inequality constraint normally allows a continuum of solutions.

(ii) The partial waves lie near the centre of the Argand diagram in the inelastic region, for small inelastic amplitudes (fig.8a). So, the unitarity constraint is unimportant.

(iii) As the high partial waves lie near the edge of the circle in elastic processes, it puts restrictions over ϕ near $Z_0: \phi(Z_0)=0$ ensures f_1 to be real. The z-discontinuity of $\tilde{F}(z)$ to be real up to the spectral function boundary z_1 , ensuring that $f_1 \rightarrow 0$ as $l \rightarrow \infty$ along the proper quadratic curve (fig.8b), it puts more restrictions over ϕ .

The ambiguity continuum corresponds to an area, or areas, on each partial-wave Argand plot, each point of which is connected to a point in a similar area for each partial wave. These areas are called islands of ambiguity. If the islands of ambiguity cover a significant fraction of the Argand circle for some waves, it is called a serious ambiguity and if the areas are small the ambiguity is not serious — even if there are infinite set of solutions.

None of the criteria, described above, restricts $\phi(Z)$ to a finite set and there is a continuum of scattering amplitudes for each set of perfect data measurements, corresponding to different functions $\phi(Z)$. The question arises as to how large is the ambiguity continuum.

If the ambiguity continuum is a functional of the phase function $\phi(z=\cos\theta)$, one has to explore the whole of an infinite dimensional function space in order to find its true boundaries. There have been explorations in particular directions in the function space which gives at least a lower limit on the size of the ambiguity continuum. However, a simple analytical way of approaching the problem quantitatively has not been done. The main results for perfect data with zero errors are essentially of the following types: (a) the ambiguity is discrete with, at most, a finite number of discrete solutions, (b) if all partial waves, except the s-wave, are not too large the amplitude is unique, apart from the trivial ambiguity ($F=-F^*$) corresponding to changing the sign of all phase shifts, (c) if the partial waves are large, then in a number of situations there is Crichton ambiguity [37].

The trivial ambiguity corresponds to reversing the sign of all real parts and thus of all phase shifts. We can remove it by observation of Coulomb interference, in the case of charged particles. It can be also removed by the inclusion of extra dynamical constraints on the amplitude of $\Pi\Pi$ scattering.

2.2 THE MODULUS AND THE PHASE OF THE SCATTERING AMPLITUDES.

The scattering amplitude $F(s, \cos \theta_s)$ for the reaction $\Pi + \Pi \rightarrow \Pi + \Pi$ is a function of two variables: s and θ_s . The scattering amplitude $F(s, \cos \theta_s)$ is a complex number and the differential cross section

$$\frac{d\sigma}{d\Omega} = \frac{4}{s} \left| F(s, \cos \theta_s) \right|^2 \quad (2.2.1)$$

is real, it is not obvious that the information exists to fix $F(s, \cos \theta_s)$. In practice, the modulus is most of the time the only possible and accessible quantity, the phase and the modulus are linked by very general relationships based on things, which are: conservation of probability, called unitarity implying in particular certain positivity properties, and causality (as expressed by an underlying field theory). It follows that the physical scattering amplitude is the boundary value of an analytic function.

For any function ϕ of energy and angle, which is real in the whole physical region, we have

$$F(s, \cos \theta_s) = \left| F(s, \cos \theta_s) \right| \exp i\phi(s, \cos \theta_s) \quad (2.2.2)$$

both sides giving exactly the same cross section.

$\left| F(s, \cos \theta_s) \right|$ is the modulus of the scattering amplitude, $\phi(s, \cos \theta_s)$ is the phase.

2.3 PHASE SHIFTS IN ELASTIC REGION.

If $Ec.m. = \sqrt{s}$ is low enough, all inelastic channels are closed and unitarity takes the simplest form [38]

$$f(s, \underline{l}_1, \underline{l}_2) = \frac{2k}{\sqrt{s}} F(s, \cos \Theta_s), \quad (2.3.1)$$

where \underline{l}_1 and \underline{l}_2 are unit vectors in the initial and the final directions of the colliding particles, so that $\cos \Theta_s = \underline{l}_1 \cdot \underline{l}_2$.

We can express unitarity by equation [38]:

$$\text{Im } f(s, \underline{l}_1, \underline{l}_2) = \int \frac{d\Omega_3}{4\pi} f^*(s, \underline{l}_1, \underline{l}_3) f(s, \underline{l}_3, \underline{l}_2) \quad (2.3.2)$$

One can expand F in terms of convergent partial waves,

$$F(s, \cos \Theta_s) = \sum_{l=0}^{\infty} (2l+1) f_l(s) P_l(\cos \Theta_s) \quad (2.3.3)$$

and unitarity equation becomes

$$\text{Im } f_l(s) = \frac{2k}{\sqrt{s}} |f_l(s)|^2 \quad (2.3.3a)$$

$$f_l(s) = \frac{\sqrt{s}}{2k} \exp(i\delta_l) \sin \delta_l \quad (2.3.3b)$$

It is the unitarity which guarantees that the phase shift, δ_l , is real.

We can consider equation (2.3.2) as a non-linear integral equation for the phase; once we know the modulus,

$$f(\underline{l}_1, \underline{l}_2) = |f(\underline{l}_1, \underline{l}_2)| \exp i\phi(\underline{l}_1, \underline{l}_2), \quad (2.3.4)$$

it is sufficient to find the angular dependent phase $\phi(s, \cos \Theta_s)$ of the whole amplitude, which is obtained as the solution of the non-linear integral equation

$$|f(\underline{l}_1, \underline{l}_2)| \sin \phi(\underline{l}_1, \underline{l}_2) = \frac{1}{4\pi} \int d\Omega_3 \frac{|f(\underline{l}_1, \underline{l}_3)| |f(\underline{l}_3, \underline{l}_2)|}{\cos[\phi(\underline{l}_1, \underline{l}_3) - \phi(\underline{l}_2, \underline{l}_3)]} \quad (2.3.5)$$

$$\text{or } \sin \phi(\underline{l}_1, \underline{l}_2) = \frac{1}{4\pi} \int d\Omega_3 \frac{|f(\underline{l}_1, \underline{l}_3)| |f(\underline{l}_3, \underline{l}_2)|}{|f(\underline{l}_1, \underline{l}_2)|} \cos[\phi(\underline{l}_1, \underline{l}_3) - \phi(\underline{l}_2, \underline{l}_3)] \quad (2.3.6)$$

Any function ϕ substituted in the right-hand side of (2.3.6) yields another function ϕ' on the left-hand side, and each of these functions is a point in a suitable space so that $\phi' = O(\phi)$. If the output region of the function space ϕ' produced by the mapping lies entirely within the input region for any choice of ϕ , and any pair of points are brought closer together by the mapping, we call it a contraction mapping. On applying such successive mappings, we get smaller regions and so there can always exist a fixed point, which is mapped onto itself. The fixed-point value of the phase function ϕ is the unitary solution. These fixed-point theorems in non linear analysis have been applied to the problems by Klepikov [38a], Newton [39], Martin [40] and Atkinson [41].

In order to have at least one point fixed in the mapping (2.3.6), we need a limit on

$$\sin \alpha \equiv \text{Max} \left[\frac{\int \frac{d\Omega_3}{4\pi} \frac{|f(\frac{1}{2}, \frac{1}{3})| |f(\frac{1}{3}, \frac{1}{2})|}{|f(\frac{1}{2}, \frac{1}{2})|} \right] \quad (2.3.7)$$

For the slowly varying phase, (2.3.6) goes roughly to the maximum value of $\sin \alpha$. And this to be physical we should have $\sin \alpha < 1$, which ensures that (2.3.6) is a contraction mapping and so we must have at least one fixed point. Its phase gives us the guarantee that elastic unitarity is satisfied. By iteration procedure on a computer, one can find out convergence to give the solution. The condition $\sin \alpha < 1$ is very restrictive; for an example, due to the presence of the denominator of (2.3.7) it excludes differential cross sections with deep dips.

In order to remove the trivial ambiguity, we require that the real part should be positive, then

$$0 < \phi(\cos \theta) < \alpha < \pi/2 \quad (2.3.8)$$

or $\text{Re} f(\cos \theta) > 0, \text{Im} f(\cos \theta) > 0 \quad (2.3.8a)$

and there are no sign changes. For $k \geq 1$,

$$\text{Re} f_0 \pm \text{Re} f_1 = \frac{1}{2} \int_{-1}^1 dz \text{Re} f(z) [1 \pm P_1(z)] > 0, \quad (2.3.9)$$

as $|P_1(z)| < 1$ and similarly for the $\text{Im}(f_0 + f_1)$. These partial waves are on the unitary circle in the elastic region and we have

$$\text{Im}f_1 < \frac{1}{2} \text{ or } |\delta_1| < \Pi/2, \quad (2.3.10)$$

it has been improved to

$$|\delta_1| \leq \Pi/6, \quad l \geq 1 \quad (2.3.11)$$

In short, all the waves except the s wave must be fairly small, and certainly non-resonant for these results to hold good.

It is possible to prove, on the basis of analyses of authors [38a, 39, 40, 41], that the iterative solution converges if

$$\sup_{\text{all angles } s} \int \frac{d\Omega_3}{4\Pi} \frac{|f(l_1, l_3)| |f(l_2, l_3)|}{|f(l_1, l_2)|} < 0.79 \quad (2.3.12)$$

Therefore, in a situation where we are close to a resonance ($\delta_1 \sim \Pi/2$), the condition (2.3.12) will be violated. The partial wave amplitudes are exponentially decreasing, even then the existence and uniqueness of the solutions is not clear; different sufficient conditions of some stronger and some weaker nature are obtained. However, it has been shown by Martin [40] that for $\sin \kappa < 1/\sqrt{2}$ the solution is unique.

Crichton [37] has shown that there exist the two sets of phase shifts which give identical cross sections without violating the Martin uniqueness theorems:

$$\begin{array}{lll} \delta_0 = -23^\circ 20' & \delta_1 = -43^\circ 27' & \delta_2 = 20^\circ \\ \delta_0 = 98^\circ 50' & \delta_1 = -26^\circ 33' & \delta_2 = 20^\circ \end{array} \quad (2.3.13)$$

One may hope that the Crichton ambiguity could be the only sort of ambiguity which can be found in the elastic unitarity situation. It has been shown by Martin [40] in the form of a relationship:

$$\frac{15}{2} \exp(i\delta_2) \sin \delta_2 \cdot \left[\cos \theta - x_1(\delta_2) \pm iy_1(\delta_2) \right] \left(\cos \theta - \frac{4}{5} + \frac{1}{5} i \cot \delta_2 \right) \quad (2.3.14)$$

Atkinson et al. [42] and Cornille and Drouffe [43] have extended Crichton ambiguity to the case of four fold and five fold ambiguities. On the other hand, Itzykson and Martin [44] have found the same result for entire functions, which are not polynomials.

Berends and Ruysenaars [45] put forward the idea that there can be, at most, a two fold ambiguity. And one can choose the option of writing the amplitude as a product over its zeros:

$$F(Z) = \beta \prod_{i=1}^L (z - z_i), \quad (2.3.15)$$

where the coefficient of z^L is proportional to F_L ,

$$\beta = \exp(i\delta_L) \sin\delta_L (2L+1) \frac{2L!}{2^L (L!)^2} \quad (2.3.16)$$

And the cross-section can be written:

$$\frac{d\sigma}{d\Omega} = \frac{1}{k^2} |\beta|^2 \prod_{i=1}^L (z - z_i^*)(z - z_i) \quad (2.3.17)$$

Gersten [46] observed it for the first time that the cross section would be unaffected if we replace any of its roots z_n by its complex conjugate.

2.4 PHASE SHIFT SOLUTIONS IN INELASTIC REGION.

When the collision energy of π and $\bar{\pi}$ is sufficiently high other reactions compete with the elastic reaction



Then the conservation of probability is not so simple expression and we do not have anymore an integral equation for the phase. Unitarity, which in the elastic region directly relates real and imaginary parts of the amplitude for each partial wave, now only provides an inequality constraint between them, requiring each partial-wave amplitude to lie inside or upon its unitary circle. If all partial waves lie inside and at finite distance from the edge, there is a whole family of phase functions $\phi(Z)$ of limited magnitude but of infinite variety of functional form, which does not move any wave outside its circle. One must make sure that the transformation ϕ keeps the waves inside their circles.

There is a continuum of scattering amplitudes for each set of perfect data measurements, corresponding to different functions $\phi(Z)$. The ambiguity continuum corresponds to an area, or areas, on each partial-wave Argand plot, each point of which is linked to a point in a similar area for each partial wave. If the islands of ambiguity cover a fraction of the Argand circle for some waves, it is clearly serious, which is the usual situation in inelastic region. The ambiguity continuum is a functional of the phase factor $\phi(Z)$ and to find its true boundaries is a very difficult problem, which involves exploring the whole of an infinite dimensional function space.

The partial wave amplitudes should lie inside the unitary circle:

$$\left| \frac{2k}{\sqrt{s}} f_1(s) - i/2 \right| \leq \frac{1}{2} \quad (2.4.1)$$

$$\text{and } \text{Im} f_1(s) \geq 0. \quad (2.4.2)$$

Consequently, $\text{Im}f(s, \underline{l}_1, \underline{l}_2)$ is a function of positive type over the rotation group and for any reasonable function Q of the direction \underline{l}_1 , we have [38]:

$$\int Q^*(\underline{l}_1) \text{Im}F(s, \underline{l}_1, \underline{l}_2) Q(\underline{l}_2) d\Omega_2 d\Omega_1 \geq 0, \quad (2.4.3)$$

which is obtained by inserting the partial wave expansion of $\text{Im}F$ for every l by taking $Q(\underline{l}_1) = P_l(\underline{l}_1 \cdot \underline{l}_0)$ with \underline{l}_0 some fixed direction.

In the forward direction ($\theta_s = 0$), we have

$$\text{Im}F(s, \cos\theta_s = 1) = \sum (2l+1) \text{im}f_l(s), \quad (2.4.4)$$

a sum of positive terms, which is positive. $\text{Im}F(s, \cos\theta_s = 1)$ can not vanish unless the scattering amplitude is identically zero at all energies and all angles. Hence, we have

$$\text{Im}F = \sin\phi |F| > 0$$

$$\text{and } 0 < \phi(s, \cos\theta_s = 1) < \pi \quad (2.4.5)$$

At a particular energy s_0 , one has $0 < \phi(s_0, \cos\theta_s = 1) < \pi$ to remove the $2\pi n$ ambiguity. This phase satisfies inequality (2.4.5).

On the other hand, in the physical region ($-1 < \cos\theta_s < +1$) the imaginary part of the amplitude is not necessarily positive, even at very close to the forward direction.

From the result $|P_l(\cos\theta_s)| < P_l(\cos\theta_s = 1) = 1$, we have the inequality

$$|\text{Im} F(s, \cos\theta_s)| < \text{Im}F(s, \cos\theta_s = 1). \quad (2.4.6)$$

Kinoshita and Martin [47] have derived an inequality

$$\frac{\text{Im}F(s, \cos\theta_s)}{\text{Im} F(s, \cos\theta_s = 1)} > -\frac{1}{2}, \quad \cos\theta_s > -\frac{1}{2} \quad (2.4.7)$$

This inequality gives new information on the phase.

We measure $(d\sigma/d\Omega)(\cos\theta_s)$ as a continuous function of $\cos\theta_s$.

There is some angular interval ($0 < \theta_s < \theta_0$) in which

$$\frac{d\sigma}{d\Omega}(\cos\theta_s) > \left(\frac{1}{4}\right) \frac{d\sigma}{d\Omega}(\cos\theta_s=1) \quad (2.4.8)$$

$$\text{and } |F(s, \cos\theta_s)| > \frac{1}{2} |F(s, 1)| > \frac{1}{2} \text{Im}F(s, 1) \quad (2.4.9)$$

In the case of $\theta_0 < 2\pi/3$, we have

$$\text{Im}F(s, \cos\theta_s) > -\frac{1}{2} \text{Im}F(s, \cos\theta_s=1) \quad (2.4.10)$$

It is obvious from the equations (2.4.10) and (2.4.9) that $\text{Re} F=0$ $\text{Im}F < 0$. So, the phase factor $\phi(s, \cos\theta_s)$ can not be equal to $-\pi/2 + 2n\pi$. For the forward scattering, we have

$0 < \phi(s, 1) < \pi$ and on using continuity in θ_s , we conclude that

$$-\pi/2 < \phi(s, \cos\theta_s) < 3\pi/2 \text{ for } 0 \leq \theta_s \leq \theta_0 \leq 2\pi/3 \quad (2.4.11)$$

Although this information about the phase comes from the modulus, it is considered to be a weak one.

By considering detailed properties of Legendre polynomials, Cornille and Martin [48] have found the result:

$$|\phi(s, \cos\theta_s)| < \pi + \frac{(\pi(1/4))^4}{\pi^3} \sup_{\theta_s' \leq \theta_s} \frac{\frac{d\sigma}{d\Omega}(s, \cos\theta_s=1)}{\frac{d\sigma}{d\Omega}(s, \cos\theta_s')} \quad (2.4.12)$$

Here we no longer have restriction $\theta_s < 2\pi/3$.

Bowcock et al. [49] chose particular forms for $\phi(z)$ and varied the coefficients of expansion until the unitarity limit is found out in some partial waves:

$$\phi(z) = \sum_i \mathcal{A}_i \phi_i(z) \quad (2.4.13)$$

They made a very limited exploration of this phase ambiguity on selecting a particular form of ϕ , with one parameter b :

$$\phi(z) = b \left[(1-z^2/1.5)^{\frac{1}{2}} - (1-1/1.5)^{\frac{1}{2}} \right] \quad (2.4.14)$$

Satisfying the restrictions (L), (U)-(iv) and (R). However, the method is limited to only one direction of ϕ space with the neighbourhood of $b=0$. They conclude that, while no resonance

is created or destroyed, quite large quantitative changes in resonance parameters are possible. It has since been extended by Pietarinen[50].

Bowcock and Hodgson[51] model amplitude is in the form:

$$F(z) = \frac{\gamma}{(\alpha^2 + \beta^2 - 2\alpha\beta z)^{1/2}} \quad (2.4.15)$$

$$\text{and } \phi(z) = \delta [(\alpha^2 + \beta^2 - 2\alpha\beta z)^{1/2} - (\alpha^2 + \beta^2 - 2\alpha\beta)^{1/2}] \quad (2.4.16)$$

It has been observed that for values of δ between -2 and 1 all waves (s,p, and d) lie inside the unitarity circles and corresponding points on arcs represent allowed partial waves.

The ambiguities form lines only because the phase function $\phi(z)$ has one parameter.

Atkinson[52] and co-workers have developed a new method of the partial waves which rests on the fact that there is no continuum ambiguity in elastic region, where the inelasticities are fixed and then using the latter as variables with which to parameterize the continuum. The method is systematic and powerful. They have applied the method to $\alpha\alpha$ elastic scattering at 35 Mev. The results show clearly the islands of ambiguity. The ambiguity is as large as a third of the circle for the s-wave but it has a tendency to become more one dimensional in the higher waves. Recently, they have extended this work to pion-nucleon scattering[53].

The islands are, in general, smaller than in $\alpha\alpha$ scattering, and in some cases remarkably small. There is the real possibility of suppressing the resonance in some cases where small resonance circles are involved.

The situation is more ambiguous in the case of Π^+p and k^+p , as observed by Van Driel[54]. There are islands of ambiguity which actually varies the speed on the Argand diagram and so none of the usual structures should be taken seriously as resonances.

Atkinson et al. [55] have constructed Π^+p continuum ambiguities from 1974 Sclay phase-shift analysis. It leaves unchanged the total cross-section, the differential cross-section and the polarization. They find that most of the resonant structures are stable, but that alternative solutions are possible that lack the second S_{31} or the G_{39} resonance. Further, they suggest that disagreements between different groups concerning the existence of the weak resonances, or concerning the masses and widths of stronger ones, may be caused by the existence of the continuum ambiguity.

In conclusion, we can obtain the scattering amplitude from the experimental data in the elastic region with only a few discrete alternative solutions at most. On the other hand, there has not been developed any reliable inelastic phase-shift analysis which gives convincingly justified results. The uncertainties in the amplitude produced by the continuum ambiguity are serious. Methods based on energy smoothing to find a unique amplitude are quite arbitrary, while the method of multi-energy analysis based on fixed-momentum dispersion relations seems to be a sound route to unique amplitude. It is most desirable, but very difficult, to find a sound procedure which can be justified by analytic argument and error analysis.

2.5 ANALYSES OF MARTIN AND ESTBROOKS[65]

In the low energy region ($M_{\pi\pi} \leq 2\text{Gev}$), the presence of the $p(1^+(1^-)-)$, $f(0^+(2^+)_+)$ and $g(1^+(3^-)-)$ resonances with masses and full widths ($770 \pm 10\text{Mev}$, $150 \pm 10\text{Mev}$), (1270 ± 10 , $170 \pm 30\text{Mev}$) and ($1686 \pm 20\text{Mev}$, $180 \pm 30\text{Mev}$) respectively is clear from the high statistics $\pi\pi^- p \rightarrow \pi\pi^+ \pi\pi^- n$ [56] and $\pi\pi^+ p \rightarrow \pi\pi^+ \pi\pi^-$ data[57]. The study by Flatte et al.[58] has shown the existence of the $S^*(0^+)$ resonance near the $K\bar{K}$ threshold. Although the Frascati $e^+e^- \rightarrow 2\pi(4\pi)$ data [59] is not conclusive, there is definite evidence for a p' (1600) from the photoproduction process $\gamma \text{Be} \rightarrow 2\pi(4\pi)\text{Be}$ observed at FNAL[60]. The p' is also evident in $\pi\pi$ partial wave analyses of the CERN-Munich high statistics $\pi\pi^- p \rightarrow \pi\pi^- \pi\pi^+$ data[61].

Using Barrelet zeros[62], Martin and Estbrooks [63] have made an energy independent $\pi\pi$ partial wave analysis in the energy range $1.0 < M_{\pi\pi} \leq 1.8 \text{ Gev}$, to examine in detail the possible ambiguities, and to study the resulting $\pi\pi^- \pi\pi^+$ resonance spectrum. The study has been done with a motivation for a possible E' resonance [64] under f , and p' resonance under g resonance.

Before extracting $\pi\pi^- \pi\pi^+$ partial waves from $\pi\pi^- p \rightarrow \pi\pi^- \pi\pi^+ n$ data, we have the moments $\langle Y_0^J \rangle$, $J=0, 1, \dots, 2L$, of the $\pi\pi^- \pi\pi^+ \rightarrow \pi\pi^- \pi\pi^+$ angular distribution where L denotes the highest non-negligible partial wave. $\langle Y_0^J \rangle$ determine the magnitudes and relative phases of the first $L+1$ partial waves, but not the overall phase. In addition to that, we have a discrete 2^L fold ambiguity, expressed in terms of Barrelet zeros $Z_j(s)$ of the $\pi\pi^- \pi\pi^+$ scattering amplitude in the complex $Z \equiv \cos\theta_s$ -plane:

$$F(s, Z) = f(s) \prod_{j=1}^L (Z - Z_j), \quad (2.5.1)$$

$L \rightarrow \infty$ in general. This ambiguity is due to the fact that the signs of $\text{Im}Z_j$ cannot be determined from the angular distribution.

In the low energy region; elastic unitarity may resolve this ambiguity; whereas in the inelastic region the unitarity constraint is no longer as powerful. As the $\Pi^- \Pi^+$ partial wave resonates (p, f, g, \dots), zeros are close to the physical region. It is clear from the study of Estabrooks [65] and Hyams [66] that the zero contours $Z_j(s)$ are extremely smooth in S except the S^* near the $K\bar{K}$ threshold. So, Barrelet zeros have found to be very useful in the phase shift analysis of $\Pi^- \Pi^+$ scattering in the following sense:

- (i) one can find all the 2^L solutions at a given s :
- (ii) One can keep track of the physical solution by continuity of the $Z_j(s)$ with increasing s , and can find the values of s , where alternative solutions arise ($\text{Im}Z_j \neq 0$);
- (iii) one can investigate the resonance spectrum for searching the existence of daughter resonances, and determine their parameters.

In EM's [63] study, for each $M_{\Pi^- \Pi^+}$, the data determine the values of eight parameters, namely the magnitude and relative phases of S_0, P_0, D_0, F_0 and the parameter C . The amplitude L_0 is given by

$$L_0 = (N.) \frac{M_{\Pi^- \Pi^+}}{\sqrt{k}} \sqrt{2L+1} f_L, \quad (2.5.2)$$

where the partial wave amplitudes are defined by

$$f_L^I = (n_L^I e^{2id_1^I} - 1) / 2p \quad (2.5.2a)$$

$$(N.) = \text{the overall normalisation factor.} \quad (2.5.2b)$$

$$k = \Pi \text{ momentum in } \Pi^- \Pi^+ \text{ C.m. frame.} \quad (2.5.2c)$$

$$f_L = \frac{1}{3} (2f_L^0 + f_L^2) \text{ for even } L \quad (2.5.2d)$$

$$f_L = \frac{1}{3} \text{ for odd } L, M_{\Pi^- \Pi^+} = \text{dipion mass} \quad (2.5.2e)$$

This $(N.)$ is determined by the elastic P wave phase shift to go smoothly through 90° at the p resonance. In equation (2.5.2) it is assumed that the Π exchange amplitudes L_0 have a common

t dependence, which is independent of $M_{\Pi\Pi}$. This method has been used by Hyams et al. [66], which gives reliable results below 1.4 Gev.

The solution A is defined by the magnitudes and relative phases of $\sqrt{2L+1} f_L$ and the parameter C, which determines the non Π exchange production amplitudes. The complex zeros, Z_j , are obtained from the solution:

$$\sum_{L=0}^3 (2L+1) P_L(z) |f_L| e^{i\phi_L} = a_{\Pi\Pi} \prod_{j=1}^3 (z-z_j) \quad (2.5.4)$$

One can find alternative solutions at each $M_{\Pi\Pi}$ by replacing $\text{Im} Z_j$ by $-\text{Im} z_j$ for one or more of the zeros, calculating a new set of magnitudes and relative phases of the L_0 amplitudes from equation (2.5.4), and then fitting to the data. So, one obtains eight solutions at each energy. As the existence of the f resonance requires the second zero to approach the physical region with $\text{Im} Z_2 < 0$, and similarly the g resonance requires $\text{Im} Z_3 < 0$, the ambiguity due to overall 2^L solutions at a given s is immediately reduced. Hence, one has a two-fold ambiguity depending simply on the sign of $\text{Im} Z_1$ at each $M_{\Pi\Pi}$ in the f region ($M_{\Pi\Pi} < 1.4 \text{ Gev}$). The solution A with $\text{Im} Z_1 > 0$ leads to a better description of the $\Pi^0 \Pi^0$ mass spectrum in this region, resolving the ambiguity in the f resonance region. Their solutions are classified as follows:

Solutions	Sign of $\text{Im} Z_1$	Sign of $\text{Im} Z_2$
A	-	-
B	+	-
C	+	+
D	-	+

It is found in their study that $\text{Im}Z_1 \approx 0$ around $M_{\pi\pi} = 1.24$ Gev. They define solution B in which $\text{Im}Z_1$ does not change sign at $M_{\pi\pi} = 1.24$ Gev.

The overall phase has been chosen to give reasonable continuity of the partial waves consistent with the existence of the f and g resonances, and with unitarity. It appears that solution A shows no evidence for daughter resonances in this region; whereas for solution B the S partial wave in the region of the f resonance and the P wave in the g region follow approximately circular contours in an anticlockwise direction in the Argand plot. The speed of rotation of these lower partial waves is not clear indication of resonant behaviour and these daughter resonances must be relatively broad ($\Gamma \sim 400$ Mev), and are difficult to be established. According to EM's observation the S wave of solution B is outside its unitary circle for $1.25 \leq M_{\pi\pi} \leq 1.5$ Gev, consequently, the relatively large errors on this partial wave make it possible to use unitarity to definitely eliminate this solution.

For further EM's study, the energy dependence of the solutions is needed in terms of zero contours, which is suggested by the smoothness of Z_j in S. The $Z_j(s)$ is parameterized as a ratio of polynomials in S and determine the complex coefficients from the relative magnitudes and phases of f_L . Further, $Z_3(s)$ is parameterized in the g region such that at 1.5 Gev it joins onto the value calculated in the f region on using the f and g resonance forms. The resonance form is expressed by

$$f_L = \frac{X_R Y_R(s)}{M_R^2 - s - iY_R(s)}, \quad (2.5.5)$$

$$\text{where } Y_R = Y_0 + Y_1(s - M_R^2). \quad (2.5.6)$$

The overall magnitude is specified by fitting $|f_D|$ in the range

$1 < M_{\pi\pi} < 1.4$ Gev, $|f_p|$ in the region $1.5 \text{ Gev} < M_{\pi\pi} < 1.8$ Gev to (2.5.5) and (2.5.6). Excellent fits to the amplitudes are obtained.

Now, it is clear from EM's study that s-dependence of $\text{Im } z_j(s)$ indicates the main ambiguity between solutions A and B. On changing the sign of $\text{Im } z_2$ in solutions A and B for $M_{\pi\pi} > 1.4 \text{ Gev}$, we get two other solutions C and D respectively. The resonance parameters and values of the zeros at complex pole positions show that solution C like A has only leading resonances; whereas solution D appears to have a broad D-wave resonance in the g region. The solution A shows no resonance structure other than the leading f and g resonances. However, solution B having a broad p' resonance (~ 400 Mev) in the g region, violates S wave unitarity in the f region.

EM's published figures give the impression of very smooth argand diagrams, but actually solutions (plotted from tables) are very noisy. On the other hand, the problem of truncation at $L=3$ introduces spurious uniqueness and there are continuum ambiguities clearly present.

In EM's [63] notation, on the question of the existence of a p wave p' (1600) resonance their solutions divide into two categories: (i) solutions B, D have a p' coupling relatively strongly to $\pi\pi$ (elasticity 25%); whereas (ii) solutions A, C show no evidence for a p' signal (elasticity 4%). These two categories arise because the first zero, $z_1(s)$, to enter the physical region has $\text{Im } z_1 = 0$ near $s = M_{\pi\pi} = 1.25$ Gev and so a bifurcation of solutions is possible. Above this energy, solutions of type (i) and (ii) correspond to $\text{Im } z_1 > 0$ and $\text{Im } z_1 < 0$ respectively.

Recently, Johnson, Martin and Pennington [67] have exploited analyticity to distinguish between classes of $\Pi^+ \Pi^-$ partial wave solutions. In their view, fixed-t and fixed-u dispersion relations determine the overall phase of the amplitude and clearly select solutions with a $\rho'(1600)$ resonance of 25% elasticity. The relevant question of existence of ρ' , ω' and ϕ' vector mesons, with the advent of new Ψ particles, is outstanding. There is so far only information on the ρ' resonance.

On the assumption that the truncation of the partial wave series at $L=3$ (and moment series at $J=6$) is exact, so that the unknown phase ϕ_0 depends on s and is independent of t , Johnson et al [67] conclude that analyticity overwhelmingly favours the $\Pi \Pi$ partial wave solutions (B and D) with a sizeable ρ' coupling to $\Pi \Pi$ and determines the overall phase of these solutions. Further work is continued to resolve the remaining ambiguity between the B and D solutions. It is more complicated in the sense that it depends on Barrelet zero (z_2), which unlike z_1 , is near the physical region $\sqrt{s} > 1.45$ Gev (where the bifurcation of $\text{Im } Z_2$ actually occurs) and so just outside the range of validity of fixed momentum transfer dispersion relations.

2.6 ANALYSES OF FROGGATT AND PETERSEN.

Froggatt and Petersen[68] have used extrapolated $\Pi^+\Pi^-$ moments from amplitude analysis of the 17Gev/c CERN-Munich experiment on $\Pi^-p \rightarrow \Pi^+\Pi^-n$, and reduced phase-shift ambiguities by imposing fixed-t and fixed-u analyticity. The result and solution agree qualitatively with semi-local duality. A phase-shift analysis by constraining the result to be compatible with fixed-t(-u) amplitudes have been performed. Consequently, a smooth phase-shift solution is obtained, which shows a clear p' signal.

Broadly speaking, we face 3 different classes of ambiguities in reconstructing the amplitude from experiment, described earlier. FP [68] have concentrated their work to class 3rd ambiguities (in lack of a real pion target an ordinary scattering experiment only measures the absolute magnitude of the amplitude); while using the results of Estabrooks and Martin[63].

We can write the $\Pi^+\Pi^- \rightarrow \Pi^+\Pi^-$ elastic scattering amplitude as

$$|F^{+-}(M_{\Pi\Pi}, \cos \theta)|^2 \equiv \sum_L (2L+1) A_L(M_{\Pi\Pi}) P_L(\cos \theta), \quad (2.6.1)$$

where A_L 's are real coefficients given by the Clebsch-Gordon series as bilinear functions of the f_1^I 's with known coefficients. Using the EM solutions [63] the first 7 A_L 's can be calculated. These values are independent of the overall phase ambiguity.

It seems that the most promising proposal for dealing with the phase-shift ambiguity problem consists in demanding compatibility with fixed-t and fixed-u analyticity. FP [68] introduced a crossing symmetric energy variable v :

$$v \equiv \frac{s-u}{4m_{\Pi}} \quad (2.6.2)$$

with $v=v_0(t)$ and $v=\bar{v}(t)$ the s-channel physical threshold and the start of the s-channel physical region respectively:

$$\begin{aligned} v_0(t) &= m_{\Pi^+} + t/4m_{\Pi} \\ \bar{v}(t) &= m_{\Pi^-} - t/4m_{\Pi} \end{aligned} \quad (2.6.3)$$

If we have the following information about an amplitude $F(v,t)$ for fixed t : (a) $\text{Im}F(v,t)$ is known on the unphysical cuts such that $-\bar{v}(t) \leq v \leq -v_0(t)$ and $v_0(t) \leq v \leq \bar{v}(t)$, (b) $|F(v,t)|$ be known throughout the physical regions $-\infty < v \leq -\bar{v}(t)$ and $\bar{v}(t) \leq v < \infty$ and (c) at infinite energies the growth of $|F(v,t)|$ be under control i.e. $|F(v,t)| < M \cdot |v|^{\alpha}$ for $|v| > N$, v real $\pm i\epsilon$ (M, α finite); then $F(v,t)$ is uniquely defined up to a finite-dimensional ambiguity [69]. The method for imposing fixed-momentum transfer analyticity on amplitude analysis, developed by Pietarinen [69], has been used. The input is assumed to consist of numerical information at a finite number of energies. It is optimal and capable of providing unbiased error-estimates.

We can expand the fixed- t (or fixed- u) amplitude $F(v)$ in terms of a suitably chosen set of functions $\{\Phi_{\mathbb{I}n}(v)\}$, each possessing the desired analyticity properties:

$$F(v) = \sum_{i=0}^N \alpha_i \Phi_{\mathbb{I}i}(v) \quad (2.6.4)$$

The expansion coefficients are found by minimizing

$$\chi^2(F) \equiv \chi^2(F) + \Phi(F), \quad (2.6.5)$$

where $\chi^2(F)$ is for the experimental data and $\Phi(F)$ is the convergence test function in order to give a penalty for lack of smoothness.

They have presented two analyses of $\Pi^+ \Pi^-$ scattering between 1.1 Gev and 1.8 Gev. The first one results in a set of fixed momentum-transfer amplitudes satisfying analyticity properties exactly and the second one has correspondingly good

properties at fixed energies: smoothness in $\cos \theta_s$ and unitarity. The two analyses agree to the extent that we can talk about one solution.

The FP [68] solution has the following salient features:

- (a) It reproduces the experimental Legendre-moments $\{A_{\ell}\}$.
- (b) It not only has good smoothness properties, both as a function of energy and $\cos \theta_s$, but it satisfies crucial analyticity requirements.
- (c) It agrees reasonably with unitarity.

However, the solution does not satisfy semi-local duality. And, the amount of remaining ambiguity has not been determined.

In constructing the Argand diagrams from the $\Pi^+ \Pi^-$ partial wave amplitudes an error has been made by FP [68] in the case of $l=1$. Indeed, P_1 and F_1 as given in their figures 8 & 9 as well as their values reconstructed from table 1 are too large by a factor $3/2$. secondly, the asymptotic cross-section corresponding to their fig. 7 should be 4mb . These corrections have been made by FP [68a].

It is observed that FP's partial waves are much smoother than EM's, on plotting Argand diagrams.

P A R T O N E

CHAPTER III : BOUNDS ON $\pi\pi$ SCATTERING LENGTHS.3.0. INTRODUCTION.

Martin[70] demonstrated that the constraints imposed on the scattering amplitude by the results of axiomatic field theory limit the strength of the strong interactions, at least for the case of $\pi\pi$ scattering. From the requirements of analyticity, unitarity, and crossing symmetry he proved that within its analyticity domain, including the symmetry point, the $\pi\pi$ scattering amplitude is bounded above and below as a function of the pion mass alone. Martin's numerical results were improved by Łukaszuk and Martin[71] using a refinement of Martin's original method.

These bounds are rigorous consequences of axiomatic field theory. Unlike the asymptotic bounds on scattering amplitudes (e.g. the Froissart[72] and Jin-Martin [17] bounds) they contain no arbitrary constants and represent quantitative restrictions on the size of the amplitude at finite energies. It is therefore desirable to see if they can be improved by making better use of analyticity, unitarity, and crossing symmetry.

In the real world there are no bound states in the $\pi\pi$ system, and their absence has been explicitly incorporated in the analyticity assumptions used to derive the bounds on the $\pi\pi$ amplitude.

A nice development is that rigorous phenomenology leads to some improvements over the axiomatic results. Recently, on this line of approach the lower bounds of the $\pi\pi$ S-wave scattering lengths have been developed on the basis of some estimates of the D-wave scattering lengths [20].

Bonnier[18] has derived rigorous upper and lower bounds on the $\pi\pi$ S-wave scattering lengths, starting from a given phenomenological input (upper and lower bounds of the real

and imaginary parts of the $\pi^0\pi^0$ and $\pi^+\pi^0$ amplitudes on the region $0.45\text{Gev} \leq E_{\text{c.m.}} \leq 1.9\text{Gev}, 0 \leq t \leq 4m_{\pi}^2$.

Lopez[19] has found a new lower bound to the $\pi^0\pi^0$ S-wave scattering length in terms of the D-wave scattering length. The main ingredients of the method are the exact Roy partial-wave equations and an extensive use of unitarity in the physical region. For a value of $a_2 = 7.3 \times 10^{-4}$, he gets the bound $a_0 \gg -0.33$. Further, Lopez and Mennessier[22] have improved substantially the precedent absolute lower bounds on the $\pi^0\pi^0$ S-wave scattering length. The new feature in their derivation is the exploitation of the known structure of the partial wave left hand cut discontinuity, explicitly exhibited by the Roy equations. The result is

$$a_0^{00} > -1.75 \quad (3.0.1)$$

Furthermore, Bonnier, Lopez and Mennessier[21] have used axiomatic properties to derive new absolute upper and lower bounds on $\pi^0\pi^0$ amplitude in the Mandelstam triangle. In particular, if the amplitude is so normalized that its value at threshold is the scattering length, the value at the symmetry point, which is considered as a measure of the $\pi\pi$ coupling, has been shown to lie between -13.5 and 2.75.

3.1. BONNIER'S BOUNDS ON THE $\pi\pi$ S WAVE SCATTERING LENGTHS.

3.2 Introduction.

Bonnier [18] has developed a new approach to derive rigorous phenomenological bounds on the S-wave scattering lengths, but he adopts the position of using the maximal amount of available experimental data as directly as possible, and not only through the D-waves. As a result a new class of bounds appear (upper bounds) and the lower ones are improved. However, in this approach we have to take care of the consistency of the chosen phenomenology with general principles. In the energy range $0.45 \text{ GeV} \leq E \text{ c.m.} \leq 1.9 \text{ GeV}$, the main features of $\pi\pi$ scattering are common to most of the analyses and one can define a "central" family of S, P, D, F phase shifts with associated 'errors'. In order to cover the spread of the data, he has multiplied the errors (between 0.45 GeV and 1.9 GeV) by a scaling factor ϵ ($0 \leq \epsilon \leq 1$) such that $\epsilon=0$ gives the central family and $\epsilon=1$ the band of maximal expanse. This ϵ is not a measure of the errors in a given analysis, but an estimate of the discrepancies between various analyses. In this way, for any fixed value of ϵ one can easily compute the lower and upper bounds of the $\pi\pi$ amplitudes and then derive the bounds on the scattering lengths.

3.3 NOTATIONS AND SUM-RULE INEQUALITY.

We can write the S-channel partial wave expansion of the S-channel isospin (I) $\Pi\Pi$ amplitude $F^{(I)}(s,t,u)$ in the form;

$$F^{(I)}(s,t,u) = \sum_{l=0}^{\infty} \left[\frac{1+(-)^{l+1}}{2} \right]^{(2l+I)} f_l^I(s) P_l(1+2t/(s-4)), \quad (3.3.1)$$

where $m_{\Pi\Pi} \equiv 1$,

$$f_l^I(s) = (\eta_l^I(s) e^{2i\delta_l^I(s)} - 1) / 2ip(s), \quad p(s) = ((s-4)/s)^{1/2} \quad (3.3.2)$$

and the optical theorem is in the form,

$$\text{Im } F^I(s,0) = ((s-4)/s)^{1/2} \sigma_{\text{total}}^I(s) / 16\pi \quad (3.3.3)$$

The s-wave scattering lengths for $I=0,2$ are simply

$$a_I = f_0^I(4) = F^I(4,0,0) \quad (3.3.4)$$

At fixed $t=t_0$, $0 \leq t_0 \leq 4$ the elastic amplitudes have the combinations:

$$\begin{aligned} F^0 + 2F^2 &\equiv F_N, & \text{for } \Pi^0 + \Pi^0 &\longrightarrow \Pi^0 \Pi^0 \\ F^1 + F^2 &= F_S, & \text{for } \Pi^+ + \Pi^0 &\longrightarrow \Pi^+ \Pi^0 \end{aligned} \quad (3.3.5)$$

$$z = ((s-u)/(4+t_0))^2 = ((2s+t_0-4)/(4+t_0))^2 \quad (3.3.6)$$

We find that $s \leftrightarrow u$ crossing even amplitudes are real analytic functions in the complex z -plane cut for $z \geq 1$. One can assume safely that on some part (s_1, s_2) of the physical region ($4 < s_1 < s_2$), mapped onto (z_1, z_2) , the available data are sufficiently reliable to give us upper and lower bounds of the real and imaginary parts of F_N and F_S . Also, the chosen data should satisfy the sum-rule inequality of Common [74] which expresses $s \leftrightarrow u$ crossing and positivity. So, it appears that this kind of information can be rigorously used in a powerful way on general lines.

$$\text{Mapping: } v = \frac{1 - \sqrt{w}}{1 + \sqrt{w}} \quad \text{where } w = \frac{z - z_1}{z - z_2} \quad (3.3.7)$$

It maps the cut z -plane onto a unit disk D_v of the v -plane such that the low-energy region $1 \leq z \leq z_1$ goes to the cut $v_1 \leq v \leq 1$, the intermediate energy region $z_1 \leq z \leq z_2$ (where both the real and imaginary parts of the amplitudes F_N and F_S have phenomenological bounds) goes to the circumference of an unitary circle:

$$v = v(e^{i\theta}), \quad v(z=z_2) = -1 \quad (3.3.8)$$

and finally the high-energy region $z \geq z_2$ goes to the cut $-1 \leq v \leq 0$ in order that when $z \rightarrow \infty, v \rightarrow 0^-$ like:

$$v(z) \sim -\frac{(z_2 - z_1)}{4z} \sim -\frac{(z_2 - z_1)}{4z} \sim \frac{-(z_2 - z_1)(4 + t_0)^2}{16s^2} \quad (3.3.9)$$

The mapping is shown in fig.9.

The union of the regions $[-1, 0]$ and $[v_1, 1]$ is denoted by I . If $P(v)$ and $Q(v)$ are two real analytic functions, one can construct a function $L(v)$ which is real and analytic in the unit disc and bounded on its boundary:

$$L(v) = v \left[P(v) F_N(v) + Q(v) F_S(v) \right] \quad (3.3.10)$$

Now, if $v=0$ we have corresponding point infinity in the s -plane. The Froissart-Martin bound for the amplitudes can be written as

$$|L(v)| \leq \text{const.} (\sqrt{|v|} \log^2 |v|) \quad \text{as } v \sim 0 \quad (3.3.11)$$

From (3.3.9) and (3.3.11) it follows that

$$L(0) = 0.$$

For any point v_0 inside the unit disc D_v ($0 < v_0 < v_1$), we can write from Cauchy integral:

$$L(v_0) = \frac{1}{2\pi i} \oint \frac{L(v') dv'}{v' - v_0}$$

$$\text{or } L(v_0) = \frac{1}{\Pi} \int_0^{\Pi} \text{Re} \left[\frac{L(e^{i\theta}) e^{i\theta}}{e^{i\theta} - v_0} \right] d\theta +$$

$$+ \frac{1}{\Pi} \left[\int_{-1}^0 + \int_{v_1}^1 \right] \frac{v' dv'}{v' - v_0} (P(v') \text{Im} F_N(s(v')) + Q(v') \text{Im} F_S(s(v'))) \quad (3.3.12)$$

$$\text{or } L(v_0) = L_0(v_0) + L_I(v_0), \quad (3.3.13)$$

where $L_0(v_0)$ and $L_I(v_0)$ are the contributions of the circle and the region I respectively. As the absorptive parts of F_N and F_S on I are positive, it follows from (3.3.12) that the contribution $L_I(v_0) \geq 0$ or $L_I(v_0) \leq 0$ according as P and $Q \geq 0$ or ≤ 0 respectively. In this sense, P and Q are not arbitrary.

The intermediate energy region (experimental) is on the circle and its contribution, $L_0(v_0)$, can be computed for all such P and Q to a certain accuracy, accordingly one can calculate upper and lower bounds:

$$L_0^m(v_0) \leq L_0(v_0) \leq L_0^M(v_0) \quad (3.3.14)$$

On combining the results (3.3.13) and (3.3.14) we obtain Bonnier's sum-rule inequalities for any t_0 and v_0 , $0 \leq t_0 \leq 4, 0 < v_0 \leq v_1$:

$$L(v_0) \geq L_0^m(v_0) \quad P, Q \geq 0 \text{ for all points on I} \quad (3.3.15)$$

$$L(v_0) \leq L_0^M(v_0) \quad P, Q \leq 0 \text{ for all points on I} \quad (3.3.15a)$$

They are true for any unphysical values, but there is a focus on the scattering lengths.

3.4 BOUNDS ON THE SCATTERING LENGTHS.

The S-wave scattering lengths for $l=0,2$ are

$$a_0 = f_0^0(4) = F^0(4,0,0) \quad (3.4.1)$$

$a_2 = f_0^2 = F^2(4,0,0)$ with $s \leftrightarrow u$ symmetry. For old bounds with the

choice $t_0=0, w_0=v_1$, we have the combinations

$$F_N(v_1) \equiv F^0(4,0) + 2F^2(4,0) = a_0 + 2a_2 \quad (3.4.2)$$

$$F_S(v_1) \equiv F^1(4,0) + F^2(4,0) = a_2 \quad (3.4.2a)$$

Then, we have bounds

$$L(w_0) = a_0 v_1 P(v_1) + a_2 v_1 (Q(v_1) + 2P(v_1)) \quad (3.4.3)$$

Applying inequalities (3.3.15) on (3.4.3), we get information about some combinations of a_0 and a_2 . Equation (3.3.15) needs $PQ \geq 0$ on I and since v_1 belongs to I as end point it is impossible to bound a_0 alone, that would require $2P(v_1) Q(v_1) = 0$. However, this is possible on a_2 [$P(v_1)=0, Q(v_1)=1$] but then $Q(v_1)=1$ implies $P, Q \geq 0$ on I which allows us to compute only lower bounds. This is true for $a_0 + 2a_2$. In this way we recover here the lower bounds, already obtained by Common [10], Goebel and Shaw [75] and Basdevant et al. [35]. These lower bounds can now be positive and optimized owing to the freedom allowed in the weight functions $P(v)$ and $Q(v)$.

Now on applying $s \leftrightarrow t$ crossing, we have a noticeable improvement over the bounds. Choosing $t_0=4, v_0=v(z=0)$

($0 < v_0 < v_1$), we have the combinations of the amplitudes

$$F_N(v_0) = F^0(0,4) + 2F^2(0,4) = F^0(4,0) + 2F^2(4,0) = a_0 + 2a_2 \quad (3.4.4)$$

$$F_S(v_0) = F^1(0,4) + F^2(0,4) = 2/3 \left[F^0(4,0) - F^2(4,0) \right] = 2/3(a_0 - a_2) \quad (3.4.5)$$

and the bound

$$L(w_0) = a_0 v_0 (P(v_0) + 2/3 Q(v_0)) + 2a_2 v_0 (P(v_0) - \frac{Q(v_0)}{3}) \quad (3.4.6)$$

As V_0 do not belong to I , the values of P and Q at v_0 can now be prescribed independently of their required behaviour on I . With the help of equation (3.4.6), we can compute upper and lower bounds for any linear combination of the scattering lengths, and in particular for the scattering lengths themselves. Bonnier [18] has selected to bound $a_0, a_2, 2a_0 - 5a_2$ and $a_0 + 2a_2$ with corresponding values of $P(v_0)$ and $Q(v_0)$.

To make choice of the weight functions $P(v)$ and $Q(v)$, we can select a finite subset of the infinite set of polynomials which give necessary and sufficient conditions for the solutions of the associated 'moment problem',

$$\mu_n = \int_{-1}^0 v^n g(v) dv + \int_{v_0}^1 v^n g(v) dv, \quad n=0,1,2,\dots \quad (3.4.7)$$

with $g(v)$ a non-negative function of v [76]. For the purpose, Bonnier [18] has constructed :

$$P(v) = P(v_0) R_p(v) \prod_{j \in J} \frac{(v - v_p^j)(v - \bar{v}_p^j)}{(v_0 - v_p^j)(v_0 - \bar{v}_p^j)} \prod_{k \in K} \frac{(v - v_p^k)}{(v_0 - v_p^k)} \quad (3.4.8)$$

where $v_p^j = r_p^j e^{i\theta_p^j}$, $\bar{v}_p^j = r_p^j e^{-i\theta_p^j}$, $r_p^j \geq 0$, $0 < \theta_p^j < \pi$ for all j

$$v_p^k \leq -1 \text{ or } v_p^k \geq 1 \text{ for all } k \text{ values} \quad (3.4.9)$$

$R_p = 1$ or $v(v - v_1)/v_0(v_0 - v_1)$ according to the sign of $P(v_0)$ and $Q(v_0)$ and to the nature of the wanted bound.

This parameterization (3.4.9) gives the most general expression for a polynomial of fixed degree ($\approx 2J+K$) submitted to the constraints. The number and location of real and complex zeros entering these representations are parameters which are optimized to give the best bounds for a given set of data. Bonnier has applied MINUITL to obtain the extrema of $L_0^m(v_0)$ and $L_0^M(v_0)$ with at most 48 parameters.

3.5 PHENOMENOLOGICAL INPUT.

Bonnier[18] has pointed out that these types of bounds, $L_0^m(V_0)$ and $L_0^M(V_0)$, can not be constructed from any set of data. Firstly, they should fulfil the obvious constraints

$$L_0^m(V_0) < L_0^M(V_0) \quad (3.5.1)$$

Secondly, the chosen data must satisfy the sum-rule inequality of Common[74], satisfying $s \leftrightarrow u$ crossing and positivity. Thirdly, we can also add to these requirements some $s \leftrightarrow t$ crossing sum-rules for all $0 \leq t_0 < 4$.

In the energy range $0.45 \text{ Gev} \leq E_{c.m.} \leq 1.9 \text{ Gev}$, the main features of $\pi\pi$ scattering agree with the recent analyses[77]. We can define the whole situation by a central family of S,P,D,F phase shifts with associated errors. In order to cover the spread of the data, it is convenient to select a scaling factor \mathcal{E} ($0 \leq \mathcal{E} \leq 1$) such that the central family ($\mathcal{E}=0$) is obtained, and $\mathcal{E}=1$ gives the band of maximal expanse. This \mathcal{E} is not a measure of the errors in a given analysis, but it is an estimate of the discrepancies between various analyses. We can compute the lower and upper bounds on $\pi\pi$ amplitudes, thereby, the bounds on the scattering lengths for any fixed value of \mathcal{E} . Phenomenologically, the results with $\mathcal{E}=1$ should only be taken with confidence.

3.6 CONCLUSIONS AND REMARKS.

Bonnier[18] has selected three values of ϵ ($\epsilon = 0, \frac{1}{2}$ and 1.0). The computed upper bounds on s-wave scattering lengths vary considerably with three values of ϵ and with different combinations of the scattering lengths. However, the lower bounds remain always small, in particular, for $\epsilon=1$ stay rather on a firm basis. It has already been pointed out by Basdevant et al[35] that they can increase considerably if some peculiar phase-shift analysis of Estabrooks et al.[78] are used to rule out the Weinberg values of the scattering lengths. On the contrary, this smallness of the lower bounds in all cases weakens the phenomenological interest of their present axiomatic values.

The upper bounds for $\epsilon=1$ are weak and surprisingly constraining for $\epsilon=0$. Bonnier has suggested that in order to obtain a better estimate of the scattering lengths one can stay rather far from threshold (450 Mev), then one has to reduce the errors.

It is a fortunate situation that on a definite set of coherent data, Bonnier's method[18] yields a model-independent measurement with true errors of scattering lengths.

3.7 NEW UPPER BOUNDS ON THE $\pi\pi$ S-WAVE SCATTERING LENGTHS.

3.8 Introduction.

Asymptotic bounds represent asymptotic properties and it is difficult to settle at what energy asymptotics really sets in. Therefore one can hardly over-emphasize the importance of devising rigorous bounds on closed curves in the complex plane of the energy.

In this work we derive rigorous phenomenological upper bounds on the s-wave $\pi\pi$ scattering lengths. On defining a central family of S,P,D,F phase shifts with associated errors in the energy range $0.45\text{Gev} \leq E_{c.m.} \leq 1.9\text{gev}$, we use the maximal amount of available experimental data as directly as possible. Also, proper care is taken of the consistency of the chosen phenomenology with general principles of unitarity, analyticity and crossing. As a result we have derived some new upper bounds on the $\pi\pi$ S-wave scattering lengths.

Starting from notation and normalization, sum-rule inequalities are derived. The zeros of the $\pi\pi$ scattering amplitudes and properties of analytic behaviour are discussed. The expression for the upper bounds is derived in detail. The bounds are computed in elastic ($0.45\text{Gev} \leq E_{c.m.} \leq 0.95\text{Gev}$) and in the broad energy ($0.45\text{Gev} \leq E_{c.m.} \leq 1.9\text{Gev}$) regions from $\pi^0\pi^0 \rightarrow \pi^0\pi^0$ and $\pi^+\pi^0 \rightarrow \pi^+\pi^0$ interactions. A suitable minimization program from NAG-routine manual is adopted to find the minima of the bounds with respect to parameters, for different combinations of $\pi\pi$ scattering lengths in the two regions. We compare our results with Bonnier's bounds [18]. The results show improvement over Bonnier's bounds. Finally, we compare our results with BFP [30] model results.

3.9 NOTATION AND NORMALIZATION.

The S-channel partial wave expansion of the s-channel isospin (I) $\pi\pi$ amplitude reads ($m_{\pi} = c = \hbar = 1$):

$$F^{(I)}(s, t, u) = \sum_{l=0}^{\infty} (2l+1) f_l^{(I)}(s) P_l(\cos\theta_s), \quad (3.9.1)$$

$$\text{where } f_l^{(I)}(s) = (\eta_l^I(s) e^{2i\delta_l^I(s)} - 1) / 2ip(s) \quad (3.9.2)$$

$$p(s) = \sqrt{\frac{s-4}{s}} \quad (3.9.3)$$

$$\sqrt{s} = E_{\text{c.m.}} \quad (3.9.4)$$

$$\cos\theta_s = 1 + 2t_0 / (s-4) \quad (3.9.5)$$

$$t_0 = 4m_{\pi}^2 = 4 \quad (3.9.6)$$

Partial wave amplitudes $f_l^I(s)$ for orbital angular momentum l and isospin I are related to the real phase-shift $\delta_l^I(s)$ and elasticity-coefficient $\eta_l^I(s)$ by equation (3.9.2).

The scattering lengths are defined as

$$a_l^I = \lim_{s \rightarrow 4^+} f_l^I(s) / k^{2l}, \quad a_0^I = f_0^I(4) \quad (3.9.7)$$

where k is the c.m. 3-momentum:

$$k^2 = \frac{1}{4} (s-4) \quad (3.9.8)$$

The s-wave scattering lengths are given by

$$a_l^I = f_0^I(4) = F^I(4, 0, 0), \quad l = 0, 2 \quad (3.9.9)$$

3.10 SUM RULE INEQUALITIES.

In the following we consider ($t=t_0=4m_{\pi}^2$) $\pi^0 \pi^0 \rightarrow \pi^0 \pi^0$ and $\pi^+ \pi^0 \rightarrow \pi^+ \pi^0$ elastic amplitudes and the corresponding s-wave scattering lengths:

$$F(s, 4)_{\pi^0 \pi^0 \rightarrow \pi^0 \pi^0} = 1/3. (F^0(s, 4) + 2F^2(s, 4)) = 1/3. (a_0 + 2a_2) \quad (3.10.1)$$

$$F(s, 4)_{\pi^+ \pi^0 \rightarrow \pi^+ \pi^0} = 1/2 (F^1(s, 4) + F^2(s, 4)) = 1/3. (a_0 - a_2) \quad (3.10.2)$$

these $s \leftrightarrow u$ crossing are analytic functions in the complex z-plane cut for $z \geq 1$, where

$$z = \left(\frac{2s + t_0 - 4m_{\pi}^2}{4m_{\pi}^2 + t_0} \right)^2 \quad (3.10.3)$$

On defining $G(z) \equiv F(s, t_0)$, it follows from the symmetry of amplitudes (3.10.1) and (3.10.2) under $s \leftrightarrow u$ interchange that $G(z)$ is a real analytic function of z in the whole complex z-plane cut from 1 to ∞ .

We then assume that on some part $[s_1, s_2]$ of the physical region ($4 < s_1 < s_2$), which through (3.10.3) is mapped onto $[z_1, z_2]$ ($1 < z_1 < z_2$), the available data are sufficiently reliable to yield upper and lower bounds on the real and imaginary parts of amplitudes. We can use this information in a powerful way in the framework of general principles.

First, we introduce the mapping:

$$w = A \left(\frac{z - z_1}{z - z_2} \right) \quad \text{with } A > 0 \quad (3.10.4)$$

We wish to map $w=0$ to $w=-\infty$ onto circumference of a unit disc D_v in v-plane such that the point z_1 goes to $w=0$ in the w-plane, and to $v=1$ in the v-plane; the point z_2 goes to $w=-\infty$ in the w-plane, and to $v=-1$ in the v-plane. Also, the point $z=0$ should go to $w = A \left(\frac{z_1}{z_2} \right)$ in the w-plane, and corresponding to $v=v_0$ ($-1 \leq v_0 \leq 1$) in the v-plane.

We can express this mapping by

$$v = \frac{B - \sqrt{w}}{B + \sqrt{w}}, \quad (3.10.5)$$

$$\text{where } v_0 = \frac{B - \sqrt{A \frac{z_1}{z_2}}}{B + \sqrt{A \frac{z_1}{z_2}}} \quad (3.10.6)$$

$$\text{Taking } A = z_2 / z_1, \text{ we have } v_0 = \frac{B-1}{B+1} \quad (3.10.7)$$

$$\text{hence, } B = \frac{1+v_0}{1-v_0}. \quad (3.10.8)$$

Substituting these values of A, B, w and v_0 into (3.10.5), we get

$$v = \frac{\frac{1+v_0}{1-v_0} - \sqrt{w}}{\frac{1+v_0}{1-v_0} + \sqrt{w}} = \frac{\frac{1+v_0}{1-v_0} - \sqrt{\frac{z_2}{z_1} \frac{(z-z_1)}{(z-z_2)}}}{\frac{1+v_0}{1-v_0} + \sqrt{\frac{z_2}{z_1} \frac{(z-z_1)}{(z-z_2)}}} \quad (3.10.9)$$

For threshold energy $z=1, \infty$ we have

$$v_T = \frac{\left(\frac{1+v_0}{1-v_0}\right) - \sqrt{\frac{z_2}{z_1} \left(\frac{1-z_1}{1-z_2}\right)}}{\left(\frac{1+v_0}{1-v_0}\right) + \sqrt{\frac{z_2}{z_1} \left(\frac{1-z_1}{1-z_2}\right)}} \quad (3.10.10)$$

$$v_{\infty} = \frac{\frac{1+v_0}{1-v_0} - \sqrt{\frac{z_2}{z_1}}}{\frac{1+v_0}{1-v_0} + \sqrt{\frac{z_2}{z_1}}} \quad (3.10.11)$$

The mappings are shown in figure 10.

3.11 ZERO OF THE AMPLITUDE.

If $G(0) > 0$ corresponding to the scattering length, we can prove that $G(z)$ has exactly one zero between $z=0$ and $z=-\infty$.

At a fixed $t=t_0=4m_{\text{II}}^2=4$, a dispersion relation for a scattering amplitude (symmetric in $s \leftrightarrow u$) can be written in the form:

$$F(s, t_0) = g(t_0) + \frac{s^2}{\text{II}} \int_4^{\infty} \frac{A_s(s', t_0) ds'}{s'^2(s'-s)} + \frac{u^2}{\text{II}} \int_4^{\infty} \frac{A_u(u', t_0) du'}{u'^2(u'-u)} \quad (3.11.1)$$

Introducing the variable

$$z = \left(\frac{2s+t_0-4m_{\text{II}}^2}{4m_{\text{II}}^2+t_0} \right)^2,$$

the right and left hand cuts may be folded to give

$$G(z) = G(z_0) + \frac{1}{\text{II}} \int_1^{\infty} \frac{(z-z_0) \text{Im} G(z') dz'}{(z'-z)(z'-z_0)}, \quad (3.11.2)$$

where z_0 is a pole, as shown in figure 11.

$$\text{or } G(z) = G(z_0) + \frac{1}{\text{II}} \int_1^{\infty} \text{Im} G(z') \left[\frac{1}{(z'-z)} - \frac{1}{z'-z_0} \right] dz' \quad (3.11.3)$$

As we have defined $G(z) \equiv F(s, 4)$, $\text{Im}G(z') = \text{Im}F(s, 4) \geq 0$, where

$1 < z < \infty$. Taking imaginary part of (3.11.3), we have

$$\begin{aligned} \text{Im}G(z) &= \text{Im}G(z_0) + \frac{1}{\text{II}} \int_1^{\infty} \text{Im}G(z') \text{Im}(1/(z'-z)) dz' - \\ &\quad - \frac{1}{\text{II}} \int_1^{\infty} \text{Im}G(z') \text{Im}(1/(z'-z_0)) dz' \end{aligned} \quad (3.11.4)$$

Now, $\text{Im}(1/(z'-z)) = \text{Im}(1/((z'-(x+iy))) = \text{Im}((z'-x+iy)/((z'-x-iy)(z'-x+iy)))$

$$= \text{Im}((z'-x+iy)/((z'-x)^2+y^2)) = y/((z'-x)^2+y^2). \quad (3.11.5a)$$

$$\text{Im}G(z_0) = \text{Im}G(x+i0) = 0 \quad (3.11.5b)$$

(74)

$$\begin{aligned} \operatorname{Im}\left(\frac{1}{z-z_0}\right) &= \operatorname{Im}\left(\frac{1}{z'-(x_0+i0)}\right) = \operatorname{Im}\left(\frac{z'+i0-x}{(z'-x-i0)(z'-x+i0)}\right) \\ &= \operatorname{Im}\left(\frac{z'-x+i0}{(z'-x)^2+0}\right) \quad \text{Or } \operatorname{Im}(1/(z'-z_0))=0. \end{aligned} \quad (3.11.5c)$$

Putting the results (3.11.5a,b,c) into (3.11.4), we get

$$\operatorname{Im} G(z) = \frac{1}{\pi} \int_1^{\infty} \operatorname{Im} G(z') \frac{y}{(z'-x)^2+y^2} dz' \quad (3.11.6)$$

so, we see that $\operatorname{Im} G(z)$ is positive or negative as y is positive or negative respectively:

$$y > 0, \operatorname{Im} G(z) > 0$$

$$y < 0, \operatorname{Im} G(z) < 0$$

Therefore $G(z)$ can only have zeros for z real, $-\infty < z < 1$.

Again,

$$\frac{dG(z)}{dz} = \frac{1}{\pi} \int_1^{\infty} \frac{\operatorname{Im} G(z')}{(z'-z)^2} dz' > 0 \quad (3.11.7)$$

As the denominator is always positive and $\operatorname{Im} G(z') > 0$ for $y > 0$, hence the integral is positive i.e.

$$\frac{dG(z)}{dz} > 0, \quad -\infty < z < 1. \quad (3.11.7a)$$

It is obvious that $G(z)$ can have only one zero on the cut.

On the other hand, if $G(z)$ has no zeros then

$$\frac{1}{G(z)} = \frac{1}{\pi} \int_1^{\infty} \frac{\operatorname{Im}(1/G(z'))}{(z'-z)} dz' = -\frac{1}{\pi} \int_1^{\infty} \frac{\operatorname{Im} G(z') dz'}{|G(z')|^2 (z'-z)} < 0 \quad (3.11.8)$$

As we are looking for upper bound to $G(0)$ so we can assume safely $G(0) > 0$,

Hence, $G(z)$ has exactly one zero between $z=0$ and $z=-\infty$.

Owing to our special mapping, we can define a function $G(z) \equiv g(v)$, which has exactly one zero between $v=v_0$ and $v=v_\infty$ at $v=v_1$ (say). Then we can construct a function

$$h(v) = g(v) \left[\frac{1-v_1 v}{v-v_1} \right], \quad (3.11.9)$$

which has no zeros inside the circle.

Also, on the circumference of the circle $|v|=1$, we have

$$|h(v)| = |g(v)| \quad (3.11.10)$$

3.12 DOMAIN OF ANALYTICITY OF THE FUNCTION.

We have defined the function

$$h(v) = g(v) \left[\frac{1-v_1 v}{v-v_1} \right]$$

and this function $h(v)$ has no zero inside the circle.

On the circumference of the unit circle, on which the experimental region is mapped, the absolute values of the functions $h(v)$ and $g(v)$ are the same:

$$|h(v)| = |g(v)| \quad \text{on } |v|=1 \quad (3.12.1)$$

Furthermore, we take log of the function $h(v)$, and introduce a new function $H(v)$ in its place

$$H(v) = \log h(v) \quad (3.12.2.)$$

As we have observed that $h(v)$ has no zeros inside circle, the new function $H(v)$ has the same domain of analyticity i.e. the cut circle D_v .

3.13 DERIVATION OF THE UPPER BOUND.

On using Cauchy theorem for $\frac{H(v)}{1-vv_0^*}$, keeping v_0^* constant, round the contour indicated in figure 10, we have

$$\begin{aligned} \frac{H(v)}{1-vv_0^*} = & \frac{1}{2\pi i} \int_{\text{circle}} \frac{H(v') dv'}{(1-v'v_0^*)(v'-v)} + \frac{1}{2\pi i} \int_{-1}^{v_\infty} \frac{\text{Disc } H(v') dv'}{(1-v'v_0^*)(v'-v)} \\ & + \frac{1}{2\pi i} \int_{v_T}^1 \frac{\text{Disc } H(v') dv'}{(1-v'v_0^*)(v'-v)} \end{aligned} \quad (3.13.1)$$

It is to be noted that $1-vv_0^* \neq 0$ inside or on circle, and $v_0 = v_0^*$ being real.

Taking $v=v_0$ which is real and introducing $v'=e^{i\alpha}$ for the unit circle, we can write (3.13.1) in the form

$$\begin{aligned} H(v_0) = & \frac{(1-v_0^2)}{2\pi} \int_0^{2\pi} \frac{H(e^{i\alpha}) e^{i\alpha} d\alpha}{(1-e^{i\alpha}v_0)(e^{i\alpha}-v_0)} \\ & + \frac{(1-v_0^2)}{2\pi i} \int_{-1}^{v_\infty} \frac{\text{Disc } H(v') dv'}{(1-v'v_0)(v'-v_0)} \\ & + \frac{(1-v_0^2)}{2\pi i} \int_{v_T}^1 \frac{\text{Disc } H(v') dv'}{(1-v'v_0)(v'-v_0)} \end{aligned} \quad (3.13.2)$$

Now the real parts give

$$\begin{aligned} \log |h(v_0)| = \text{Re } H(v_0) = & \frac{(1-v_0^2)}{2\pi} \int_0^{2\pi} \text{Re } H(e^{i\alpha}) \text{Re} \left[\frac{e^{i\alpha}}{(1-e^{i\alpha}v_0)(e^{i\alpha}-v_0)} \right] d\alpha \\ & - \frac{(1-v_0^2)}{2\pi} \int_0^{2\pi} \text{Im } H(e^{i\alpha}) \text{Im} \left[\frac{e^{i\alpha}}{(1-e^{i\alpha}v_0)(e^{i\alpha}-v_0)} \right] d\alpha \\ & + (1-v_0^2)/2\pi \left[\int_{-1}^{v_\infty} + \int_{v_T}^1 \right] \left\{ \frac{\text{Disc } \text{Im } H(v') dv'}{(1-v'v_0)(v'-v_0)} \right\} \end{aligned} \quad (3.13.3)$$

As we are interested in the real parts, the integrand of the second integral

$$\text{Im} \left[\frac{e^{i\alpha}}{(1-e^{i\alpha}v_0)(e^{i\alpha}-v_0)} \right] = 0 \quad (3.13.4)$$

over the limit of integration. The second integral over the limit of integration vanishes and we have,

$$\begin{aligned} \log |h(v_0)| &= \frac{(1-v_0^2)}{2\pi} \int_0^{2\pi} \frac{\log |h(e^{i\alpha})| d\alpha}{1+v_0^2-2v_0 \cos \alpha} \\ &+ \frac{(1-v_0^2)}{2\pi} \left[\int_{-1}^v + \int_{v_T}^1 \right] \left\{ \frac{\text{Disc Im } H(v') dv'}{(1-v'v_0)(v'-v_0)} \right\} \end{aligned} \quad (3.13.5)$$

Now $\text{Im } H(v'+i\epsilon) = \text{Arg } h(v+i\epsilon)$ and at the beginning of the right hand cut ($v=v_T-\epsilon$), we have

$$h(v) = \left[\frac{1-v_1v}{v-v_1} \right] g(v) > 0, \text{ since } g(v) > 0. \quad (3.13.6)$$

For $v=v_T+\epsilon+i\epsilon$ with $\epsilon > 0$, $\text{Im } h(v) > 0$ and $\text{Re } h(v) > 0$ from continuity so that $\pi/2 > \text{Argh}(v) > 0$.

As $\text{Re}(v)$ increases $\text{Re}h(v)$ may change sign but $\text{Im}h(v) > 0$ since $\text{Im}g(v) > 0$, from unitarity condition: $\text{Im } F(s,4) > 0$.

Therefore, $\pi > \text{Argh}(v+i\epsilon) > 0$. Similarly, for $v=\text{Re}v-i\epsilon$, we have $0 > \text{arg } h(v) > -\pi$. Also, from reality of $h(z)$, $h(v+i\epsilon) = h^*(v-i\epsilon)$, then for the range $1 > v > v_T$, $\text{Arg } h(v+i\epsilon) = -\text{Argh}(v-i\epsilon)$.

$$\begin{aligned} \text{Disc Im } H(v') &= \text{Arg } h(v+i\epsilon) - \text{Argh}(v-i\epsilon) = 2\text{Argh}(v+i\epsilon) \\ &= 2\text{Arg } g(v+i\epsilon). \end{aligned} \quad (3.13.8a)$$

Hence, on the right hand cut, we can replace

$$\text{Disc Im } H(v') = 2\text{Arg } g(v+i\epsilon) \quad (3.13.7)$$

Similarly, on the left hand cut of the Disc- D_v ($-1 \leq v \leq v_\infty$) we

$$\begin{aligned} \text{have } \text{Disc Im } H(v') &= \text{Arg } h(v+i\epsilon) - \text{Arg } h(v-i\epsilon) = 2\text{Arg } h(v+i\epsilon) \\ &= 2\text{Arg} \left\{ \left[\frac{1-v(v+i\epsilon)}{v+i\epsilon-v_1} \right] g(v+i\epsilon) \right\} \end{aligned}$$

$$\text{or Disc Im } H(v') = -2 \text{Arg } g(v+i\epsilon) \quad (3.13.8b)$$

And on both cuts of the disc D_v , we have

$$0 \leq \text{Arg } g(v+i\epsilon) \leq \Pi, \quad (3.13.9)$$

since $\text{Im } g(v+i\epsilon) > 0$.

Now, substituting the results of Disc Im $H(v')$ from (3.13.8a) and (3.13.8b) into the second integrals of (3.13.5), we have

$$\begin{aligned} & \frac{(1-v_0^2)}{2\Pi} \left[\int_{-1}^{\infty} + \int_{v_T}^1 \right] \left\{ \frac{\text{Disc Im } H(v') dv'}{(1-v'v_0)(v'-v_0)} \right\} \\ &= \frac{(1-v_0^2)}{2\Pi} \left[\int_{-1}^{\infty} + \int_{v_T}^1 \right] \left\{ \frac{2 \text{Arg } g(v'+i\epsilon) dv'}{(1-v'v_0)|v'-v_0|} \right\} \end{aligned} \quad (3.13.10)$$

On the circumference of unitary circle:

$$\begin{aligned} \log |h(e^{i\alpha})| &= \log |g(e^{i\alpha})|, \text{ but in the general case} \\ \log |h(v_0)| &= \log \left| \left[\frac{1-v_1v_0}{v_0-v_1} \right] g(v_0) \right| \end{aligned} \quad (3.13.11)$$

substituting (3.13.10) and (3.13.11) in (3.13.5), we get

$$\begin{aligned} \log \left| \left[\frac{1-v_1v_0}{v_0-v_1} \right] g(v_0) \right| &= \frac{(1-v_0^2)}{\Pi} \int_0^{\Pi} \frac{\log |g(e^{i\alpha})| d\alpha}{1+v_0^2-2v_0 \cos \alpha} + \\ &+ \frac{(1-v_0^2)}{\Pi} \left[\int_{-1}^{\infty} + \int_{v_T}^1 \right] \left\{ \frac{\text{Arg } g(v'+i\epsilon) dv'}{(1-v'v_0)|v'-v_0|} \right\} \end{aligned} \quad (3.13.12)$$

We have defined $G(z) = F(s, t_0) = F(s, 4) = g(v)$,

$$\text{so } \text{Arg } g(v) = \tan^{-1} \left[\frac{\text{Im } F(s, 4)}{\text{Re } F(s, 4)} \right] \quad (3.13.13)$$

and on the circumference of the circle

$$|g(e^{i\alpha})| = |F(s, 4)| \quad (3.13.14)$$

Since the zero occurs between $z=0$ and $z=-\infty$, we can write (3.13.12)

in the form:

$$g(v_0) \leq \text{Max}_{v_\infty < v_1 < v_0} \left[\frac{v_0 - v_1}{1 - v_1 v_0} \right] \text{Exp} \left\{ \frac{(1 - v_0^2)}{\Pi} \int_0^\Pi \frac{\text{LOG} |g(e^{i\alpha})| d\alpha}{(1 + v_0^2 - 2v_0 \cos \alpha)} + \right. \\ \left. \frac{(1 - v_0^2)}{\Pi} \left[\int_{-1}^{v_\infty} + \int_{v_T}^1 \right] \left\{ \frac{\text{Argg}(v' + i\epsilon) dv'}{(1 - v'v_0) |v' - v_0|} \right\} \right\} \quad (3.13.15)$$

$$\text{Now Max}_{v_\infty < v_1 < v_0} \left[\frac{v_0 - v_1}{1 - v_1 v_0} \right] = \frac{v_0 - v_\infty}{1 - v_0 v_\infty} \quad (3.13.16)$$

Hence, we obtain the expression for the upper bound

$$g(v_0) \leq \left[\frac{v_0 - v_\infty}{1 - v_\infty v_0} \right] \text{Exp} \left\{ \frac{(1 - v_0^2)}{\Pi} \int_0^\Pi \frac{\log |g(e^{i\alpha})| d\alpha}{[1 + v_0^2 - 2v_0 \cos \alpha]} + \right. \\ \left. + \frac{(1 - v_0^2)}{\Pi} \left[\int_{-1}^{v_\infty} + \int_{v_T}^1 \right] \left\{ \frac{\text{Arg} g(v' + i\epsilon) dv'}{(1 - v'v_0) |v' - v_0|} \right\} \right\} \quad (3.13.17)$$

(79a)

Later we will try to improve our bounds by the replacement $g(v) \rightarrow g_1(v) = g(v) + \sum_{i=0}^M A_{i+1} (v-v_0)^i$, where A_i are arbitrary real parameters adjusted to give the best bounds. However, $g_1(v)$ may have more zeros than $g(v)$ in the unit circle. We will show that the inequality (3.13.17) still holds when $g(v)$ is replaced by $g_1(v)$.

We have to consider two interesting cases (i) if there are N number of zeros introduced between $v=v_0$ and $v=v_\infty$, (ii) if there are N_1 -pairs of complex conjugate zeros inside the circle as well as N real zeros.

(i) Firstly, we suppose that $g_1(v)$ has N real zeros between $v=v_0$ and $v=v_\infty$ at $v=v_1, v_2, v_3, \dots, v_N$ (say). Then we can construct a function

$$h(v) = g_1(v) \prod_{i=1}^N \left[\frac{1-v_i v}{v-v_i} \right] \quad (3.13.18)$$

which has no zeros inside the circle and on the circumference of the circle $|v|=1$, we have $|h(v)| = |g(v)|$. The function $H(v) = \log h(v)$ has the same domain of analyticity as $h(v)$ i.e. the cut circle D_v .

Now $\text{Im } H(v+i\epsilon) = \text{Arg } h(v+i\epsilon)$ and at the beginning of the right hand cut ($v=v_T - \epsilon$), we have

$h(v) = \prod_{i=1}^N \left[\frac{1-v_i v}{v-v_i} \right] g_1(v) > 0$, since we can assume $g_1(v) > 0$ otherwise we would get a better bound. For $v=v_T + \epsilon + i\epsilon$ with $\epsilon > 0$, $\text{Im } h(v) > 0$ and $\text{Re } h(v) > 0$ from continuity so that $\pi \geq \text{Arg } h(v+i\epsilon)$.

On the left hand cut of the disc ($-1 \leq v \leq v_\infty$) we have

$$\begin{aligned} \text{Disc } H(v) &= \text{Arg } h(v+i\epsilon) - \text{Arg } h(v-i\epsilon) = 2\text{Arg } h(v+i\epsilon) \\ &= 2\text{Arg} \left\{ \left[\prod_{i=1}^N \frac{1-v_i(v+i\epsilon)}{v+i\epsilon-v_i} \right] g_1(v+i\epsilon) \right\} \\ &= (-1)^N 2\text{Arg } g_1(v+i\epsilon) \end{aligned} \quad (3.13.19)$$

On the circumference of unitary circle $\log |h(e^{i\alpha})| = \log |g_1(e^{i\alpha})|$,

while at $v=v_0$,

$$\log |h(v_0)| = \log \left| \left[\prod_{i=1}^N \frac{1-v_i v_0}{v_0-v_i} \right] g_1(v_0) \right| \quad (3.13.20)$$

So, we can replace (3.13.12) by

(79b)

$$\log \left| \left[\prod_{i=1}^N \frac{1-v_i v_0}{v_0 - v_i} \right] g_1(v_0) \right| = \frac{(1-v_0^2)}{\Pi} \int_0^{\Pi} \frac{\log |g_1(e^{i\lambda})| d\lambda}{1+v_0^2 - 2v_0 \cos \lambda} +$$

$$+ \frac{(1-v_0^2)}{\Pi} \left[\int_{-1}^{v_0} \frac{(-1)^{N+1} \text{Arg } g_1(v'+ie) dv'}{(1-v'v_0) |v'-v_0|} + \int_{v_T}^1 \frac{\text{Arg } g_1(v'+ie) dv'}{(1-v'v_0) |v'-v_0|} \right]$$

$$\text{or } g_1(v_0) \leq \text{Max.} \left| \prod_{i=1}^N \frac{v_0 - v_i}{1 - v_i v_0} \right| \cdot$$

$$\text{Exp} \left\{ \frac{(1-v_0^2)}{\Pi} \int_0^{\Pi} \frac{\log |g_1(e^{i\lambda})|}{(1+v_0^2 - 2v_0 \cos \lambda)} + \frac{(1-v_0^2)}{\Pi} \left[\int_{-1}^{v_0} \frac{(-1)^{N+1} \text{Arg } g_1(v'+ie) dv'}{(1-v'v_0) |v'-v_0|} + \int_{v_T}^1 \frac{\text{Arg } g_1(v'+ie) dv'}{(1-v'v_0) |v'-v_0|} \right] \right\} \quad (3.13.21)$$

$$\text{Now, } \text{Max.} \left[\prod_{i=1}^N \frac{v_0 - v_i}{1 - v_i v_0} \right] = \left[\frac{v_0 - v_{\infty}}{1 - v_0 v_{\infty}} \right]^N \quad (3.13.22)$$

Hence, we obtain the expression for the upper bound

$$g_1(v_0) \leq \left[\frac{v_0 - v_{\infty}}{1 - v_0 v_{\infty}} \right]^N \text{Exp} \left\{ \frac{(1-v_0^2)}{\Pi} \int_0^{\Pi} \frac{\log |g_1(e^{i\lambda})|}{[1+v_0^2 - 2v_0 \cos \lambda]} + \frac{(1-v_0^2)}{\Pi} \left[\int_{-1}^{v_0} \frac{(-1)^{N+1} \text{Arg } g_1(v'+ie) dv'}{(1-v'v_0) |v'-v_0|} + \int_{v_T}^1 \frac{\text{Arg } g_1(v'+ie) dv'}{(1-v'v_0) |v'-v_0|} \right] \right\} \quad (3.13.23)$$

$$\text{If } N > 1, \left[\frac{v_0 - v_\infty}{1 - v_\infty v_0} \right]^N < \left[\frac{v_0 - v_\infty}{1 - v_\infty v_0} \right] \quad (3.13.24)$$

$$\text{and } (-1)^{N+1} \text{Arg } g_1(v'+ie) \leq \text{Arg } g_1(v'+ie), \quad (3.13.25)$$

and consequently, we get lower value of the bound numerically.

As we are looking for the upper bound, the inequality (3.13.17) holds when $g(v)$ is replaced by $g_1(v)$.

(ii) If as well as the above real zeros $g_1(v)$ has N_1 pairs of complex zeros $v_i, \bar{v}_i, i=N+1, N+2, \dots, N+N_1$, then we construct the function,

$$h(v) = g_1(v) \prod_{i=N+1}^{N_1+N} \left[\frac{1-v_i v}{v-v_i} \right] \left[\frac{1-\bar{v}_i v}{v-\bar{v}_i} \right] \prod_{i=1}^N \left(\frac{1-v_i v}{v-v_i} \right) \quad (3.13.26)$$

which has no zeros in the unit circle.

Now $\left[\frac{1-v_i v}{v-v_i} \right] \left[\frac{1-\bar{v}_i v}{v-\bar{v}_i} \right]$ is real positive when v real so that for

$-1 \leq v \leq v_\infty$ we again have

$$\text{disc } H(v) = (-1)^{N_1+N} 2 \text{Arg } g_1(v+ie) \text{ and for } v_T \leq v \leq 1,$$

$$\text{disc } H(v) = 2 \text{Arg } g_1(v+ie).$$

$$\text{Also on the unit circle } \left| \frac{1-v_i v}{v-v_i} \right| \left| \frac{1-\bar{v}_i v}{v-\bar{v}_i} \right| = 1.$$

So we can this time replace (3.13.12) by,

$$\begin{aligned} & \log \left| \left[\prod_{i=1}^N \left(\frac{1-v_i v_0}{v_0 - v_i} \right) \right] \prod_{i=N+1}^{N_1+N} \left(\frac{1-v_i v_0}{v_0 - v_i} \right) \left(\frac{1-\bar{v}_i v_0}{v_0 - \bar{v}_i} \right) g_1(v_0) \right| \\ &= \frac{(1-v_0^2)}{\pi} \int_0^\pi \frac{\log |g_1(e^{i\lambda})| d\lambda}{1+v_0^2 - 2v_0 \cos \lambda} + \frac{(1-v_0^2)}{\pi} \left[\int_{-1}^{v_\infty} \frac{dv' (-1)^{N_1+N} \text{Arg } g_1(v'_0)}{(1-v'v_0) |v'-v_0|} \right. \\ & \left. + \int_{v_T}^1 \frac{\text{Arg } g_1(v'+ie) dv'}{(1-v'v_0) |v'-v_0|} \right] \quad (3.13.27) \end{aligned}$$

(79d)

Exponentiating and using the fact that $\left| \frac{(v_i - v_0)(\bar{v}_i - v_0)}{(1 - v_i v_0)(1 - \bar{v}_i v_0)} \right| \leq 1$

for all v_i inside unit circle, (3.13.23) again holds so that the inequality (3.13.17) holds when $g(v)$ is replaced by $g_1(v)$.

3.14 NUMERICAL CALCULATIONS.

We calculate $|g(e^{i\alpha})| = |F(s,4)|$ from phase shifts, and so $\int_0^{\Pi} \frac{\log |g(e^{i\alpha})| d\alpha}{(1+v_0^2 - 2v_0 \cos \alpha)}$ can be calculated.

Above $\sqrt{s} \sim 2\text{Gev}$, $\text{Im } F(s,4) \gg \text{Re } F(s,4)$ so in this region $\text{Arg } g(v'+i\epsilon) \approx \Pi/2$, and we can evaluate the integral

$\int_{-1}^v \frac{\text{Arg } g(v'+i\epsilon) dv'}{(1-v'v_0)|v'-v_0|}$ by varying the arg F between

0 to $\Pi/2$ in the high energy region ($\sqrt{s} \sim 2\text{Gev}$).

Finally, we need an estimate on upper bound for

$\int_{v_T}^1 \frac{\text{Arg } g(v'+i\epsilon) dv'}{(1-v'v_0)|v'-v_0|}$. The amplitude can be expanded

in terms of partial waves in the two regions. In the region $4 \leq s < [500 \text{ Mev}]^2$, $\text{Re } f_1^I(s) \sim (s-4)^{(2l+1)/2}$ and $\text{Im } f_1^I(s) \sim (s-4)^{2l+1}$. Hence we can approximate the ratio

$$\frac{\text{Im } F^I(s,4)}{\text{Re } F^I(s,4)} \approx \frac{\text{Im } f_0^I(s)}{\sum_{l=0}^{\infty} (2l+1) \text{Re } f_1^I(s) P_1(1+\frac{8}{s-4})} \quad (3.14.1)$$

For certain isospin combinations, $\text{Limit}_{s \rightarrow 4} \frac{\text{Re } f_1^I(s)}{(s-4)^{(2l+1)/2}} = \mathcal{L}_1 > 0; l=2,4,8,\dots$ (3.14.2)

We expect from Froissart-Gribov formula that $\text{Re } f_1^I(s) > 0$ in the range $[500 \text{ Mev}]^2 \gg s > 4$ for $l=2,4,8,\dots$

Also, we assume $F(4,0) = \mathcal{L}_0 = \frac{2f_0^I(4)}{(\frac{s-4}{4})^{\frac{1}{2}}} > 0$, and hence

$$\frac{\text{Im } F^I(s,4)}{\text{Re } F^I(s,4)} \leq \frac{\text{Im } f_0^I(s)}{\text{Re } f_0^I(s)}, \quad 4 \leq s < [500 \text{ Mev}]^2 \quad (3.14.3)$$

Now, $f_0(s) = 1/3 \cdot (f_0^0(s) + 2f_0^2(s))$ and $f_0^I(s) \simeq e^{i\delta_0^I} \sin \delta_0^I$ and $|\delta_0^0| > |\delta_0^2|$, we expect the order $f_0(s) \sim 1/3 \cdot (f_0^0(s))$. Considering these results, we obtain the ratio

$$\text{Arg } F(s, 4) = \tan^{-1} \frac{\text{Im } F(s, 4)}{\text{Re } F(s, 4)} \leq \tan^{-1} \frac{\text{Im } f_0^0(s)}{\text{Re } f_0^0(s)} \approx \delta_0^0(s) \quad (3.4.4)$$

Looking at the data, it seems to be a good approximation to take $\delta_0^0(s) \leq \pi/6$ for $4 \leq s \leq (500 \text{ Mev})^2$. Then in the low energy region: $0 \leq \text{Arg } F(s, 4) \leq \pi/6$ and in the high energy region: $0 < \text{Arg } F(s, 4) \leq \pi/2$ seem to be true[†]. If one does not want to make such assumptions rigorously, we can apply $0 \leq \text{Arg } F(s, 4) \leq \pi$, and can get bound to

$$\int_{v_T}^1 \frac{\text{Arg } g(v' + i\epsilon) dv'}{(1 - v'v_0) |v' - v_0|}$$

Putting all these conclusions together, we can evaluate the upper bounds on the s-wave scattering lengths:

$$g(v_0) \leq \left[\frac{v_0 - v_\infty}{1 - v_\infty v_0} \right] \text{Exp} \left\{ \frac{(1 - v_0^2)}{\pi} \int_0^\pi \frac{\log |g(e^{i\alpha})| d\alpha}{[1 + v_0^2 - 2v_0 \cos \alpha]} + \frac{(1 - v_0^2)}{\pi} \left[\int_{-1}^{v_\infty} + \int_{v_T}^1 \right] \frac{\text{Arg } g(v' + i\epsilon) dv'}{(1 - v'v_0) |v' - v_0|} \right\} \quad (3.4.5)$$

[†] We define $\text{Arg } F(s, 4) = \text{Arg } g(v) \equiv \text{GR}$ for computational purpose and select the set of arguments $\{\text{GR} = \pi/6, \text{GR} = \pi/2\}$, $\{\text{GR} = \pi/6, \text{GR} = \pi\}$, $\{\text{GR} = \pi/2, \text{GR} = \pi\}$ and $\{\text{GR} = \pi, \text{GR} = \pi\}$ according as $\{v \equiv X > VI \equiv v_0, X < VI\}$ for the function $g(v) \equiv F(s, 4)$. The above arguments suggest that $0 \leq \text{Arg } F(s, 4) \leq \pi/6$ do not apply to the case $\pi^+ \pi^0 \rightarrow \pi^+ \pi^0$ since in that case the $I=1$ contributions to $\text{Re } F(s, 4)$ can be negative.

We replace

$$g(v) \rightarrow g(v) + A_1 + \sum_{i=1}^N A_{i+1} (v-v_0)^i \equiv h(v) \quad (3.14.6)$$

so that the central wave has the upper bound

$$|h(v)| \leq |h_c(v)| + |\Delta g(v)| \quad (3.14.7)$$

The first expansion coefficient A_1 should be selected to

give an upper bound $|g(v_0) + A_1| \leq M(A_1)$, and

$$0 \leq g(v_0) \leq M(A_1) - A_1.$$

The amplitude has a band of variation on the plot of energy (E) against phase (d_0):

$$F(s, 4) = F_c \pm \epsilon \Delta F, \quad (3.14.8)$$

where F_c corresponds to the central case with positive and negative errors. The integral over the bound involves lots of internal cancellations, which lead to stable upper bounds.

In order to improve the upper bounds further, we include four coefficients to replace

$$g(e^{i\alpha}) \rightarrow g(v) + A_1 + A_2(v-v_0) + A_3(v-v_0)^2 + A_4(v-v_0)^3 \quad (3.14.9)$$

in (3.14.5). On the other hand, the arguments (GR) of the amplitude are varied between sets:

$\{GR = \pi, GR = \pi/2\}$ and $\{GR = \pi, GR = \pi\}$ according as

$\{X > VI = v_0 \text{ or } X < VI\}$ respectively. The last set should give the

worst values; whereas the first set should give the best

values. The set of arguments are selected accordingly.

We can not use the more restrictive bounds $0 \leq \text{Arg } g_1(v' + ie) \leq \pi/6$ in this case because the real part of $g_1(v)$ on the cut is modified by the addition of a real polynomial.

We keep z_1 fixed at value corresponding to

$\sqrt{s} = 450$ Mev, and vary two parameters (v_0 and z_2). This z_2 is varied from values corresponding to $\sqrt{s} = 950$ Mev to 1900 Mev at 100 Mev intervals. Also, v_0 is varied from $v_0 = -0.9$ to 0.5 at intervals 0.1. The first two coefficients A_1 and A_2 are varied from 0.05 to 1.0 at intervals 0.05; and -0.05 to -0.096 at intervals -0.05 respectively.

To find the amplitudes by interpolation, we apply inverse mapping:

$$v = \frac{B\sqrt{w}}{B+\sqrt{w}} = e^{i\kappa} \text{ on unitary circle.} \quad (3.14.9)$$

$$\text{or } vB + v\sqrt{w} = B - \sqrt{w}$$

$$\text{or } \sqrt{w} = \left(\frac{1-v}{1+v} \right) B$$

$$w = \left[\frac{(1-v)}{(1+v)} B \right]^2 = A \cdot \frac{z-z_1}{z-z_2}, \quad A > 0. \quad (3.14.10)$$

$$\text{Hence } z = \frac{Az_1 - wz_2}{A-w} = \frac{\frac{z_2}{z_1} z_1 - wz_2}{\frac{z_2}{z_1} - w} = \frac{z_1 z_2 (1-w)}{z_2^{-wz_1}}$$

$$z = \left(\frac{(2s+t_0-4)}{4+t_0} \right)^2 = (2s/8)^2 = (s/4)^2, \quad t_0 = 4. \quad (3.14.11)$$

$$z_1 = (s_1/4)^2, \quad z_2 = (s_2/4)^2 \quad (3.14.12)$$

So, if we are given a $v(e^{i\kappa})$ point on the unitary circle, we have to follow the following order of calculations:

$$(i) \quad B = \frac{1+v_0}{1-v_0} \quad (3.14.13a)$$

$$(ii) \quad w = \left[\frac{1-v}{1+v} B \right]^2, \quad v = \frac{B-\sqrt{w}}{B+\sqrt{w}} \quad (3.14.13b)$$

$$(iii) \quad z = \frac{z_1 z_2 (1-w)}{z_2^{-wz_1}} \quad (3.14.13c)$$

$$(iv) \quad s = \frac{(4+t_0)\sqrt{z} - (t_0-4)}{2} \quad (3.14.13d)$$

(v) Given this s , we calculate the amplitude $F(s, 4) \equiv G(Y)$ by interpolation.

3.15 UPPER BOUNDS IN THE ELASTIC REGION.

In order to include errors in phase shift measurement, Δd_1^I , we suppose that they are all correlated to give error in total amplitude in the elastic region:

$$F^I = \sum_{l=0,1} \left| \frac{\partial F}{\partial d_1^I} \right| (\Delta d_1^I), \text{ where } d_1^I \text{ are in radians. (3.15.1)}$$

$$\text{Hence, } \Delta F^I = \sum_{l=0,1} e^{2i d_1^I} |P_1(\cos \theta_3)| |\Delta d_1^I| \quad (3.15.2)$$

Taking the right combinations for $\Pi^O + \Pi^O \rightarrow \Pi^O + \Pi^O$ scattering, we have error,

$$\Delta F' \equiv (1/3 \Delta F^O + 2/3 \Delta F^2) = 1/3 |e^{2i d_0^O}| |P_0(\cos \theta_3)| (\Delta d_0^O) + 2/3 |e^{2i d_0^2}| |P_0(\cos \theta_3)| (\Delta d_0^2) \quad (3.15.3)$$

Now, we replace

$$|g(e^{i\alpha})| \rightarrow |g(v) + A_1 + A_2(v-v_0) + A_3(v-v_0)^2 + A_4(v-v_0)^3| + \epsilon \Delta F',$$

where $\epsilon = 0, 0.5$ and 1 . (3.15.4)

Consequently, we have

$$\text{ANS1} \equiv \left[\frac{v_0 - v_\infty}{1 - v_\infty v_0} \right] \text{Exp} \left\{ \frac{(1-v_0^2)}{\Pi} \right\}$$

$$\int_0^\Pi \log \left\{ |g(e^{i\alpha}) + A_1 + A_2(v-v_0) + A_3(v-v_0)^2 + A_4(v-v_0)^3| + \epsilon \Delta F' \right\} d\alpha$$

$$(1 + v_0^2 - 2v_0 \cos \alpha)$$

$$\text{ANS2} \equiv \left[\frac{v_0 - v_\infty}{1 - v_\infty v_0} \right] \text{Exp} \left\{ \frac{(1-v_0^2)}{\Pi} \int_{-1}^{v_\infty} \frac{\text{Arg } g_1(v'+i\epsilon) dv'}{(1-v'v_0) |v'-v_0|} \right\} \quad (3.15.5)$$

$$(3.15.6)$$

$$\text{ANS3} \equiv \left[\frac{v_0 - v_\infty}{1 - v_\infty v_0} \right] \text{Exp} \left\{ \frac{(1-v_0^2)}{\Pi} \int_{v_T}^1 \frac{\text{Arg } g_1(v'+i\epsilon) dv'}{(1-v'v_0) |v'-v_0|} \right\} \quad (3.15.7)$$

$$g(v_0) \leq \text{FINANS.} = \text{ANS1} + \text{ANS2} + \text{ANS3}$$

$$(3.15.8)$$

So, equation (3.15.8) computes equation (3.14.5) to give the upper bounds in the elastic region ($0.45 \text{ GeV} \leq E_{c.m.} < 0.95 \text{ GeV}$). For the function (3.15.4), we have $0 < d < \pi$ for $v_T < v < 1$.

The data for central values and errors used, to compute the bounds for the real and imaginary parts of the amplitude, are given in table 1 [18]. The phase shifts are given in degrees and the inelasticities fulfil

$$\sup \{ 0, \eta - \Delta\eta \} \leq \eta \leq \inf \{ 1, \eta + \Delta\eta \}.$$

The computational results of upper bounds are given in table 2.

For $\pi^+ + \pi^0 \rightarrow \pi^+ + \pi^0$ scattering, we take the combination $F_{\pi^+ \pi^0 \rightarrow \pi^+ \pi^0}(s, 4) = \frac{1}{2} [F^1 + F^2]$. If errors are correlated,

$$\Delta F^I = \sum_{l=0,1} |e^{2i\delta_l^I}| |P_l(\cos\theta_s)| (\Delta d_l^I) \quad (3.15.9)$$

$$\Delta F^1 = |e^{2i\delta_1^1}| P_1(\cos\theta_s) (\Delta d_1^1)$$

$$\Delta F^2 = |e^{2i\delta_0^2}| P_0(\cos\theta_s) (\Delta d_0^2)$$

$$\therefore \Delta F' = \frac{1}{2} (\Delta F^1 + \Delta F^2) = \frac{1}{2} |e^{2i\delta_1^1}| P_1(\cos\theta_s) (\Delta d_1^1) + \frac{1}{2} |e^{2i\delta_0^2}| P_0(\cos\theta_s) (\Delta d_0^2) \quad (3.15.10)$$

The amplitude should be successively replaced by

$$F_{\pi^+ \pi^0 \rightarrow \pi^+ \pi^0}(s, 4) \equiv g(e^{i\alpha})$$

$$|g(e^{i\alpha})| \rightarrow |g(v) + A_1 + A_2(v - v_0) + A_3(v - v_0)^2 + A_4(v - v_0)^3| \equiv \epsilon \Delta F', \quad (3.15.11)$$

$\epsilon = 0, 0.5$ and 1.0 . The computational results of upper bounds are given in table 3. The sets of arguments are $\{\pi, \pi/2\}$ and $\{\pi, \pi\}$ according as $\{X > v_0, X < v_0\}$ for this combination.

- Table 1

$E_{c.m.}$ Gev	0.45	0.5	0.55	0.6	0.65	0.7	0.75	0.8	0.85	0.9	0.95
d_0^0	40 \pm 9	44 \pm 9	50 \pm 9	58 \pm 9	63 \pm 11	70 \pm 11	75 \pm 11	82 \pm 11	89 \pm 13	97 \pm 14	130 \pm 36
$-d_0^2$	7 \pm 3	10 \pm 4	12 \pm 4	14 \pm 5	15 \pm 5	16 \pm 5	17 \pm 5	18 \pm 7	19 \pm 7	20 \pm 7	20 \pm 7
d_1^1	3.5 \pm 1	6.5 \pm 1.5	10 \pm 1.5	15.5 \pm 1.5	25 \pm 1.5	42 \pm 2	75 \pm 2.5	115 \pm 3.5	140 \pm 2.5	150 \pm 2.5	154 \pm 2.5
$E_{c.m.}$ Gev	1.0	1.05	1.10	1.2	1.3	1.4	1.5	1.6	1.7	1.8	1.9
d_0^0	180 \pm 60	240 \pm 20	250 \pm 15	270 \pm 15	290 \pm 15	312 \pm 15	332 \pm 15	358 \pm 15	380 \pm 15	400 \pm 15	405 \pm 15
n_0^0	0.25 \pm 0.25	0.5 \pm 0.25	0.7 \pm 0.25	0.9 \pm 0.3	0.95 \pm 0.3	0.95 \pm 0.3	0.9 \pm 0.3	0.85 \pm 0.3	0.75 \pm 0.3	0.7 \pm 0.3	0.6 \pm 0.3
$-d_0^2$	20 \pm 7	20 \pm 7	21 \pm 7	21 \pm 9	22 \pm 9	22 \pm 11	23 \pm 11	23 \pm 11	24 \pm 15	25 \pm 15	25 \pm 15
n_0^2	1	1	1	1	1	1	1	1	1	1	1
d_1^1	154 \pm 10	157 \pm 10	159 \pm 10	163 \pm 11	165 \pm 11	166 \pm 11	167 \pm 11	168 \pm 11	169 \pm 11	169 \pm 11	169 \pm 11
n_1^1	1 \pm 0.15	1.0 \pm 0.15	0.95 \pm 0.15	0.95 \pm 0.15	0.9 \pm 0.15	0.85 \pm 0.15	0.7 \pm 0.15	0.5 \pm 0.15	0.85 \pm 0.15	1 \pm 0.15	1 \pm 0.15
d_2^0	8 \pm 5	12 \pm 6	17 \pm 6	42 \pm 10	100 \pm 13	142 \pm 11	157 \pm 11	160 \pm 11	160 \pm 11	160 \pm 11	160 \pm 11
n_2^0	1 \pm 0.2	1 \pm 0.2	1.0 \pm 0.2	0.9 \pm 0.2	0.65 \pm 0.2	0.75 \pm 0.2	0.82 \pm 0.2	0.86 \pm 0.2	0.9 \pm 0.2	0.94 \pm 0.2	0.98 \pm 0.2
d_3^1	1 \pm 3	1 \pm 3	2 \pm 3	2 \pm 3	3 \pm 3	4 \pm 3	6 \pm 3	10 \pm 3	5 \pm 3	-10 \pm 3	-8 \pm 3
n_3^1	1 \pm 0.5	1 \pm 0.5	1 \pm 0.5	1 \pm 0.5	1 \pm 0.5	1 \pm 0.5	0.92 \pm 0.5	0.8 \pm 0.5	0.5 \pm 0.5	0.7 \pm 0.5	0.9 \pm 0.5

TABLE 2:

Funct.	ϵ	$\frac{X \gg VI}{XVI} \frac{GR}{\epsilon, R}$	v_0	A_1	A_2	A_3	Upper Bounds (Minimum)
$ g(u) \rightarrow g(v) + \epsilon \Delta F'$	0	$\Pi/6, \Pi/2$	0.172				0.7595
		$\Pi, \Pi/2$	0.088				11.73
		$\Pi/6, \Pi$	0.235				1.0476
		Π, Π	0.088				14.74
	0.5	$\Pi/6, \Pi/2$	0.171				0.847
		$\Pi, \Pi/2$	0.087				13.08
		$\Pi/6, \Pi$	0.17				1.064
		Π, Π	0.087				16.44
	1.0	$\Pi/6, \Pi/2$	0.085				0.935
		$\Pi, \Pi/2$	0.089				14.43
		$\Pi/6, \Pi$	0.085				1.174
		Π, Π	0.089				18.13
$ g(u) \rightarrow g(v) + A_1 + A_2(v-v_0) + \epsilon \Delta F'$	0	$\Pi, \Pi/2$	0.108	-0.039	-0.472		3.0770940
		Π, Π	0.1085	-0.039	-0.472		3.8661006
	0.5	$\Pi, \Pi/2$	0.532	0.091	-0.769		5.0187147
		Π, Π	0.532	0.091	-0.769		6.3055740
	1.0	$\Pi, \Pi/2$	0.532	0.0861	-0.766		6.5502428
		Π, Π	0.532	0.086	-0.767		8.2298045
$ g(u) \rightarrow g(v) + A_1 + A_2(v-v_0) + A_3(v-v_0)^2 + \epsilon \Delta F'$	0	$\Pi, \Pi/2$	0.100	-0.031	-0.471	0.00689	2.9330533
		Π, Π	0.100	-0.031	-0.471	0.0069	3.6848775
	0.5	$\Pi, \Pi/2$	0.463	0.083	-0.696	0.051	5.0462178
		Π, Π	0.517	0.092	-0.755	0.019	6.2955831
	1.0	$\Pi, \Pi/2$	0.5199	0.088	-0.756	0.0114	6.5478322
		Π, Π	0.5199	0.088	-0.757	0.0114	8.2267758

TABLE 2 (CONTINUED):

Funct.	ϵ	XVI:GR= v ₀	A ₁	A ₂	A ₃	A ₄	Upper Bounds. (Minimum)	
$ g(v) \rightarrow g(v) + A_1(v-v_0) + A_2(v-v_0)^2 + A_3(v-v_0)^3 + \epsilon \Delta F'$	0	II, II/2	0.098	-0.031	-0.471	0.00689	-0.0009	3.0566328
		II, II	0.098	-0.031	-0.471	0.0689	-0.0009	3.8374145
	0.5	II, II/2	0.144	0.065	-0.639	0.1398	-0.163	4.1947098
		II, II	0.144	0.065	-0.639	0.1398	-0.1629	5.2702844
	1	II, II/2	0.144	0.067	-0.637	0.141	-0.161	5.8221501
		II, II	0.14	0.067	-0.637	0.141	-0.161	7.315099

Table 3: (Set of arguments: $X > VI$: GR=II, II/2)
 $X < VI$: GR=II, II

Function	ϵ	v_0	A_1	A_2	A_3	A_4	Upper bounds (Minimum).
$ g(e^{i\kappa}) + \epsilon \Delta F'$	0	0.101					8.7950186
		0.101					11.050168
	0.5	0.101					9.7196570
		0.101					12.211895
	1.0	0.101					10.600076
		0.101					13.318064
$ g(e^{i\kappa}) \rightarrow g(v) + A_1 + A_2(v-v_0) + \epsilon \Delta F'$	0	0.4239	0.0799	-0.269			9.3249948
		0.42	0.079	-0.269			11.716036
	0.5	0.464	-0.094	-0.318			12.093706
		0.464	-0.0939	-0.318			15.194679
	1.0	0.568	-0.028	-0.459			14.392596
		0.568	-0.0278	-0.459			18.083038
$ g(e^{i\kappa}) \rightarrow g(v) + A_1 + A_2 \cdot (v-v_0) + A_3(v-v_0)^2 + \epsilon \Delta F'$	0	0.468	0.0256	-0.4399	0.0304		3.2810942
		0.468	0.0256	-0.4399	0.0305		4.1093775
	0.5	0.531	0.093	-1.166	1.082		6.8624974
		0.531	0.093	-1.166	1.080		8.622125
	1.0	0.524	0.154	-1.283	1.222		8.7712799
		0.523	0.152	-1.277	1.213		11.020651
$ g(e^{i\kappa}) \rightarrow g(v) + A_1 + A_2 \cdot (v-v_0) + A_3(v-v_0)^2 + A_4(v-v_0)^3 + \epsilon \Delta F'$	0	0.025	0.081	-0.264	0.00083	-0.0023	9.7238868
		0.025	0.081	-0.264	0.0008	-0.0023	12.217233
	0.5	0.310	0.158	-1.008	1.164	-0.565	5.6873326
		0.3105	0.143	-1.094	1.146	-0.565	7.1331543
	1.0	0.649	0.198	-1.748	1.586	0.918	8.4311597
		0.649	0.200	-1.749	1.589	0.919	10.584160

3.16 UPPER BOUNDS IN THE BROAD ENERGY REGION

In order to calculate the upper bounds in the energy region ($0.45 \text{ Gev} \leq E_{c.m.} \leq 1.9 \text{ Gev}$), we assume the errors to be correlated for two combinations of amplitudes.

$$\Delta f(x_i) = \sum_{i=1}^N |\Delta x_i| \left| \frac{\partial f}{\partial x_i} \right| \quad (3.16.1)$$

$$\text{so, } \frac{\partial F^I}{\partial d_1^I} = \sum_{l=0}^{\infty} (s/(s-4))^{\frac{1}{2}} (2l+1) \left[n_1^I 2ie^{2id_1^I} \right] / 2i \cdot P_1(x)$$

$$\text{or } \frac{\partial F^I}{\partial d_1^I} = \sum_{l=0}^{\infty} (s/(s-4))^{\frac{1}{2}} (2l+1) n_1^I e^{2id_1^I} \cdot P_1(x), \quad (3.16.2)$$

$$\text{where } X = \left(1 + 4 \cdot \frac{2m_{\Pi}^2}{s - 4m_{\Pi}^2} \right).$$

$$\text{Similarly, } \frac{\partial F^I}{\partial n_1^I} = \sum_{l=0}^{\infty} \left(\frac{s}{s-4} \right)^{\frac{1}{2}} (2l+1) \left[e^{2id_1^I} \right] / 2i \cdot P_1(x) \quad (3.16.3)$$

Putting the results (3.16.2) and (3.16.3) into (3.16.1), we have

$$\Delta F^I = \sum_{l=0,1,2,3}^{\infty} (s/(s-4))^{\frac{1}{2}} (2l+1) \left[|n_1^I e^{2id_1^I} P_1(x) \cdot \Delta d_1^I| + \left| \frac{e^{2id_1^I}}{2i} \Delta n_1^I P_1(x) \right| \right] \quad (3.16.4)$$

Now $\Delta F^I \equiv (1/3 \cdot \Delta F^0 + 2/3 \cdot \Delta F^2)$ for $\Pi^0 \Pi^0 \rightarrow \Pi^0 \Pi^0$.

$$\begin{aligned} &= 1/3 \cdot (s/(s-4))^{\frac{1}{2}} \left\{ \left[|n_0^0 e^{2id_0^0} \Delta d_0^0| + \left| \frac{e^{2id_0^0}}{2i} \Delta n_0^0 \right| \right] P_0(x) \right. \\ &\quad \left. + 5 \left[|n_2^0 e^{2id_2^0} \Delta d_2^0| + \left| \frac{e^{2id_2^0}}{2i} \Delta n_2^0 \right| \right] P_2(x) \right\} \\ &+ 2/3 \cdot (s/(s-4))^{\frac{1}{2}} \left\{ |n_0^2 e^{2id_0^2} \Delta d_0^2| + \left| \frac{e^{2id_0^2}}{2i} \Delta n_0^2 \right| \right\} \cdot P_0(x) \end{aligned}$$

(3.16.5)

And for $\Pi^+ \Pi^0 \rightarrow \Pi^+ \Pi^0$ scattering,

$$\Delta F' = \frac{1}{2} (\Delta F^1 + \Delta F^2)$$

$$= \frac{1}{2} \left[(s/(s-4))^{\frac{1}{2}} \left\{ 3 \left[|n_1^1 e^{2i d_1^1} \Delta d_1^1| + \left| \frac{e^{2i d_1^1}}{2i} \Delta n_1^1 \right| \right] P_1(x) + \right. \right. \\ \left. \left. + 7 \left[|n_3^1 e^{2i d_3^1} \Delta d_3^1| + \left| \frac{e^{2i d_3^1} \Delta n_3^1}{2i} \right| \right] P_3(x) + \right. \right. \\ \left. \left. + \left[|n_0^2 e^{2i d_0^2} \Delta d_0^2| + \left| \frac{e^{2i d_0^2} \Delta n_0^2}{2i} \right| \right] P_0(x) \right\} \right]$$

(3.16.6)

In the elastic region, we assume $n=1$ and the partial wave amplitudes are calculated by

$$f_1^I(s) = (s/(s-4))^{\frac{1}{2}} e^{i d_1^I(s)} \text{sind}_1^I(s), \quad (3.16.7)$$

whereas in the inelastic region we use equation (3.9.1)

and (3.9.2). On calculating amplitudes in the respective

regions, we apply the same mapping and the expression (3.4.5)

to calculate upper bounds on s-wave scattering lengths in

the broad energy region with $\epsilon = 0, 0.5, 1.0$. Errors (3.16.5)

and (3.16.6) are taken into due consideration. The results

are given in tables 4 and 5.

TABLE 4:

(92)

Funct. ϵ	$XVI:GR=$ $XVI:GR=$	v_0	A_1	A_2	A_3	A_4	Upper Bounds (Minimum.)		
$ g(u) \rightarrow g(u) + \epsilon \Delta F'$	0	$\Pi/6, \Pi/2$	0.235					0.9904	
		$\Pi, \Pi/2$	0.236					14.7303	
	0.5	$\Pi/6, \Pi$	0.112					1.163	
		Π, Π	0.236					15.5811	
	1.0	$\Pi/6, \Pi/2$	0.112					1.099	
		$\Pi, \Pi/2$	0.112					16.35	
		$\Pi/6, \Pi$	0.113					2.43	
		Π, Π	0.112					17.29	
	1.0	$\Pi/6, \Pi/2$	0.224					4.1759	
		$\Pi, \Pi/2$	0.112					17.49	
		$\Pi/6, \Pi$	0.224					4.242	
		Π, Π	0.112					18.50	
	$ g(u) \rightarrow g(u) + A_1 + A_2(v-v_0) + \epsilon \Delta F'$	0	$\Pi, \Pi/2$	0.123	0.005	-0.479			3.73156
			Π, Π	0.123	0.0052	-0.479			3.9471
		0.5	$\Pi, \Pi/2$	0.111	0.0067	-0.475			4.3402
			Π, Π	0.111	0.0067	-0.475			4.5909
1.0		$\Pi, \Pi/2$	0.111	0.0068	-0.475			4.7302	
		Π, Π	0.111	0.0067	-0.475			5.0034	
$ g(u) \rightarrow g(u) + A_1 + A_2(v-v_0) + A_3(v-v_0)^2 + A_4(v-v_0)^3 + \epsilon \Delta F'$	0	$\Pi, \Pi/2$	0.102	-0.019	-0.482	0.012		3.8445	
		Π, Π	0.101	-0.019	-0.482	0.012		4.06661	
	0.5	$\Pi, \Pi/2$	0.101	-0.020	-0.482	0.010		4.6501	
		Π, Π	0.101	-0.020	-0.482	0.010		4.9187	
	1.0	$\Pi, \Pi/2$	0.101	-0.020	-0.481	0.010		4.8753	
		Π, Π	0.101	-0.020	-0.481	0.010		5.1569	

TABLE 4 (CONTINUED):

Funct	ϵ	XVI:GR=	v_0	A_1	A_2	A_3	A_4	Upper bounds.
		XVI:GR=						(minimum.)
$ g(v) \rightarrow g(v) + A_1 + A_2(v-v_0) + A_3(v-v_0)^2 + A_4(v-v_0)^3 + \epsilon \Delta F$	0	$\Pi, \Pi/2$	0.108	-0.019	-0.482	0.012	0.003	3.7461
		Π, Π	0.108	-0.019	-0.482	0.012	0.003	3.9625
	0.5	$\Pi, \Pi/2$	0.113	-0.020	-0.481	0.010	0.006	4.53618
		Π, Π	0.113	-0.020	-0.481	0.010	0.006	4.7982
	1.0	$\Pi, \Pi/2$	0.112	-0.020	-0.481	0.010	0.005	4.98216
		Π, Π	0.112	-0.020	-0.481	0.010	0.005	5.26993

Table 5:

Funct.	ϵ	$X > VI:$ GR= $X < VI:$ GR=	v_0	A_1	A_2	A_3	A_4	Upper bounds (Minimum).
$ g(e^{i\theta}) \rightarrow g(u) + \epsilon \Delta F'$	0	$\pi, \pi/2$	0.099					10.096549
		π, π	0.099					10.679722
	0.5	$\pi, \pi/2$	0.112					11.115231
		π, π	0.112					11.757243
	1	$\pi, \pi/2$	0.112					11.898424
		π, π	0.112					12.585673
$ g(e^{i\theta}) \rightarrow g(u) + A_1 + A_2(u^2) + \epsilon \Delta F'$	0	$\pi, \pi/2$	0.078	0.153	-0.257			7.1247006
		π, π	0.078	0.153	-0.257			7.5362216
	0.5	$\pi, \pi/2$	0.077	0.153	-0.257			7.9012722
		π, π	0.077	0.153	-0.257			8.3579170
	1	$\pi, \pi/2$	0.078	0.153	-0.257			8.4747998
		π, π	0.078	0.153	-0.257			8.9642957
$ g(e^{i\theta}) \rightarrow g(u) + A_1 + A_2(u^2) + A_3(u^3) + A_4(u^4) + \epsilon \Delta F'$	0	$\pi, \pi/2$	0.077	0.154	-0.257	0.0003		7.1711222
		π, π	0.077	0.154	-0.257	0.0003		7.5853239
	0.5	$\pi, \pi/2$	0.077	0.154	-0.257	0.0003		7.9918524
		π, π	0.077	0.154	-0.257	0.0003		8.4534586
	1	$\pi, \pi/2$	0.076	0.154	-0.257	0.0004		8.4901218
		π, π	0.076	0.154	-0.257	0.0004		8.9805088
$ g(e^{i\theta}) \rightarrow g(u) + A_1 + A_2(u^2) + A_3(u^3) + A_4(u^4) + A_5(u^5) + \epsilon \Delta F'$	0	$\pi, \pi/2$	0.077	0.154	-0.257	0.0001	0.00027	7.0290661
		π, π	0.077	0.154	-0.257	0.0001	0.00027	7.4350620
	0.5	$\pi, \pi/2$	0.077	0.154	-0.257	0.0009	0.00027	7.8803580
		π, π	0.077	0.154	-0.257	0.0009	0.00027	8.3355271
	1	$\pi, \pi/2$	0.077	0.154	-0.258	0.0002	0.00002	8.4729797
		π, π	0.076	0.154	-0.258	0.0002	0.00002	8.9623751

Table 6 :

	$\epsilon=0$	$\epsilon=0.5$	$\epsilon=1.0$
U.B.	0.86	6.8	12.2
a_0 L.B.	-0.07	-0.31	-0.47
U.B.	0.60	2.65	4.5
a_2 L.B.	-0.02	-0.17	-0.27
U.B.	1.71	17.2	32
$2a_0 - 5a_2$ L.B.	-2.8	-9	-16
U.B.	1.28	7.2	12.5
$a_0 + 2a_2$ L.B.	0.126	-0.12	-0.22

3.17 DISCUSSION OF RESULTS.

In the present work, we have adopted the main features of $\Pi\Pi$ scattering in the energy region $0.45\text{Gev} \leq E_{c.m.} \leq 1.9\text{ Gev}$, defining the same central family of S,P,D and F phase shifts with associated errors. Furthermore, we have also defined and multiplied the errors in the (A)elastic region and in the (B) broad energy region by the same scaling factor \mathcal{E} ($0 \leq \mathcal{E} \leq 1$) such that $\mathcal{E}=0$ gives the central family and $\mathcal{E}=1$ gives the bands of maximal expanse. For any fixed value of \mathcal{E} , we compute the upper bounds of $\Pi\Pi$ amplitudes in the two regions of energy for $\Pi^0 + \Pi^0 \rightarrow \Pi^0 + \Pi^0$ and $\Pi^+ \Pi^0 \rightarrow \Pi^+ \Pi^0$ interactions. We have used Bonnier's [18] normalization factor:

$$p(s) = [(s-4)/s]^{1/2} \quad (3.17.1)$$

In the elastic region for $\Pi^0 + \Pi^0 \rightarrow \Pi^0 + \Pi^0$, we have selected one third and two third combinations of amplitudes for isospin zero and two respectively. For $\Pi^+ + \Pi^0 \rightarrow \Pi^+ + \Pi^0$ we have taken half and half combinations of amplitudes for isospins one and two.

For comparing the results, Bonnier's bounds [18] are given in table 6. Numerical values (for different values of \mathcal{E}) of the bounds on $a_0, a_2, 2a_0 - 5a_2$ and $a_0 + 2a_2$ have been obtained by him on using data (table 1). Bonnier's bounds [18] are approximately linear with \mathcal{E} ($0 \leq \mathcal{E} \leq 1$). Our results are to be compared with the upper bounds on $a_0 + 2a_2$ with different values of $\mathcal{E} = 0, 0.5$ and 1 .

²The bounds given in tables 3&5 are upper bounds for $\frac{1}{2}(F^1(0,4) + F^2(0,4)) = 1/3 \cdot (a_0 - a_2)$ (see 3.4.5)

(A) Elastic region ($0.45\text{Gev} \leq E_{c.m.} \leq 0.95\text{Gev}$):

$\pi^0 + \pi^0 \rightarrow \pi^0 + \pi^0$: In the beginning, we select some sets of arguments, namely $(\pi/6, \pi/2)$, $(\pi/6, \pi)$, $(\pi, \pi/2)$ & (π, π) then we have sets of arguments: $(\pi, \pi/2)$ and (π, π) .

The first set, in the latter case, should give the best results, while the last one should give the maximum value. The minimum is found at $v_0 \approx 0.08$ consistently. Firstly, in the best case of arguments $(\pi, \pi/2)$ the numerical values of the bounds are 11.73, 13.08 and 14.43 for $\epsilon = 0, 0.5$ and 1 respectively. In the worst case of arguments (π, π) , the numerical values are 14.74, 16.44 and 18.13 for $\epsilon = 0, 0.5$ and 1.0 respectively, which can be compared with Bonnier's result 12.5.

On expanding the total amplitude in terms of powers of $(v-v_0)$ with the help of certain coefficients, like A_1 and A_2 , we find lots of cancellations going on and finally it leads to stable bounds. The numerical values of the bounds drop to 3.077, 5.019 and 6.55 corresponding to the set of arguments $(\pi, \pi/2)$ and $\epsilon = 0, 0.5$ and 1.0 respectively. In the worst case, the numerical values are 3.866, 6.306 and 8.229 which show considerable improvement over Bonnier's result 12.5. On inclusion of more coefficients of expansion, the bounds improve a lot down to our numerical value 7.31 in the worst case of arguments, which shows a considerable drop of 41.6% as compared to Bonnier's value 12.5.

$\Pi^+ + \Pi^0 \rightarrow \Pi^+ \Pi^0$: We select same sets of arguments $(\Pi, \Pi/2)$ & (Π, Π) for this isospin combination. We find that the numerical values of the upper bounds are 8.79, 9.72 and 10.6 for $E=0, 0.5$ and 1.0 respectively with the argument $(\Pi, \Pi/2)$. The minima are found consistently at $v_0=0.101$. In the worst case of arguments (Π, Π) , the numerical values are 11.05, 12.21 and 13.32 for $E=0, 0.5$ and 1.0 respectively. On inclusion of coefficients of expansion for $(v-v_0)$, we have considerable improvement over the previous numerical values of bounds, down to our result 10.58 in the worst case of arguments with $E=1.0$, which is still lower than Bonnier's result [18].

(B) In the second part of this work, we have selected the broad energy region with the same mappings and expression for the upper bound. The central family ($E=0$) shows some increase in the values of upper bounds as compared to our initial results in the elastic region. There is the reverse case with other values of E , the bounds improve as compared to corresponding cases in pure elastic region. It is a remarkable observation that minimum values of upper bounds are found at $v_0 \approx 0.1$ in almost all cases of expansion with different values of E (0, 0.5, and 1.0) in this case; while in the elastic region the minimum values of upper bounds are found at values of v_0 varying from $v_0=0.08$ to $v_0=0.53$ in different cases of power expansion of the amplitudes.

$\Pi^0 + \Pi^0 \rightarrow \Pi^0 + \Pi^0$: In the beginning, we have selected four sets of arguments $(\sqrt{6}, \sqrt{6}/2)$, $(\sqrt{6}, \sqrt{6})$, $(\sqrt{3}, \sqrt{3}/2)$ & $(\sqrt{3}, \sqrt{3})$; and then two sets of arguments $(\Pi, \Pi/2)$ and (Π, Π) are selected. In the case of central family ($E=0$), the numerical values of upper bounds are 14.73, 16.35 and 17.49 for the set of arguments $(\Pi, \Pi/2)$; while the numerical values for the set

of arguments (Π, Π) are 15.58, 17.29 and 18.50.

On inclusion of different power expansion of $(v-v_0)$ in terms of coefficients, the bounds improve a lot and the best value is 3.73 at $v_0=0.123, A_1=0.005, A_2=-0.479$

after minimization; while the worst value is 5.269 at $v_0=0.112, A_1=-0.020, A_2=-0.481, A_3=0.001$ and $A_4=0.005$. Both results show great improvement over Bonnier's results.

$\Pi^+ \Pi^0 \rightarrow \Pi^+ \Pi^0$: We have selected same sets of arguments of the amplitude for this combination: $(\pi, \pi/2)$ & (π, π) .

In the former case, we have numerical values of the bounds 10.09, 11.15 and 11.898 for $\epsilon=0, 0.5$ and 1.0 respectively; whereas in the latter case of arguments their values are 10.679, 11.757 and 12.586 respectively. They show considerable improvement over the corresponding results in the elastic region.

On inclusion of the power series in $(v-v_0)$ with four coefficients, we get the best numerical values 7.029, 7.880 and 8.473 for $\epsilon=0, 0.5, 1$; whereas in the case of arguments (Π, Π) their values are 7.435, 8.335, 8.962 for $\epsilon=0, 0.5$ and 1.0 respectively on minimization. All these results show much more improvement over previous results.

3.18 CONCLUSIONS.

We find that all values of upper bounds, given in tables (2, 3, 4, and 5), depend strongly on E and the set of arguments used. The best values of upper bounds on s -wave scattering lengths are obtained for $E=0$ and arguments $(\Pi/6, \Pi/2)$ or $(\Pi, \Pi/2)$

; whereas the worst upper bounds are obtained for $E=1$ with arguments (Π, Π) . On replacing $g(e^{i\alpha}) = F(s, 4)$ by a power series in $(v-v_0)$, the integrals over the upper bounds involve lots of internal cancellations and lead to stable upper bounds.

In the elastic region ($0.45 \text{ GeV} \leq E_{c.m.} \leq 0.95 \text{ GeV}$), the upper bounds get stabilised on introduction of coefficients A_1, A_2, A_3, A_4 of the power series. There is much improvement over Bonnier's [18] results with same normalisation factor in all cases of E -values.

On selecting broad energy region with the same mapping and expression for upper bounds, the central family ($E=0$) shows some deterioration. However, reverse is the case with other E -values—— bounds improve as compared to those in the elastic region. The minima are almost stable at $v_0 \approx 0.1$, except in few cases of E -values; whereas in pure elastic region they are found at values of v_0 varying from $v_0 \approx 0.08$ to $v_0 \approx 0.53$ under different conditions of parameterization.

Finally, our method is model independent and it gives new upper bounds on s -wave scattering lengths and their any linear combinations, on defining central family of S, P, D, F phase shifts with associated errors.

We would like to compare our results with general s-wave phenomenology based on BFP model[30] with the same normalization factor.

Both Saclay and Berkeley data restrict the isoscalar s-wave scattering length to the range

$$-0.05 < a_0^0 < 0.6,$$

while the CM-EM1 phases require $a_0^0 > 0.15$. The BFP model[30] gives the following s-wave parameters for Saclay and CM-EM1 phase shifts, as shown in table 7:

Table 7:

Saclay data: a_0^0	a_0^2	$\frac{1}{3}(a_0^0 + 2a_0^2)$	CM-EM1 data: a_0^0	a_0^2	$\frac{1}{3}(a_0^0 + 2a_0^2)$
-0.056	-0.108	-0.087	0.17	-0.066	0.013
0.16	-0.037	0.029	0.31	-0.030	-0.083
0.30	-0.006	0.096	0.40	-0.010	0.127
0.58	0.047	0.224	0.59	0.028	0.178

From BFP model[30], it is apparent that

$$-0.087 < \frac{1}{3}(a_0^0 + 2a_0^2) < 0.224 \text{ for Saclay data}$$

and
$$-0.083 < \frac{1}{3}(a_0^0 + 2a_0^2) < 0.178 \text{ for CM-EM1 data.}$$

On the basis of our model, the best results on s-wave scattering lengths in the (A) elastic and (B) broad energy region are (with arguments $(\pi, \pi/2)$ and $\epsilon=0$):

(A) Elastic region: $\frac{1}{3}(a_0^0 + 2a_0^2) \leq 3.057$; $v_0 = 0.098$, $A_1 = -0.0312$,

$$A_2 = -0.4709, A_3 = 0.0068,$$

$$A_4 = -0.0009.$$

(B) Broad Energy Region: $1/3.(a_0 + 2a_2) \leq 3.73, v_0 = 0.123, A_1 = 0.005,$
 $A_2 = -0.479.$

On the other hand, the upper bounds on s-wave scattering lengths with arguments $(\Pi/6, \Pi/2)$ and $G=0$ are :

(A) Elastic Region: $1/3.(a_0 + 2a_2) \leq 0.7595, v_0 = 0.172$

(B) Broad Energy Region: $1/3.(a_0 + 2a_2) \leq 0.9904, v_0 = 0.235.$

The upper bounds from BFP[30] models for Saclay and CM-EM1 data are 0.224 and 0.178 respectively. As compared to BFP results from Saclay and CM-EM1 data our bounds for arguments $(\Pi/6, \Pi/2)$ with $G=0$ are 3.39 and 4.27 times higher in the elastic region respectively; while in the broad energy region our bounds are 4.42 and 5.56 times higher.

For $\Pi^+ \Pi^0 \rightarrow \Pi^+ \Pi^0$ scattering, our bounds are higher with the set of arguments $(\Pi, \Pi/2)$ and $G=1$:

(A) Elastic Region: $1/3.(a_0 - a_2) \leq 8.43, v_0 = 0.649, A_1 = 0.198, A_2 = -1.748,$
 $A_3 = 1.586, A_4 = 0.918.$

(B) Broad Energy Region : $1/3.(a_0 - a_2) \leq 8.47, v_0 = 0.077, A_1 = 0.154, A_2 = -0.258,$
 $A_3 = 0.0002,$
 $A_4 = 0.000002.$

The corresponding upper bounds from BFP[30] models for Saclay and CM-EM1 data are $1/3.(a_0 - a_2) \leq 0.177$ and 0.190 respectively. As compared to these bounds our bounds are much higher in both the elastic and broad energy regions. However, our model shows closer bounds to BFP results.

This method is model independent and is capable of producing new class of upper bounds on s-wave $\Pi \Pi$ scattering lengths and their linear combinations, defining central family of S, P, D and F phase shifts with associated errors in the low energy region.

P A R T T W O

CHAPTER IV: $\pi\pi$ SUM-RULES AND PHASE SHIFT

SOLUTIONS IN THE INELASTIC REGION.

4.0. INTRODUCTION.

We can derive sumrules for pion-pion scattering amplitudes using analyticity, crossing symmetry and rigorous bounds. If they involve integrals only over physical quantities, they are called superconvergent. Ordinarily, superconvergent sum rules involve only absorptive parts of amplitudes. Wanders[7] superconvergent sum rules differ from the simplest superconvergent relations because absorptive parts as well as derivatives of absorptive parts with respect to the momentum transfer appear in the integrals. On the basis of the three basic ingredients of the imaginary parts of the partial wave amplitudes, Roskies[8] has derived inequalities on integrals involving the low partial waves of elastic $\pi^0\pi^0$ scattering in the physical region. The integrals have been found sensitive only to the low-energy region, and they can be tested once we know a phase shift analysis. Also, the relations can be used to discriminate between various proposed $\pi^0\pi^0$ phase shifts. On expansion of the work, Roskies[8] has obtained sum rules involving the absorptive parts of all partial waves for each isospin. Using these absorptive parts, we can re-obtain the sum rules as inequalities involving integrals of the low partial-wave amplitudes which are sensitive only to the low-energy region. Furthermore, it is observed that the necessity for subtractions in the dispersion relations implies that no results can be obtained for s and p waves. It has been proved by different authors that two subtractions are necessary in $\pi\pi$ dispersion relations. This is confirmed by axiomatic field theory[17].

On the other hand, sum-rules on pseudoscalar meson-meson scattering amplitudes in the physical region have been studied by Grassberger[79] to show that a broad f is preferred by sum rules which are derived from crossing and analyticity. A class of sum-rules dominated by the ρ, f, g meson and the ρ regge amplitude has emerged. Furthermore, Grassberger[79] has observed that in the absence of the Pomeron, there is perfect agreement if both the f and the g are as narrow as given by Veneziano model, to some extent narrower than experimentally observed; but on inclusion of the high-energy contribution due to the Pomeron, one sees that the f must be much broader to get saturation.

Common[74] has derived sum rule inequalities on the $\Pi \Pi$ scattering amplitudes from analyticity, $s \leftrightarrow u$ crossing and positivity of these amplitudes, connecting the real and imaginary parts of the amplitude in the energy region where they may be calculated from phase-shift analysis, and they do not require knowledge of these quantities at low energies or in the high energy region. These inequalities are obtained by mapping the region, where the phase shifts are known experimentally, onto the circumference of the circle, while the remaining parts of the physical cuts are mapped onto cuts in this circle. They put constraints, over the forward amplitude for the process $\Pi^+ \Pi^0 \rightarrow \Pi^+ \Pi^0$ and $\Pi^0 \Pi^0 \rightarrow \Pi^0 \Pi^0$, which are violated by the two solutions for the phase shifts given by Estabrooks[80]. However, the violation is found to be of the order of experimental errors, so neither solution can be ruled out completely. The results are in favour of solution 1, in agreement with $\Pi^+ \Pi^- \rightarrow \Pi^0 \Pi^0$ and the behaviour of the amplitude at the S^* threshold.

4.1 Description of sum-rule and sum-rule Inequalities.

We can write the sum-rules in the most general form

$$\sum_{j=4}^{\infty} A(s, t_i) Q(t_i, t_j, t_k, s) ds = 0, \quad (4.1.1)$$

cyclic permutations

of $i, j, k=1, 2, 3$

where $A(s, t)$ is the absorptive part of the $\Pi \Pi$ scattering amplitude, Q is a known function of its arguments and $|t_i| \leq 4m_{\Pi}^2$. These types of sum rules have been derived by Wanders [7] and Roskies [8] from dispersion relations containing derivatives of $A(s, t)$.

On selecting $s \leftrightarrow u$ symmetric combinations of the amplitudes for different isospins and transforming to the symmetric variable $z = (s - 2m_{\Pi}^2)^2$ and defining $G(z) = F(s, 0)$ it follows that $G(z)$ is a real analytic function of z in the whole complex z -plane cut from $4m_{\Pi}^4$ to ∞ . Common [74] has used the mapping for the sum-rule,

$$z \rightarrow v = \frac{1 + \frac{1}{\frac{-(z_1+z_2)}{(z_1-z_2)} + \frac{2z}{(z_1-z_2)}}}{1 + \frac{1}{\frac{-(z_1+z_2)}{(z_1-z_2)} + \frac{2z}{z_1-z_2}}} - \frac{1 - \frac{1}{\frac{-(z_1+z_2)}{(z_1-z_2)} + \frac{2z}{(z_1-z_2)}}}{1 - \frac{1}{\frac{-(z_1+z_2)}{z_1-z_2} + \frac{2z}{(z_1-z_2)}}}, \quad (4.1.2)$$

where the region $z_1 \leq z \leq z_2$ is mapped onto the circumference of the unitary circle. The high energy region ($z \gg z_2$) is mapped onto the cut $-1 \leq v \leq 0$ and the low energy region $z \leq z_1$ is mapped onto the cut $v < v_0 < 1$ with $v_0 \rightarrow z = 4m_{\Pi}^4$.

If $w(v)$ is chosen to be a polynomial, which is positive for $-1 \leq v \leq 0$ and $v_0 \leq v \leq 1$, one gets a sum-rule inequality:

$$-\text{Re} \int_0^{\Pi} f(e^{i\theta}) w(e^{i\theta}) e^{i\theta} d\theta \geq 0 \quad (4.1.3)$$

From this mapping, we can prove the convergence

$$\int \text{Im} f(v+i\epsilon) w(v) dv \sim \int \frac{A(s,0) ds}{s^3} \quad \text{as } s \rightarrow \infty, v \rightarrow 0 \quad (4.1.4)$$

There can be an infinite set of polynomials to test the inequality (4.1.3), but we should be sure about necessary and sufficient conditions of the connected moment problem, described by equation (3.4.7) in chapter III.

Furthermore, if we know either $\text{Im}f(v+i\epsilon)$ on part of the real axis, or have a lower bound for it; the inequality can be improved:

$$\text{Im}f(v+i\epsilon) \geq h(v) \geq 0, \quad -1 \leq v \leq v_1 < 0$$

$$-\text{Re} \left[\int_0^{\Pi} f(e^{i\theta}) w(e^{i\theta}) d\theta \right] - \int_{-1}^{v_1} h(v) w(v) dv \geq 0, \quad (4.1.5)$$

where $h(v)$ is a known function like $h(v) \equiv \text{Im}f(v+i\epsilon) \equiv A(s,0)$

According to Common[74], the data of Estabrooks et al [80] on $\Pi \Pi$ phase shifts up to $\sqrt{s} = 1.38 \text{ GeV}$ for their two solutions (1 and 2) are normalised for $I=0$ s-wave to $2/3$, to $(2/3)\sqrt{5}$ for the D-wave and $I=1$ P-wave to $\sqrt{3}$. The region $0.45 \text{ GeV} \leq \sqrt{s} \leq 0.97 \text{ GeV}$ (elastic) is mapped onto the circumference of the circle in the complex v -plane with $v_0 = 0.7$. There is an overall phase ambiguity due to inelasticity, but the ambiguity is not large.

For the process $\Pi^+ + \Pi^0 \rightarrow \Pi^+ + \Pi^0$, the inequality (4.1.5) should be non-negative. They ^{are} satisfied better by solution 1 than by solution 2. More precisely, for the latter solution many of conditions are violated by less than one standard deviation. In the case of the process $\Pi^0 + \Pi^0 \rightarrow \Pi^0 + \Pi^0$, the constraints are violated in a number of cases by both solution 1 and solution 2. This violation is always smaller than one standard deviation in the former case, while in the latter case some constraints are violated up to 1.5 standard deviations. So, Common [74] observes that solution 1 is more likely to be correct than solution 2, but we cannot rule out solution 2. In this way, it has been found by Common [74] that this violation of constraints is of the order of experimental error so neither solution of Estabrooks [80] can be ruled out completely.

4.2. INTRODUCTION.

In the present work, we derive sum-rule inequality on $\pi^+\pi^-\rightarrow\pi^+\pi^-$ scattering amplitudes in the inelastic region from analyticity and positivity of these amplitudes. They connect the real and imaginary parts of the amplitude in the region where they are calculated from phase shifts analysis, and do not require knowledge of these quantities at low energies or in the high energy region. We choose a polynomial, $P(v)$, so that it has zeros at $v=0$ and $v=v_0$, the point which corresponds to infinity in the complex s -plane. It is arranged such that $\text{Im}F(v)P(v)$ has a constant sign from $v=-1$ to $v=0$ and $v=v_0$ to $v=+1$. The experimental inelastic region, $s_1 \leq s \leq s_2$ is mapped onto the unitary circle in v -plane. As the phase shifts are known in the inelastic region this information can be used in the sum rule. So, we need definite sign of $\text{Im}F(v)P(v)$ for $-1 \leq v \leq 0$ and $v_0 \leq v \leq 1$.

The data from Estabrooks and Martin solutions A, B, C, D [81] and Froggatt-Petersen [68, 68a] are used to test the sum-rule inequality. Furthermore, the EM-solutions A, B, C, D have been rotated by Common [82] in a special way, the rotated data are also used to test the sum-rule inequality. The local minimization programs are used to find the minima with respect to zeros and its parameterizations.

We consider the $s \leftrightarrow u$ crossing $\frac{\text{non-}}{\text{invariant}}$ amplitude:

$$F(s, 0) = 2/3 \cdot F^0(s, 0) + 1/3 \cdot F^2(s, 0) + F^1(s, 0), \quad (4.2.1)$$

where $F^I(s, 0)$ is the forward scattering amplitude in s -channel with total isotopic spin I . The forward scattering amplitudes $F(s, 0)$ are analytic in the complex s -plane cut from $4m_{\pi}^2$ to ∞ and 0 to $-\infty$. We choose normalization such that

$$F^I(s, t) = \sum_{l=0}^{\infty} (2l+1) f_l^I(s) P_l(\cos \Theta), \quad (4.2.2)$$

$$f_1^I(s) = (n_1^I(s) e^{2id_1^I(s)} - 1) / 2ip(s) \quad \& \quad (4.2.3)$$

$1/p(s) = (s/(s-4))^{1/2}$. We adopt natural units ($c = \hbar = m_{\pi} = 1$) in our calculations. s, t, u are usual Mandelstam variables. If $\pi^+ \pi^-$ phase shifts are known for a particular energy, $\sqrt{s} = E_{c.m.}$, then both the real and imaginary parts of $F_s^I(s, 0)$ can be calculated. A set of sum rules, which connect both real and imaginary parts, are derived. On using the positivity of $A(s, 0)$ in the experimental region ($1.01 \text{ GeV} \leq E_{c.m.} \leq 1.79 \text{ GeV}$) we deduce inequalities from these equalities by mapping the region where the phase shifts are known onto the circumference of a unitary circle, while mapping the remaining parts of the physical cuts onto cuts in this circle.

4.3 Derivation of sum-rule Inequalities.

On defining $G(s) \equiv F(s, 0)$, it becomes analytic in the complex s -plane cuts, where $\sqrt{s} = E_{c.m.}$. If the phase shifts for $\Pi^+ \Pi^-$ scattering are known in the region $s_2 \geq s \geq s_1$, and s is transformed to the complex v -plane by

$$s \rightarrow v = \frac{\sqrt{\frac{s-s_2}{-s_2}} - \sqrt{\frac{s-s_1}{-s_1}}}{\sqrt{\frac{s-s_2}{-s_2}} + \sqrt{\frac{s-s_1}{-s_1}}}, \quad \sqrt{s_1} = 1.01 \text{ Gev and } \sqrt{s_2} = 1.79 \text{ Gev}, \quad (4.3.1)$$

such that $s_1 \rightarrow v = +1$, $s_2 \rightarrow v = -1$, $s = 0 \rightarrow v = 0$, $\sqrt{s} = 4m_{\Pi}^2 \rightarrow v_0 = 0.0137$, $s = \infty \rightarrow v_{\infty} = -0.2786$. It maps the cut s -plane onto a cut circle in the complex v -plane of unit radius, centre the origin as shown in figure 13. The region $s_1 \leq s \leq s_2$, where both real and imaginary parts of the function $G(s)$ are known, is mapped onto the circumference of the circle. The high energy region $s \geq s_2$ is mapped onto the cut $-1 \leq v \leq v_{\infty}$ and the low energy region $4m_{\Pi}^2 \leq s \leq s_1$ is mapped onto the cut $v_0 \leq v \leq 1$, where v_0 is determined by the mapping and corresponds to $s = 4m_{\Pi}^2$. The left hand cut $-\infty \leq s \leq 0$ is mapped onto the cut $v_{\infty} \leq v \leq 0$, as shown in figure 13.

The sum-rules are obtained by using the fact that if $P(v)$ is any function analytic in the cut circle, then

$$\int_C f(P) P(v) dv = 0, \quad (4.3.2)$$

where $f(v) = G(s) \equiv F(s, 0)$. We consider the simplest case when $P(v)$ is a polynomial in v :

$$P(v) = v(v - v_{\infty}) \prod_{j \in J} (v - v_p^j)(v - \bar{v}_p^j) \prod_{k \in K} \frac{(v - v_p^k)}{(-v_p^k)}, \quad (4.3.3)$$

$$\text{where } v_p^j = r_p^j e^{i\theta_p^j} \quad (4.3.4a)$$

$$\bar{v}_p^j = r_p^j e^{-i\theta_p^j}, \quad r_p^j \geq 0, \quad 0 \leq \theta_p^j < \pi \text{ for all } j \quad (4.3.4b)$$

$$v_p^k \leq -1 \text{ or } v_p^k \geq 1 \text{ for all } k. \quad (4.3.4c)$$

For computation, we have defined

$$j \in N_1, \theta \in A, v_p^k \in VPK, r \in R \quad (4.3.4d)$$

In our calculation, this parameterization gives the most general expression for a polynomial of fixed degree $(2J+K+1)$ submitted to our constraints. The number and location of real and complex zeros entering these representations are parameters, which are optimized to give the best results for a given set of data.

Now, $A(s, 0) = \text{Im}f(s+i\epsilon, 0)$ from unitarity for $s \geq 4m^2/\pi$, so $\text{Im}f(v+i\epsilon) \geq 0$ for $v_0 \leq v \leq +1$ and $-1 \leq v \leq 0$. If we choose $P(v)$ to be a polynomial which has positive values for $v_0 \leq v \leq 1$ and $-1 \leq v \leq 0$, then $\mathcal{P} \cdot \text{Im}f(v+i\epsilon)$ becomes positive.

Then we have

$$-\text{Re} \left[\int_0^\pi f(e^{i\theta}) P(e^{i\theta}) e^{i\theta} d\theta \right] = + \int_{-1}^{v_\infty} \text{Im} f(v+i\epsilon) P(v) dv +$$

$$+ \int_{v_\infty}^0 \text{Im}f(v+i\epsilon) P(v) dv +$$

$$+ \int_{v_0}^1 \text{Im}f(v+i\epsilon) P(v) dv \quad (4.3.5)$$

The right hand side integrals of (4.3.5) are positive so that

$$-\text{Re} \left[\int_0^\pi f(e^{i\theta}) P(e^{i\theta}) e^{i\theta} d\theta \right] \geq 0 \quad (4.3.6)$$

4.4 Convergence of s.

In the case of $s=0, v=0$ the right hand side of (4.3.5) vanishes. For a small negative value of v , we have to prove the convergence

$$\int_{v_{\infty}}^0 \text{Im}f(v+i\epsilon)P(v)dv \sim \int \frac{A(s,0)}{s^3} ds \quad (4.4.1)$$

$$\begin{aligned} \text{For that } \int \text{Im}f(v+i\epsilon)P(v)dv &= \int A(s,0) \left[P(v) \frac{dv}{ds} \right] ds \\ &\sim \int A(s,0) \left[v(v-v_{\infty}) \frac{dv}{ds} \right] ds \text{ as } s \rightarrow \infty \end{aligned} \quad (4.4.2)$$

The proof is given in the appendix:

$$\begin{aligned} \int_{v_{\infty}}^0 \text{Im}f(v+i\epsilon)P(v)dv &\sim \int A(s,0) \left[v(v-v_{\infty}) \frac{dv}{ds} \right] ds \\ &\sim \int A(s,0) \left[\left(\frac{1}{s} \right)^3 \right] ds \end{aligned} \quad (4.4.3)$$

From the results of Jin and Martin [17], the integrals of (4.3.5) exist as $s \rightarrow \infty$ and that on the left hand side as $v \rightarrow v_{\infty}$. In this way all the integrals of (4.3.5) exist.

4.5 Numerical results.

The EM[81] data is for $\Pi^+ \Pi^-$ partial wave magnitudes ($|L|$) and relative phase (δ_L) in the inelastic region ($1.01 \text{ GeV} \leq \sqrt{s} \leq 1.79 \text{ GeV}$). The amplitude is expressed by

$$F^{(\pm-)}(s, t) = \frac{\sqrt{s}}{2k} \sum_{L=0}^3 |L| e^{i\delta_L} P_L(\cos\theta_s) \quad (4.5.1)$$

The four solutions A, B, C, D are classified by the signs of the imaginary parts of the first two zeros in the g region:

$$\sum_{L=0}^3 (2L+1) P_L(z) |f_L| e^{i\phi_L} = a \prod_{i=1}^3 (z - z_i) \quad (4.5.2)$$

The phases are all relative to a 90° D-wave. The combination of the signs of $\text{Im } z_1$ and $\text{Im } z_2$ define the solutions; described in chapter II:

Solution	Sign of $\text{Im } z_1$	Sign of $\text{Im } z_2$	} (4.5.3)
A	-	-	
B	+	-	
C	+	+	
D	-	+	

The partial wave amplitudes ($|L|$) are given at energy values 1.01, 1.03, 1.05 GeV etc. by Martin. The phase shifts are interpolated at energy values 1.01, 1.03, 1.05 GeV etc. Then we add to each phase $\delta_D - 90^\circ$ of EM[81] data. In this special way, Common[82] has rotated EM data.

(A) ROTATED DATA:

The amplitude is expressed in the form

$$F^{(\pm-)}(s, t) = (s/(s-4))^{1/2} \{ f_0 + \sqrt{3} f_1 + \sqrt{5} f_2 + \sqrt{7} f_3 \}, \quad (4.5.4)$$

where $f_0 = |s| e^{i\phi_s} \cdot P_0(\cos\theta_s)$

$$f_1 = |P| e^{i\phi_P} \cdot P_1(\cos\theta_s)$$

$$f_2 = |D| e^{i\phi_D} \cdot P_2(\cos\theta_s)$$

$$f_3 = |F| e^{i\phi_F} \cdot P_3(\cos\theta_s) \quad (4.5.5)$$

$\cos\theta_s = 1 + 2t/(s-4) = 1$ for $t=0$, forward scattering.

$$\text{Then, } F^{(+)}(s, 0) = (s/(s-4))^{1/2} \left\{ |s| e^{i\phi_s} \cdot P_0(\cos\theta_s) + \sqrt{3} |P| e^{i\phi_P} \cdot P_1(\cos\theta_s) + \sqrt{5} |D| e^{i\phi_D} \cdot P_2(\cos\theta_s) + \sqrt{7} |F| e^{i\phi_F} \cdot P_3(\cos\theta_s) \right\} \quad (4.5.6)$$

If errors are uncorrelated, we have

$$\left[f(x_i) \right]^2 = \sum_{i=1}^N |\Delta x_i|^2 \left| \frac{\partial f(x_i)}{\partial x_i} \right|^2 \quad (4.5.7)$$

and

$$\begin{aligned} \left[\Delta F^{(+)}(s, 0) \right]^2 &= (s/(s-4)) \left[|e^{i\phi_s} \cdot P_0(\cos\theta_s)|^2 \cdot |\Delta s|^2 + |s| e^{i\phi_s} \cdot P_0(\cos\theta_s) \right. \\ &\quad \left. |\Delta\phi_s|^2 + \sqrt{3} e^{i\phi_P} \cdot P_1(\cos\theta_s) \right]^2 \cdot |\Delta P|^2 + |\sqrt{3} |P| e^{i\phi_P} \cdot P_1(\cos\theta_s)|^2 \cdot |\Delta\phi_P|^2 \\ &\quad + |\sqrt{5} e^{i\phi_D} \cdot P_2(\cos\theta_s)|^2 \cdot |\Delta D|^2 + \sqrt{5} |D| e^{i\phi_D} \cdot P_2(\cos\theta_s) \right]^2 \cdot |\Delta\phi_D|^2 \\ &\quad + |\sqrt{7} e^{i\phi_F} \cdot P_3(\cos\theta_s)|^2 \cdot |\Delta F|^2 + \sqrt{7} |F| e^{i\phi_F} \cdot P_3(\cos\theta_s) \right]^2 \cdot |\Delta\phi_F|^2 \end{aligned} \quad (4.5.8)$$

By defining $F^{(+)}(s, 0) \equiv f(v)$, we have tested the sum-rule inequality

$$I \equiv -\text{Re} \left[\int_0^\pi f(e^{i\theta}) P(e^{i\theta}) e^{i\theta} d\theta \right] + \int_0^\pi |\Delta f(e^{i\theta})| |P(e^{i\theta})| d\theta \geq 0 \quad (4.5.9)$$

We define this equation for computational purpose:

$$\text{FINANS} \equiv \text{ANS1} + \text{ANS2}, \quad (4.5.10)$$

Fortran minimization programs are applied to find out the minimum values of the integrals (4.5.9) with respect to parameterizations (4.3.3) and (4.3.4.a, b, c, d):

$$0 \leq r_j \leq 0.99, \quad 0.01 \leq \theta_p^j \leq \pi - 0.01, \quad v_p^k \geq 1.01 \text{ or } \leq -1.01 \quad (4.5.11)$$

The rotated data are given in tables 8, 9, 10 and 11, the computational results after local minimization with respect to parameters are given in table 12. EM data [81] are given in tables 13, 14, 15 & 16.

(B) EM'S Unrotated Data:

Now, we use EM data for solutions A,B,C,D to test the sum-rule inequality for $\Pi^+\Pi^-$ scattering in the inelastic region. If the errors are uncorrelated, then

$$[\Delta f(x_i)]^2 = \sum_{i=1}^N |\Delta x_i|^2 \left| \frac{\partial f(x_i)}{\partial x_i} \right|^2 \quad (4.5.12)$$

gives the square of the error in function f of x_i . The amplitude is expressed by

$$F^{(+)}(s,0) = (s/(s-4))^{\frac{1}{2}} \{ f_0 + \sqrt{3}f_1 + \sqrt{5}f_2 + \sqrt{7}f_3 \} \quad (4.5.13)$$

and the error is expressed by (4.5.12). The same program is applied to get the minimum values of integrals (4.5.9) with respect to the parameterization. The results are presented in table 17.

(C) FP data [68,68a]:

We use FP DATA [68,68a] to test the sum-rule inequality (4.5.9). The forward amplitude has the combination:

$$F^{(+)}(s,0) = 2/3.F^{(0)}(s,0) + F^{(1)}(s,0) + 1/3.F^{(2)}(s,0). \quad (4.5.14)$$

The corresponding errors are supposed to be uncorrelated:

$$[\Delta F^{(+)}(s,0)]^2 = 4/9.|\Delta F^{(0)}|^2 + |\Delta F^{(1)}|^2 + 1/9.|\Delta F^{(2)}|^2 \quad (4.5.15)$$

The results correspond to smoother behaviour of partial waves for $S_0, D_0, P_1, F_1, S_2, D_2$. " S_0 " wave is out of unitary circle from 1.23Gev to 1.37Gev of energy. However, D_0 wave is completely inside the unitary circle. Similar is the situation with P_1 and F_1 waves. S_2 and D_2 are confined to a very small region of argand diagrams. The scattering amplitude $F^{(+)}(s,0)$ has similar movement as in the published paper [68,68a].

The data are presented in table 18. The results of test for sum-rule inequality are given in table 19, and our phase shift analysis in the inelastic region are given in table 20.

Table 8:EM -solution A (Rotated by Common)

M_{Tl} GeV	$ s $	$\pm \Delta s $	d_s	$\pm \Delta d_s$	$ p $	$\pm \Delta p $	d_p	$\pm \Delta d_p$	$ D $	$\pm \Delta D $	d_D	$\pm \Delta d_D$	$ F $	$\pm \Delta F $	d_F	$\pm \Delta d_F$
1.01063	0.07		80.1	6.8	0.40	0.11	151.5	4.6	0.40	0.05	29.8	0.0	0.03	0.0	18.50	0.0
1.03064	0.06		83.0	6.5	0.32	0.10	146.9	4.2	0.43	0.05	29.4	0.0	0.03	0.0	16.70	0.0
1.05056	0.10		88.3	5.7	0.46	0.10	153.9	4.5	0.43	0.04	29.0	0.0	0.03	0.0	14.8	0.0
1.07071	0.06		81.7	7.1	0.35	0.11	150.1	4.6	0.42	0.05	31.0	0.0	0.04	0.0	14.9	0.0
1.09061	0.09		91.4	5.4	0.45	0.10	157.0	4.6	0.50	0.04	33.0	0.0	0.04	0.0	14.7	0.0
1.11061	0.10		92.4	4.8	0.42	0.11	156.0	5.4	0.65	0.03	35.2	0.0	0.05	0.0	14.2	0.0
1.13045	0.16		88.8	12.8	0.46	0.15	142.6	14.2	0.74	0.03	37.2	0.0	0.05	0.0	13.2	0.0
1.15064	0.10		98.8	4.3	0.29	0.11	147.9	4.1	0.69	0.03	40.0	0.0	0.06	0.0	11.5	0.0
1.17056	0.10		93.4	5.3	0.29	0.08	144.4	3.9	0.87	0.03	45.2	0.0	0.06	0.0	11.6	0.0
1.19073	0.09		101.8	4.7	0.18	0.12	139.1	12.8	0.88	0.04	50.4	0.0	0.07	0.0	10.3	0.0
1.21064	0.14		97.9	10.4	0.19	0.20	127.6	33.5	1.07	0.03	57.8	0.0	0.07	0.0	9.6	0.0
1.23070	0.11		107.2	9.3	0.23	0.22	139.5	27.8	1.11	0.03	67.4	0.0	0.08	0.0	9.3	0.0
1.25064	0.13		97.2	17.3	0.36	0.24	146.2	14.6	1.26	0.03	77.0	0.0	0.09	0.0	7.6	0.0
1.27062	0.11		102.6	19.6	0.30	0.22	149.6	23.0	1.27	0.03	87.8	0.0	0.10	0.0	6.4	0.0

Table 8 (Continued)

TT GeV	S	$\pm\Delta S $	δ_s	$\pm\Delta\delta_s$	P	$\pm\Delta P $	δ_p	$\pm\Delta\delta_p$	D	$\pm\Delta D $	δ_D	$\pm\Delta\delta_D$	F	$\pm\Delta F $	δ_F	$\pm\Delta\delta_F$
1.29	0.63	0.08	109.9	10.2	0.53	0.12	172.5	4.5	1.16	0.03	98.6	0.0	0.11	0.0	5.8	0.0
1.31	0.65	0.08	105.6	14.8	0.40	0.13	161.6	13.9	1.19	0.03	107.6	0.0	0.12	0.0	4.8	0.0
1.33	0.67	0.13	95.7	18.1	0.32	0.15	141.3	20.3	1.11	0.05	114.8	0.0	0.13	0.0	3.8	0.0
1.35	0.62	0.11	116.6	12.1	0.47	0.12	180.0	9.3	0.94	0.04	122.0	0.0	0.14	0.0	4.6	0.0
1.37	0.54	0.10	125.9	14.3	0.53	0.15	192.7	10.0	0.87	0.05	126.8	0.0	0.11	0.01	48.7	26.8
1.39	0.47	0.08	134.9	9.5	0.60	0.20	201.4	10.4	0.79	0.09	131.6	0.0	0.11	0.02	45.6	35.1
1.41	0.53	0.20	132.5	24.8	0.41	0.30	191.3	35.7	0.79	0.09	134.2	0.0	0.13	0.08	160	60.2
1.43	0.57	0.13	132.6	14.6	0.25	0.06	160.4	9.9	0.78	0.08	134.6	0.0	0.23	0.07	0.7	15.1
1.45	0.53	0.11	137.7	19.1	0.23	0.06	152.9	46.9	0.72	0.08	135.0	0.0	0.27	0.06	234	15.0
1.47	0.47	0.12	127.5	18.0	0.45	0.15	189.9	10.0	0.51	0.06	135.4	0.0	0.17	0.04	35.2	29.2
1.49	0.34	0.18	144.8	37.4	0.47	0.27	199.0	20.0	0.55	0.14	135.8	0.0	0.16	0.03	339	20.1
1.51	0.36	0.12	132.8	27.2	0.23	0.09	174.9	33.4	0.59	0.07	136.4	0.0	0.27	0.05	9.3	10.6
1.53	0.33	0.10	139.7	22.1	0.28	0.05	162.4	23.5	0.59	0.07	137.2	0.0	0.32	0.05	28.1	5.9
1.55	0.36	0.07	132.7	13.7	0.30	0.05	134.4	18.6	0.58	0.09	138.0	0.0	0.39	0.04	56.2	24.3
1.57	0.46	0.46	134.3	10.0	0.26	0.04	147.3	14.4	0.62	0.13	140.0	3.4	0.42	0.03	513	0.0
1.59	0.42	0.42	130.2	13.2	0.25	0.05	139.5	29.0	0.57	0.12	142.0	3.9	0.45	0.04	468	0.0
1.61	0.39	0.39	129.9	10.3	0.33	0.03	159.3	9.3	0.64	0.09	143.6	3.5	0.43	0.03	517	0.0

Table 8 (continued)

$M_{\pi\pi}$ Gev	$ s $	$\pm\Delta s $	δ_s	$\pm\Delta\delta_s$	$ p $	$\pm\Delta p $	δ_p	$\pm\Delta\delta_p$	$ D $	$\pm\Delta D $	δ_D	$\pm\Delta\delta_D$	$ F $	$\pm\Delta F $	δ_F	$\pm\Delta\delta_F$
1.63	0.38	0.15	124.4	10.6	0.29	0.06	134.8	20.5	0.59	0.11	144.8	3.2	0.57	0.03	60.2	0.0
1.65	0.39	0.05	123.3	8.5	0.29	0.03	118.2	12.4	0.61	0.13	146.0	2.4	0.64	0.03	59.7	0.0
1.67	0.40	0.13	123.8	11.8	0.25	0.06	139.1	23.6	0.61	0.10	150.0	3.7	0.60	0.03	74.7	0.0
1.69	0.40	0.13	124.9	13.2	0.22	0.06	118.1	28.0	0.55	0.13	154.0	4.0	0.67	0.03	77.0	0.0
1.71	0.43	0.11	124.0	16.1	0.23	0.06	144.9	32.1	0.58	0.10	156.0	5.9	0.64	0.03	96.2	0.0
1.73	0.40	0.12	115.5	20.6	0.31	0.10	153.0	25.0	0.56	0.07	156.0	6.0	0.63	0.03	101.5	0.0
1.75	0.37	0.11	117.8	20.8	0.35	0.11	184.7	16.5	0.49	0.08	156.0	11.3	0.56	0.03	118.0	0.0
1.77	0.38	0.05	111.9	19.9	0.29	0.04	174.2	11.4	0.54	0.11	155.2	5.3	0.55	0.04	112.8	0.0
1.79	0.42	0.05	117.4	16.1	0.21	0.06	95.4	55.3	0.53	0.06	154.4	7.4	0.55	0.03	105.0	0.0

Table 9: EM -solution B (Rotated by Common)

M_{TT} GeV	$ s_1 $	$ \Delta s_1 $	d_s	Δd_s	$ p_1 $	$ \Delta p_1 $	d_p	Δd_p	$ D_1 $	$ \Delta D_1 $	d_D	Δd_D	$ F_1 $	$ \Delta F_1 $	d_F	Δd_F
1.01	0.63	0.07	81.9	6.8	0.40	0.11	153.3	4.6	0.40	0.05	31.6	0.0	0.03	0.0	20.3	0.0
1.03	0.64	0.06	84.4	6.5	0.32	0.10	148.3	4.2	0.43	0.05	30.8	0.0	0.03	0.0	18.1	0.0
1.05	0.56	0.10	89.3	5.7	0.46	0.10	154.9	4.5	0.43	0.04	30.0	0.0	0.03	0.0	15.8	0.0
1.07	0.71	0.06	81.5	7.1	0.35	0.11	149.9	4.6	0.42	0.05	30.8	0.0	0.04	0.0	14.7	0.0
1.09	0.61	0.09	90.0	5.4	0.45	0.10	155.6	4.6	0.50	0.04	31.6	0.0	0.04	0.0	13.3	0.0
1.11	0.61	0.10	92.0	4.8	0.42	0.11	155.6	5.4	0.65	0.03	34.8	0.0	0.05	0.0	13.8	0.0
1.13	0.45	0.16	91.6	12.8	0.46	0.15	145.4	14.2	0.74	0.03	40.4	0.0	0.05	0.0	16.0	0.0
1.15	0.64	0.10	104.8	4.3	0.29	0.11	153.9	4.1	0.69	0.03	46.0	0.0	0.06	0.0	17.5	0.0
1.17	0.56	0.10	97.8	5.3	0.29	0.08	148.8	3.9	0.87	0.03	49.6	0.0	0.06	0.0	16.0	0.0
1.19	0.73	0.09	104.6	4.7	0.18	0.12	141.9	12.8	0.88	0.04	53.2	0.0	0.07	0.0	13.1	0.0
1.21	0.64	0.14	99.5	10.4	0.19	0.20	129.2	33.5	1.07	0.03	59.4	0.0	0.07	0.0	11.2	0.0
1.23	0.70	0.11	108.0	9.3	0.23	0.22	140.3	27.8	1.11	0.03	68.2	0.0	0.08	0.0	10.1	0.0
1.25	0.75	0.06	108.3	8.7	0.19	0.11	117.1	30.1	1.23	0.03	77.0	0.0	0.09	0.0	7.6	0.0
1.27	0.71	0.10	114.1	11.9	0.16	0.10	93.3	40.1	1.25	0.05	85.4	0.0	0.10	0.0	4.0	0.0
1.29	0.89	0.07	128.5	6.3	0.21	0.10	73.9	40.9	1.10	0.06	93.8	0.0	0.11	0.0	1.0	0.0
1.31	0.76	0.08	128.5	10.5	0.40	0.16	57.3	17.9	1.13	0.03	100.8	0.0	0.12	0.0	-20.0	0.0
1.33	0.67	0.07	125.5	12.6	0.32	0.11	80.2	27.0	1.11	0.02	106.4	0.0	0.13	0.0	-46.0	0.0

Table 9 (continued)

RF GeV	S	$\pm\Delta S $	δ_s	$\pm\Delta\delta_s$	P	$\pm\Delta P $	δ_p	$\pm\Delta\delta_p$	D	$\pm\Delta D $	δ_D	$\pm\Delta\delta_D$	F	$\pm\Delta F $	δ_F	$\pm\Delta\delta_F$
1.35	0.72	0.11	140.7	10.8	0.54	0.19	61.5	13.1	0.84	0.07	112.0	0.0	0.14	0.0	5.4	0.0
1.37	0.71	0.11	138.5	14.7	0.30	0.26	77.0	30.5	0.86	0.05	114.4	0.0	0.11	0.02	66.4	7.00
1.39	0.71	0.11	144.6	13.2	0.28	0.29	82.3	40.2	0.79	0.05	116.8	0.0	0.11	0.02	66.1	82.3
1.41	0.64	0.23	141.6	19.9	0.30	0.25	84.5	30.7	0.77	0.10	119.4	0.0	0.11	0.02	61.3	60.6
1.43	0.52	0.17	140.1	29.1	0.52	0.30	69.8	24.5	0.67	0.13	122.2	0.0	0.23	0.08	9.4	15.0
1.45	0.47	0.16	150.4	22.6	0.56	0.25	76.0	16.2	0.57	0.13	125.0	0.0	0.27	0.06	7.2	15.7
1.47	0.48	0.18	143.2	31.0	0.41	0.20	80.0	28.9	0.51	0.05	129.0	0.0	0.17	0.02	58.3	26.4
1.49	0.51	0.14	161.5	13.1	0.29	0.16	101.6	20.4	0.54	0.06	133.0	0.0	0.16	0.03	48.7	31.1
1.51	0.32	0.12	168.0	26.1	0.45	0.13	88.1	15.6	0.48	0.08	136.2	0.0	0.27	0.05	2.0	12.7
1.53	0.27	0.09	178.0	19.9	0.53	0.13	106.8	11.0	0.43	0.10	138.6	0.0	0.32	0.03	22.1	7.7
1.55	0.20	0.08	160.5	46.4	0.59	0.12	109.1	11.9	0.42	0.13	141.0	0.0	0.39	0.04	34.5	7.1
1.57	0.14	0.09	173.9	30.5	0.73	0.08	120.6	10.6	0.32	0.14	141.8	8.2	0.42	0.05	54.4	0.0
1.59	0.12	0.07	160.7	50.2	0.67	0.08	114.0	6.7	0.33	0.15	142.6	7.2	0.45	0.04	43.6	0.0
1.61	0.10	0.07	160.5	50.2	0.71	0.08	124.4	7.3	0.38	0.14	143.0	6.4	0.43	0.04	49.7	0.0
1.65	0.09	0.15	99.6	40.4	0.68	0.08	128.2	8.4	0.36	0.15	143.0	7.2	0.57	0.04	62.0	0.0
1.65	0.10	0.14	85.1	45.2	0.69	0.07	120.1	6.7	0.35	0.17	143.0	6.2	0.65	0.03	59.4	0.0
1.67	0.15	0.13	68.7	32.9	0.68	0.06	144.0	7.3	0.34	0.13	144.6	12.6	0.60	0.03	81.9	0.0

Table 9(continued)

Mid Gen	S	$\pm\Delta S $	σ_s	$\pm\Delta\sigma_s$	P	$\pm\Delta P $	σ_p	$\pm\Delta\sigma_p$	D	$\pm\Delta D $	σ_D	$\pm\Delta\sigma_D$	F	$\pm\Delta F $	σ_F	$\pm\Delta\sigma_F$
1.71	0.30	0.12	87.5	20.9	0.59	0.07	168.7	9.9	0.37	0.09	147.6	17.7	0.64	0.03	1100	0.0
1.73	0.33	0.12	91.8	21.5	0.52	0.10	162.4	13.6	0.44	0.10	148.8	15.0	0.63	0.03	1064	0.0
1.75	0.37	0.13	111.7	20.9	0.35	0.11	178.7	16.8	0.49	0.08	150.0	11.5	0.56	0.03	1120	0.0
1.77	0.36	0.11	101.9	30.8	0.40	0.18	179.7	21.9	0.49	0.12	152.4	20.9	0.55	0.03	1179	0.0
1.79	0.41	0.15	101.0	29.3	0.46	0.31	187.4	24.1	0.35	0.07	154.8	61.5	0.55	0.03	1460	0.0

Table 10: EM-solution C (Rotated by Common)

M_{DF} Gev	$ S $	$\pm \Delta S $	d_s	$\pm \Delta d_s$	$ P $	$\pm \Delta P $	d_p	$\pm \Delta d_p$	$ D $	$\pm \Delta D $	d_D	$\pm \Delta d_D$	$ F $	$\pm \Delta F $	d_F	$\pm \Delta d_F$
1.01	0.63	0.07	81.9	6.8	0.40	0.11	153.3	4.6	0.40	0.05	31.6	0.0	0.03	0.0	20.3	0.0
1.03	0.64	0.06	84.4	6.5	0.32	0.10	148.3	4.2	0.43	0.05	30.8	0.0	0.03	0.0	18.1	0.0
1.05	0.56	0.10	89.3	5.7	0.46	0.10	154.9	4.5	0.43	0.04	30.0	0.0	0.03	0.0	15.8	0.0
1.07	0.71	0.06	81.5	7.1	0.35	0.11	149.9	4.6	0.42	0.05	30.8	0.0	0.04	0.0	14.7	0.0
1.09	0.61	0.09	90.0	5.4	0.45	0.10	155.6	4.6	0.50	0.04	31.6	0.0	0.04	0.0	13.3	0.0
1.11	0.61	0.10	92.0	4.8	0.42	0.11	155.6	5.4	0.65	0.03	34.8	0.0	0.05	0.0	13.8	0.0
1.13	0.45	0.16	91.6	12.8	0.46	0.15	145.4	14.2	0.74	0.03	40.4	0.0	0.05	0.0	16.0	0.0
1.15	0.64	0.10	104.8	4.3	0.29	0.11	153.9	4.1	0.69	0.03	46.0	0.0	0.06	0.0	17.5	0.0
1.17	0.56	0.10	97.0	5.3	0.29	0.08	148.0	3.9	0.87	0.03	48.8	0.0	0.06	0.0	15.2	0.0
1.19	0.73	0.09	103.0	4.7	0.18	0.12	140.3	12.8	0.88	0.04	51.6	0.0	0.07	0.0	11.5	0.0
1.21	0.64	0.14	97.9	10.4	0.19	0.20	127.6	33.5	1.07	0.03	57.8	0.0	0.07	0.0	9.6	0.0
1.23	0.70	0.11	107.2	9.3	0.23	0.22	139.5	27.8	1.11	0.03	67.4	0.0	0.08	0.0	9.3	0.0
1.25	0.64	0.13	97.2	17.3	0.36	0.24	146.2	14.6	1.26	0.03	77.0	0.0	0.09	0.0	7.6	0.0
1.27	0.62	0.11	103.4	19.6	0.30	0.22	150.4	23.0	1.27	0.03	88.6	0.0	0.10	0.0	7.2	0.0
1.29	0.63	0.08	111.5	10.2	0.53	0.12	174.1	4.5	1.16	0.03	100.2	0.0	0.11	0.0	7.4	0.0
1.31	0.65	0.08	106.2	14.8	0.40	0.13	162.2	13.9	1.19	0.03	108.2	0.0	0.12	0.0	5.4	0.0
1.33	0.67	0.13	93.5	18.1	0.32	0.15	139.1	20.3	1.11	0.05	112.6	0.0	0.13	0.0	1.6	0.0

Table 10 (continued)

RT GeV	s	$\pm\Delta s $	δ_s	$\pm\Delta\delta_s$	p	$\pm\Delta p $	δ_p	$\pm\Delta\delta_p$	D	$\pm\Delta D $	δ_D	$\pm\Delta\delta_D$	F	$\pm\Delta F $	δ_F	$\pm\Delta\delta_F$
1.35	0.62	0.11	111.6	12.1	0.47	0.12	175.0	9.3	0.94	0.04	117.0	0.0	0.14	0.0	0.4	0.0
1.37	0.54	0.10	123.7	14.3	0.53	0.15	190.5	10.0	0.87	0.05	124.6	0.0	0.11	0.01	50.9	26.8
1.39	0.47	0.08	135.5	9.5	0.60	0.21	202.0	10.4	0.79	0.09	132.2	0.0	0.11	0.02	45.0	35.1
1.41	0.53	0.20	134.1	24.8	0.41	0.30	192.9	35.7	0.79	0.09	135.8	0.0	0.13	0.08	15.3	60.2
1.43	0.57	0.13	133.4	14.6	0.25	0.06	161.2	9.9	0.78	0.08	135.4	0.0	0.23	0.07	10.0	15.1
1.45	0.53	0.11	137.7	19.1	0.23	0.06	152.9	46.9	0.72	0.08	135.0	0.0	0.27	0.06	23.4	15.0
1.47	0.46	0.42	125.9	70.5	0.44	0.41	188.8	58.2	0.51	0.05	136.2	0.0	0.17	0.02	35.3	28.9
1.49	0.51	0.15	108.8	21.5	0.29	0.28	168.1	54.0	0.54	0.05	137.4	0.0	0.16	0.03	40.0	78.4
1.51	0.50	0.09	105.4	23.3	0.17	0.06	109.3	50.9	0.50	0.09	138.6	0.0	0.27	0.05	3.3	12.4
1.53	0.55	0.07	103.4	19.5	0.28	0.10	93.1	37.6	0.40	0.10	139.8	0.0	0.32	0.05	21.1	19.0
1.55	0.54	0.09	110.2	20.2	0.34	0.12	95.6	29.8	0.40	0.14	141.0	0.0	0.39	0.04	33.8	8.0
1.57	0.64	0.09	127.2	14.0	0.32	0.17	98.5	39.6	0.39	0.15	143.8	7.4	0.42	0.03	55.9	0.0
1.59	0.59	0.07	120.1	9.0	0.33	0.06	98.0	14.0	0.39	0.20	146.6	5.7	0.45	0.03	46.6	0.0
1.61	0.65	0.10	115.9	11.8	0.32	0.10	107.0	37.4	0.39	0.18	145.6	6.2	0.43	0.04	52.4	0.0
1.63	0.62	0.08	121.2	8.9	0.37	0.11	93.9	22.8	0.28	0.20	140.8	11.3	0.57	0.03	62.3	0.0
1.65	0.61	0.07	114.4	8.5	0.41	0.09	77.5	15.7	0.26	0.16	136.0	9.4	0.64	0.03	54.6	0.0
1.67	0.64	0.06	134.3	8.8	0.37	0.11	90.7	21.2	0.23	0.15	129.6	34.1	0.60	0.03	80.9	0.0

Table 10(Continued)

$M_{\pi\pi}$ Gev	$ S $	$\pm\Delta S $	δ_s	$\pm\Delta\delta_s$	$ P $	$\pm\Delta P $	δ_p	$\pm\Delta\delta_p$	$ D $	$\pm\Delta D $	δ_D	$\pm\Delta\delta_D$	$ F $	$\pm\Delta F $	δ_F	$\pm\Delta\delta_F$
1.69	0.60	0.05	125.2	7.8	0.36	0.08	73.9	16.2	0.21	0.12	123.2	15.2	0.67	0.03	68.8	0.0
1.71	0.61	0.07	150.6	9.7	0.35	0.11	96.5	24.3	0.30	0.05	116.8	35.2	0.64	0.03	104.6	0.0
1.73	0.58	0.08	156.7	12.4	0.36	0.08	113.4	30.6	0.33	0.05	110.4	33.5	0.63	0.03	119.4	0.0
1.75	0.54	0.06	143.8	14.2	0.22	0.05	133.4	48.1	0.39	0.06	104.0	23.7	0.66	0.03	116.8	0.0
1.77	0.54	0.11	153.8	20.1	0.26	0.14	104.1	48.8	0.42	0.08	104.4	30.1	0.55	0.04	121.0	0.0
1.79	0.42	0.15	168.5	26.5	0.46	0.15	72.5	47.5	0.35	0.06	104.8	51.9	0.55	0.03	113.0	0.0

(124)

Table 11: EM-solution D (Rotated by Common)

IT Gev	S	$\pm\Delta S $	δ_s	$\pm\Delta\delta_s$	P	$\pm\Delta P $	δ_p	$\pm\Delta\delta_p$	D	$\pm\Delta D $	δ_D	$\pm\Delta\delta_D$	F	$\pm\Delta F $	δ_F	$\pm\Delta\delta_F$
1.01	0.63	0.07	81.9	6.8	0.40	0.11	153.3	4.6	0.40	0.05	31.6	0.0	0.03	0.0	20.3	0.0
1.03	0.64	0.06	84.4	6.5	0.32	0.10	148.3	4.2	0.43	0.05	30.8	0.0	0.03	0.0	18.1	0.0
1.05	0.56	0.10	89.3	5.7	0.46	0.10	154.9	4.5	0.43	0.04	30.0	0.0	0.03	0.0	15.8	0.0
1.07	0.71	0.06	81.5	7.1	0.35	0.11	149.9	4.6	0.42	0.05	30.8	0.0	0.04	0.0	14.7	0.0
1.09	0.61	0.09	90.0	5.4	0.45	0.10	155.6	4.6	0.50	0.04	31.6	0.0	0.04	0.0	13.3	0.0
1.11	0.61	0.10	90.0	4.8	0.42	0.11	153.6	5.4	0.65	0.03	32.8	0.0	0.05	0.0	11.8	0.0
1.13	0.45	0.16	85.6	12.8	0.46	0.15	139.4	14.2	0.74	0.03	34.4	0.0	0.05	0.0	10.0	0.0
1.15	0.64	0.10	94.8	4.3	0.29	0.11	143.9	4.1	0.69	0.03	36.0	0.0	0.06	0.0	7.5	0.0
1.17	0.56	0.10	89.8	5.3	0.29	0.08	140.8	3.9	0.87	0.03	41.6	0.0	0.06	0.0	8.0	0.0
1.19	0.73	0.09	98.6	4.7	0.18	0.12	135.9	12.8	0.88	0.04	47.2	0.0	0.07	0.0	7.1	0.0
1.21	0.64	0.14	94.5	10.4	0.19	0.20	124.2	33.5	1.07	0.03	54.4	0.0	0.07	0.0	6.2	0.0
1.23	0.70	0.11	103.0	9.3	0.23	0.22	135.3	27.8	1.11	0.03	63.2	0.0	0.08	0.0	5.1	0.0
1.25	0.75	0.06	103.3	8.7	0.19	0.11	112.1	30.1	1.23	0.03	72.0	0.0	0.09	0.0	2.6	0.0
1.27	0.71	0.10	108.7	11.9	0.16	0.10	87.9	40.1	1.25	0.05	80.0	0.0	0.10	0.0	-1.4	0.0
1.29	0.89	0.07	122.7	6.3	0.21	0.10	68.1	40.9	1.10	0.06	88.0	0.0	0.11	0.0	-4.8	0.0
1.31	0.76	0.08	123.7	10.5	0.40	0.16	52.5	17.9	1.13	0.03	96.0	0.0	0.12	0.0	-6.8	0.0
1.33	0.67	0.07	123.1	12.6	0.32	0.11	77.8	27.0	1.11	0.02	104.0	0.0	0.13	0.0	-7.0	0.0

(125)

Table 11(Continued)

M_{II} Gev	$ s $	$\pm\Delta s $	δ_s	$\pm\Delta\delta_s$	$ p $	$\pm\Delta p $	δ_p	$\pm\Delta\delta_p$	$ D $	$\pm\Delta D $	δ_D	$\pm\Delta\delta_D$	$ F $	$\pm\Delta F $	δ_F	$\pm\Delta\delta_F$
1.35	0.72	0.11	140.7	10.8	0.54	0.19	61.5	13.1	0.84	0.07	112.0	0.0	0.14	0.0	5.4	0.0
1.37	0.71	0.11	141.7	14.7	0.30	0.26	80.2	30.5	0.86	0.05	117.6	0.0	0.11	0.02	63.2	7.00
1.39	0.71	0.11	151.0	13.2	0.28	0.29	88.7	40.2	0.79	0.05	123.2	0.0	0.11	0.02	59.7	82.3
1.41	0.47	0.13	126.6	24.9	0.57	0.14	62.4	11.6	0.73	0.06	127.8	0.0	0.13	0.05	30.3	38.8
1.43	0.40	0.17	122.1	30.2	0.67	0.15	63.7	18.4	0.62	0.12	131.4	0.0	0.23	0.07	4.7	12.8
1.45	0.29	0.15	101.1	50.4	0.77	0.12	62.1	16.6	0.43	0.13	135.0	0.0	0.27	0.06	7.3	7.5
1.47	0.44	0.45	146.0	78.4	0.45	0.41	83.8	56.1	0.51	0.06	138.6	0.0	0.17	0.02	50.6	30.7
1.49	0.33	0.10	133.1	23.0	0.47	0.04	78.9	7.4	0.55	0.08	142.2	0.0	0.16	0.02	47.7	19.9
1.51	0.20	0.06	113.0	14.4	0.57	0.06	73.6	11.0	0.41	0.07	145.2	0.0	0.27	0.06	5.5	12.7
1.53	0.25	0.07	77.4	16.4	0.63	0.06	80.6	5.6	0.27	0.06	147.6	0.0	0.32	0.04	11.4	4.6
1.55	0.27	0.07	96.4	15.1	0.66	0.06	97.5	4.9	0.26	0.05	150.0	0.0	0.40	0.03	32.3	4.3
1.57	0.28	0.06	101.7	15.7	0.75	0.05	125.9	6.4	0.11	0.07	150.0	30.6	0.43	0.04	67.4	0.0
1.59	0.11	0.07	167.8	60.5	0.67	0.08	121.4	6.7	0.33	0.15	150.0	7.2	0.45	0.04	51.0	0.0
1.6	0.36	0.08	62.1	14.3	0.72	0.05	95.6	8.9	0.14	0.05	131.6	14.8	0.43	0.04	32.9	0.0
1.63	0.42	0.09	88.2	14.2	0.65	0.08	117.9	12.1	0.06	0.07	94.8	80.1	0.57	0.03	63.5	0.0
1.65	0.40	0.13	84.1	14.9	0.67	0.07	110.3	11.7	0.04	0.03	58.0	100.9	0.64	0.03	60.2	0.0
1.67	0.48	0.06	107.7	12.4	0.58	0.07	143.5	8.1	0.19	0.05	58.4	20.0	0.60	0.02	94.6	0.0

Table 11(continued)

\sqrt{s} GeV	$ S $	$\pm\Delta S $	δ_s	$\pm\Delta\delta_s$	$ P $	$\pm\Delta P $	δ_p	$\pm\Delta\delta_p$	$ D $	$\pm\Delta D $	δ_D	$\pm\Delta\delta_D$	$ F $	$\pm\Delta F $	δ_F	$\pm\Delta\delta_F$
1.69	0.42	0.10	115.6	15.2	0.57	0.09	153.4	12.1	0.19	0.14	58.8	42.3	0.68	0.03	104.20	0.0
1.71	0.52	0.06	108.2	14.0	0.42	0.08	140.4	14.7	0.37	0.06	62.0	12.4	0.64	0.03	98.60	0.0
1.75	0.55	0.06	117.4	17.3	0.35	0.09	125.5	31.5	0.39	0.11	68.0	21.0	0.63	0.03	101.30	0.0
1.75	0.54	0.06	113.8	13.9	0.22	0.05	103.1	49.9	0.39	0.06	74.0	23.1	0.56	0.03	86.90	0.0
1.77	0.53	0.09	128.8	25.2	0.22	0.07	114.9	69.5	0.45	0.12	80.4	24.2	0.55	0.03	108.20	0.0
1.79	0.42	0.13	123.6	43.4	0.20	0.25	143.8	103.4	0.53	0.19	86.8	17.7	0.55	0.03	136.60	0.0

Table 12: Test of sum-rule Inequality of EM'S Rotated solutions.

sol	N_1	R	A	VPK	ANS 1	Ans 2	FINANS
A	1	0.99	0.010000122	1.0000000	-9.0453	4.3329	-4.712
	2	0.99	0.01000000	1.0000000			
		0.99	0.01000000	1.0174767	-90.2949	26.309	-63.986
	3	0.99	0.94988243	1.000094	-258.8537		
		0.99	0.0100000	1.0000004			
		0.99	0.0100000	1.0000087	-258.8537	106.74	-152.115
B	1	0.5438	0.015491386	1.0000006	-6.8938	2.4918	-4.402
	2	0.99	0.0100000	1.0000006	-95.3637	35.8037	-59.56
		0.99	0.0100000	1.0047628			
	3	0.99	0.0100000	1.0000005			
		0.99	0.0140748	1.0000045			
		0.99	0.0100000	1.0000005	-273.9860	151.145	-22.839
C	1	0.693	0.0100000	1.000000	-7.8839	3.6456	-4.238
	2	0.99	0.010000	1.0006153			
		0.99	0.0100000	1.00000	-94.0818	38.166	-55.916
	3	0.99	0.073761499	1.000000			
		0.99	0.96557566	1.0000117			
		0.99	0.0100000	1.0000032	-335.1028	168.714	-166.39
D	1	0.4956	0.0100000	1.0000000	-7.6083	2.2043	-5.4039
	2	0.99	0.01000000	1.0000001			
		0.99	0.0100000	1.0000098	-101.2619	35.269	-65.993
	3	0.99	0.0100000	1.0000079			
		0.99	1.0769872	1.0000041			
		0.99	0.0100000	1.0000001	-289.3262	141.69	-147.65

Table 13: EM-data for solution A.

M_{FF} Gev.	$ S $	$\pm\Delta S $	d_S	$\pm\Delta d_S$	$ P $	$\pm\Delta P $	d_p	$\pm\Delta d_p$	$ D $	$\pm\Delta D $	d_D	$\pm\Delta d_D$	$ F $	$\pm\Delta F $	d_F	$\pm\Delta d_F$
1.01	0.63	0.07	140.3	6.8	0.40	0.11	211.7	4.6	0.40	0.05	90.0	0.0	0.03	0.0	78.7	0.0
1.03	0.64	0.06	143.6	6.5	0.32	0.10	207.5	4.2	0.43	0.05	90.0	0.0	0.03	0.0	77.3	0.0
1.05	0.56	0.10	149.3	5.7	0.46	0.10	214.9	4.5	0.43	0.04	90.0	0.0	0.03	0.0	75.8	0.0
1.07	0.71	0.06	140.7	7.1	0.35	0.11	209.1	4.6	0.42	0.05	90.0	0.0	0.04	0.0	73.9	0.0
1.09	0.61	0.09	148.4	5.4	0.45	0.10	214.0	4.6	0.50	0.04	90.0	0.0	0.04	0.0	71.7	0.0
1.11	0.61	0.10	147.2	4.8	0.42	0.11	210.8	5.4	0.65	0.03	90.0	0.0	0.05	0.0	69.0	0.0
1.13	0.45	0.16	141.2	12.8	0.46	0.15	195.0	14.2	0.74	0.03	90.0	0.0	0.05	0.0	65.6	0.0
1.15	0.64	0.10	148.8	4.3	0.29	0.11	197.9	4.1	0.69	0.03	90.0	0.0	0.06	0.0	61.5	0.0
1.17	0.56	0.10	138.2	5.3	0.29	0.08	189.2	3.9	0.87	0.03	90.0	0.0	0.06	0.0	56.4	0.0
1.19	0.73	0.09	141.4	4.7	0.18	0.12	178.7	12.8	0.88	0.04	90.0	0.0	0.07	0.0	49.9	0.0
1.21	0.64	0.14	130.1	10.4	0.19	0.2	159.8	33.5	1.07	0.03	90.0	0.0	0.07	0.0	41.8	0.0
1.23	0.70	0.11	129.8	9.3	0.23	0.22	162.1	27.8	1.11	0.03	90.0	0.0	0.08	0.0	31.9	0.0
1.25	0.64	0.13	110.2	17.3	0.36	0.24	159.2	14.6	1.26	0.03	90.0	0.0	0.09	0.0	20.6	0.0
1.27	0.62	0.11	104.8	19.6	0.30	0.22	151.8	23.0	1.27	0.03	90.0	0.0	0.10	0.0	8.6	0.0
1.29	0.63	0.08	101.3	10.2	0.53	0.12	163.9	4.5	1.16	0.03	90.0	0.0	0.11	0.0	-2.8	0.0
1.31	0.65	0.08	88.0	14.8	0.40	0.13	144.0	13.9	1.19	0.03	90.0	0.0	0.12	0.0	-12.8	0.0
1.33	0.67	0.13	70.9	18.1	0.32	0.15	116.5	20.3	1.11	0.05	90.0	0.0	0.13	0.0	-21.0	0.0

(129)

Table 13 (Continued)

(130)

HT GeV	S	$\pm\Delta S $	d_s	$\pm\Delta d_s$	P	$\pm\Delta P $	d_p	$\pm\Delta d_p$	D	$\pm\Delta D $	d_D	$\pm\Delta d_D$	F	$\pm\Delta F $	d_F	$\pm\Delta d_F$
1.35	0.62	0.11	84.6	12.1	0.47	0.12	148.0	9.3	0.94	0.04	90.0	0.0	0.14	0.0	-27.4	0.0
1.37	0.54	0.10	89.1	14.3	0.53	0.15	155.9	10.0	0.87	0.05	90.0	0.0	0.11	0.01	-85.5	26.8
1.39	0.47	0.08	93.3	9.5	0.60	0.21	159.8	10.4	0.79	0.09	90.0	0.0	0.11	0.02	-87.2	35.1
1.41	0.53	0.20	88.3	24.8	0.41	0.30	147.1	35.7	0.79	0.09	90.0	0.0	0.13	0.08	-61.1	60.2
1.43	0.57	0.13	88.0	14.6	0.25	0.06	115.8	9.9	0.78	0.08	90.0	0.0	0.23	0.07	-35.4	15.10
1.45	0.53	0.11	92.7	19.1	0.23	0.06	107.9	46.9	0.72	0.08	90.0	0.0	0.27	0.06	-21.6	15.0
1.47	0.47	0.12	82.1	18.0	0.45	0.15	144.5	10.0	0.51	0.06	90.0	0.0	0.17	0.04	-80.6	29.2
1.49	0.34	0.18	99.0	37.4	0.47	0.27	153.2	20.2	0.55	0.14	90.0	0.0	0.16	0.03	-79.7	20.1
1.51	0.36	0.12	86.4	27.2	0.23	0.09	115.2	33.4	0.59	0.07	90.0	0.0	0.27	0.05	-37.1	10.6
1.53	0.33	0.00	92.5	22.1	0.28	0.05	86.4	23.5	0.59	0.07	90.0	0.0	0.32	0.05	-19.1	5.9
1.55	0.36	0.07	84.7	13.7	0.30	0.05	97.3	18.6	0.58	0.00	90.0	0.0	0.39	0.04	-11.8	4.3
1.57	0.46	0.06	84.3	10.0	0.26	0.04	87.5	14.4	0.62	0.13	90.0	3.4	0.42	0.03	1.3	0.0
1.59	0.42	0.16	78.2	13.2	0.25	0.05	105.7	29.0	0.57	0.12	90.0	3.9	0.45	0.04	-5.2	0.0
1.61	0.39	0.04	76.3	10.3	0.33	0.03	80.0	9.3	0.64	0.09	90.0	3.5	0.43	0.03	-1.9	0.0
1.63	0.38	0.15	69.6	10.6	0.29	0.06	62.2	20.5	0.59	0.11	90.0	3.2	0.57	0.03	5.4	0.0
1.65	0.39	0.05	67.3	8.5	0.29	0.03	79.1	12.4	0.61	0.13	90.0	2.4	0.64	0.03	3.7	0.0
1.67	0.40	0.13	63.8	11.8	0.25	0.06	54.1	23.6	0.61	0.10	90.0	3.7	0.60	0.03	14.7	0.0

Table 13 (continued)

M_{TF} GeV	$ S $	$\pm\Delta S $	δ_s	$\pm\Delta\delta_s$	$ P $	$\pm\Delta P $	δ_p	$\pm\Delta\delta_p$	$ D $	$\pm\Delta D $	δ_D	$\pm\Delta\delta_D$	$ F $	$\pm\Delta F $	δ_F	$\pm\Delta\delta_F$
1.69	0.40	0.13	60.9	13.2	0.22	0.06	54.1	28.0	0.55	0.13	90.0	4.0	0.67	0.03	13.0	0.0
1.71	0.43	0.11	58.0	20.6	0.23	0.06	78.9	25.0	0.58	0.10	90.0	6.0	0.64	0.03	30.2	0.0
1.73	0.40	0.12	49.5	16.1	0.31	0.10	87.0	32.1	0.56	0.07	90.0	5.9	0.63	0.03	35.5	0.0
1.75	0.37	0.11	51.8	20.8	0.35	0.11	118.7	16.5	0.49	0.08	90.0	11.3	0.56	0.03	52.0	0.0
1.77	0.38	0.05	46.7	19.9	0.29	0.04	109.0	11.4	0.54	0.11	90.0	5.3	0.55	0.04	47.6	0.0
1.79	0.42	0.05	53.0	16.1	0.21	0.06	31.0	55.3	0.53	0.06	90.0	7.4	0.55	0.033	40.5	0.0

(131)

Table 14: Data for EM-solution B

$M_{\text{GeV}}^{\text{THN}}$	$ s $	$\pm \Delta s$	d_s	$\pm \Delta d_s$	$ p $	$\pm \Delta p $	d_p	$\pm \Delta d_p$	$ D $	$\pm \Delta D $	d_D	$\pm \Delta d_D$	$ F $	$\pm \Delta F $	d_F	$\pm \Delta d_F$
1.01	0.63	0.07	140.3	6.8	0.40	0.11	211.7	4.6	0.40	0.05	90.0	0.0	0.03	0.0	78.7	0.0
1.03	0.64	0.06	143.6	6.5	0.32	0.10	207.5	4.2	0.43	0.05	90.0	0.0	0.03	0.0	77.3	0.0
1.05	0.66	0.10	149.3	5.7	0.46	0.10	214.9	4.5	0.43	0.04	90.0	0.0	0.03	0.0	75.8	0.0
1.07	0.71	0.06	140.7	7.1	0.35	0.11	209.1	4.6	0.42	0.05	90.0	0.0	0.04	0.0	73.9	0.0
1.09	0.61	0.09	148.4	5.4	0.45	0.10	214.0	4.6	0.50	0.04	90.0	0.0	0.04	0.0	71.7	0.0
1.11	0.61	0.10	147.2	4.8	0.42	0.11	210.8	5.4	0.65	0.03	90.0	0.0	0.05	0.0	69.0	0.0
1.13	0.45	0.16	141.2	12.8	0.46	0.15	195.0	14.2	0.74	0.03	90.0	0.0	0.05	0.0	65.6	0.0
1.15	0.64	0.10	148.8	4.3	0.29	0.11	197.9	4.1	0.69	0.03	90.0	0.0	0.06	0.0	61.5	0.0
1.17	0.56	0.10	138.2	5.3	0.29	0.08	189.2	3.9	0.87	0.03	90.0	0.0	0.06	0.0	56.4	0.0
1.19	0.73	0.09	141.4	4.7	0.18	0.12	178.7	12.3	0.88	0.04	90.0	0.0	0.07	0.0	49.9	0.0
1.21	0.64	0.14	130.1	10.4	0.19	0.20	159.8	33.5	1.07	0.03	90.0	0.0	0.07	0.0	41.8	0.0
1.23	0.70	0.11	129.8	9.3	0.23	0.22	162.1	27.8	1.11	0.03	90.0	0.0	0.08	0.0	31.9	0.0
1.25	0.76	0.06	121.3	8.7	0.19	0.11	130.1	30.1	1.23	0.03	90.0	0.0	0.09	0.0	20.6	0.0
1.27	0.71	0.10	118.7	11.9	0.16	0.10	97.9	40.1	1.25	0.05	90.0	0.0	0.10	0.0	8.6	0.0
1.29	0.89	0.07	124.7	6.3	0.21	0.10	70.1	40.9	1.10	0.06	90.0	0.0	0.11	0.0	-2.8	0.0
1.31	0.76	0.08	117.7	10.5	0.40	0.16	46.5	17.9	1.13	0.03	90.0	0.0	0.12	0.0	-12.8	0.0

Table 14 (continued)

$M_{\pi\pi}$ Gev.	$ s $	$\pm s $	δ_s	$\pm \Delta \delta_s$	$ P $	$\pm \Delta P $	δ_p	$\pm \Delta \delta_p$	$ D $	$\pm \Delta D $	δ_D	$\pm \Delta \delta_D$	$ F $	$\pm \Delta F $	δ_F	$\pm \Delta \delta_F$
1.33	0.67	0.07	109.1	12.6	0.32	0.11	63.8	27.0	1.11	0.02	90.0	0.0	0.13	0.0	-21.0	0.0
1.35	0.72	0.11	118.7	10.8	0.54	0.19	39.6	13.1	0.84	0.07	90.0	0.0	0.14	0.0	-27.4	0.0
1.37	0.71	0.11	114.1	14.7	0.30	0.26	52.6	30.5	0.86	0.05	90.0	0.0	0.11	0.02	-90.8	70.0
1.39	0.71	0.11	117.8	13.2	0.28	0.29	55.5	40.2	0.79	0.05	90.0	0.0	0.11	0.02	-92.9	82.3
1.41	0.64	0.28	112.2	19.9	0.30	0.25	55.1	30.7	0.77	0.10	90.0	0.0	0.11	0.02	-90.7	60.6
1.43	0.52	0.17	107.9	29.1	0.52	0.30	37.6	24.5	0.67	0.13	90.0	0.0	0.23	0.08	-41.6	15.0
1.45	0.47	0.16	115.4	22.6	0.56	0.25	41.0	16.2	0.57	0.13	90.0	0.0	0.27	0.06	-27.8	15.7
1.47	0.48	0.18	104.2	31.0	0.41	0.20	41.0	28.9	0.51	0.05	90.0	0.0	0.17	0.02	-97.3	26.4
1.49	0.51	0.14	118.5	13.1	0.29	0.16	58.6	20.4	0.54	0.06	90.0	0.0	0.16	0.03	-91.7	31.1
1.51	0.32	0.12	121.8	26.1	0.45	0.13	41.9	15.6	0.48	0.08	90.0	0.0	0.27	0.05	-48.2	12.7
1.53	0.27	0.09	129.4	19.9	0.53	0.13	58.2	11.0	0.43	0.10	90.0	0.0	0.32	0.03	-26.5	7.7
1.55	0.20	0.08	109.5	46.4	0.59	0.12	58.1	11.9	0.42	0.13	90.0	0.0	0.39	0.04	-16.5	7.1
1.57	0.14	0.09	122.1	30.5	0.73	0.08	68.8	10.6	0.32	0.14	90.0	8.2	0.42	0.05	2.6	0.0
1.59	0.12	0.07	108.1	50.2	0.67	0.08	61.4	6.7	0.33	0.15	90.0	7.2	0.46	0.04	-90.0	0.0
1.61	0.10	0.07	107.5	50.2	0.71	0.08	71.4	7.3	0.38	0.14	90.0	6.4	0.43	0.04	-3.3	0.0
1.63	0.09	0.15	46.6	40.4	0.68	0.08	75.2	8.4	0.36	0.15	90.0	7.2	0.57	0.04	9.0	0.0

Table 14(continued)

$M_{\pi\pi}$ Gev	$ S $	$\pm \Delta S $	d_S	$\pm\Delta d_S$	$ P $	$\pm\Delta P $	d_P	$\pm\Delta d_P$	$ D $	$\pm D $	d_D	$\pm\Delta d_D$	$ F $	$\pm\Delta F $	d_F	$\pm\Delta d_F$
1.65	0.10	0.14	32.1	45.2	0.69	0.07	67.1	6.7	0.35	0.17	90.0	6.2	0.68	0.03	6.4	0.0
1.67	0.15	0.13	14.1	32.9	0.68	0.06	89.4	7.3	0.34	0.13	90.0	12.6	0.60	0.03	27.3	0.0
1.69	0.18	0.11	0.1	30.6	0.64	0.06	84.3	16.2	0.29	0.14	90.0	15.6	0.67	0.03	26.7	0.0
1.71	0.30	0.12	29.9	20.9	0.59	0.07	111.1	9.9	0.37	0.09	90.0	17.7	0.64	0.03	52.4	0.0
1.73	0.33	0.13	33.0	21.5	0.52	0.10	103.6	13.6	0.44	0.10	90.0	15.0	0.63	0.03	47.6	0.0
1.75	0.37	0.11	51.7	20.9	0.35	0.11	118.7	16.8	0.49	0.08	90.0	11.5	0.56	0.03	52.0	0.0
1.77	0.36	0.15	39.5	30.8	0.40	0.18	117.3	21.9	0.49	0.12	90.0	20.9	0.55	0.03	55.5	0.0
1.79	0.41	0.20	36.2	29.3	0.46	0.31	122.6	24.1	0.36	0.07	90.0	61.5	0.55	0.03	81.2	0.0

Table 15: Data for EM-solution C

M_{III} Gev	$ s $	$\pm \Delta s $	d_s	$\pm \Delta d_s$	$ p $	$\pm \Delta p $	d_p	$\pm \Delta d_p$	$ D $	$\pm \Delta D $	d_D	$\pm \Delta d_D$	$ F $	$\pm \Delta F $	d_F	$\pm \Delta d_F$
1.01	0.63	0.07	140.3	6.8	0.40	0.11	211.7	4.6	0.40	0.05	90.0	0.0	0.03	0.0	78.7	0.0
1.03	0.64	0.06	143.6	6.5	0.32	0.10	207.5	4.2	0.43	0.05	90.0	0.0	0.03	0.0	77.3	0.0
1.05	0.56	0.10	149.3	5.7	0.46	0.10	214.9	4.5	0.43	0.04	90.0	0.0	0.03	0.0	75.8	0.0
1.07	0.71	0.06	140.7	7.1	0.35	0.11	201.1	4.6	0.42	0.05	90.0	0.0	0.04	0.0	73.9	0.0
1.09	0.61	0.09	148.4	5.4	0.45	0.10	214.0	4.6	0.50	0.04	90.0	0.0	0.04	0.0	71.7	0.0
1.11	0.61	0.10	147.2	4.8	0.42	0.11	210.8	5.4	0.63	0.03	90.0	0.0	0.05	0.0	69.0	0.0
1.13	0.45	0.16	141.2	12.8	0.46	0.15	195.0	14.2	0.74	0.03	90.0	0.0	0.05	0.0	65.6	0.0
1.15	0.64	0.10	148.8	4.3	0.29	0.11	197.9	4.1	0.69	0.03	90.0	0.0	0.06	0.0	61.5	0.0
1.17	0.56	0.10	138.2	5.3	0.29	0.08	189.2	3.9	0.87	0.03	90.0	0.0	0.06	0.0	56.4	0.0
1.19	0.73	0.09	141.4	4.7	0.18	0.12	178.7	12.8	0.88	0.04	90.0	0.0	0.07	0.0	49.9	0.0
1.21	0.64	0.14	130.1	10.4	0.19	0.20	159.8	33.5	1.07	0.03	90.0	0.0	0.07	0.0	41.8	0.0
1.23	0.70	0.11	129.8	9.3	0.23	0.22	162.1	27.8	1.11	0.03	90.0	0.0	0.08	0.0	31.9	0.0
1.25	0.64	0.13	110.2	17.3	0.36	0.24	159.2	14.6	1.26	0.03	90.0	0.0	0.09	0.0	20.6	0.0
1.27	0.62	0.11	104.8	19.6	0.30	0.22	151.8	23.0	1.27	0.03	90.0	0.0	0.10	0.0	8.6	0.0
1.29	0.63	0.08	101.3	10.2	0.53	0.12	163.9	4.5	1.16	0.03	90.0	0.0	0.11	0.0	-2.8	0.0
1.31	0.65	0.08	88.0	14.8	0.40	0.13	144.0	13.9	1.19	0.03	90.0	0.0	0.12	0.0	-12.8	0.0

Table 15 (Continued)

M_{III} Gev.	$ S $	$\pm AS $	d_S	$\pm \Delta d_S$	$ P $	$\pm \Delta P $	d_p	$\pm d_p$	$ D $	$\pm \Delta D $	d_D	$\pm \Delta d_D$	$ F $	$\pm \Delta F $	d_F	$\pm \Delta d_F$
1.33	0.67	0.13	70.9	18.1	0.32	0.32	116.5	20.3	1.11	0.05	90.0	0.0	0.13	0.0	-21.0	0.0
1.35	0.62	0.11	84.6	12.1	0.47	0.47	148.0	9.3	0.94	0.04	90.0	0.0	0.14	0.0	-27.4	0.0
1.37	0.54	0.10	89.1	14.3	0.53	0.53	155.9	10.0	0.87	0.05	90.0	0.0	0.11	0.01	-85.5	26.8
1.39	0.47	0.10	93.3	9.5	0.60	0.60	159.8	10.4	0.79	0.09	90.0	0.0	0.11	0.02	-87.2	35.1
1.41	0.53	0.20	88.3	24.8	0.41	0.41	147.1	35.7	0.79	0.09	90.0	0.0	0.13	0.08	-61.1	60.2
1.43	0.57	0.13	88.0	14.6	0.25	0.25	115.8	9.9	0.78	0.08	90.0	0.0	0.23	0.07	-35.4	15.1
1.45	0.53	0.11	92.7	19.1	0.23	0.23	107.9	46.9	0.72	0.08	90.0	0.0	0.27	0.06	-21.6	15.0
1.47	0.46	0.42	79.7	70.5	0.44	0.44	142.6	58.2	0.51	0.05	90.0	0.0	0.17	0.02	-81.5	28.9
1.49	0.51	0.15	61.4	21.5	0.29	0.29	120.7	54.0	0.54	0.06	90.0	0.0	0.16	0.03	-87.4	78.4
1.51	0.50	0.09	56.8	23.3	0.17	0.17	60.7	60.9	0.50	0.0-	90.0	0.0	0.275	0.05	-45.3	12.4
1.53	0.55	0.07	53.6	19.5	0.28	0.28	43.3	37.6	0.40	0.10	90.0	0.0	0.32	0.05	-28.7	9.0
1.55	0.54	0.09	59.2	20.2	0.34	0.34	44.6	29.8	0.40	0.14	90.0	0.0	0.393	0.04	-17.2	8.0
1.57	0.64	0.09	73.4	14.0	0.32	0.17	44.7	39.6	0.39	0.15	90.0	7.4	0.424	0.03	2.1	0.0
1.59	0.59	0.07	63.5	9.0	0.33	0.06	41.4	14.0	0.39	0.20	90.0	5.7	0.45	0.03	-10.0	0.0
1.61	0.65	0.10	60.3	11.8	0.32	0.10	51.6	37.4	0.39	0.18	90.0	6.2	0.43	0.04	-3.2	0.0
1.63	0.62	0.08	70.4	8.9	0.37	0.11	43.1	22.8	0.28	0.20	90.0	11.3	0.57	0.03	11.5	0.0

Table 15(continued)

$M_{\pi\pi}$ Gev.	$ S $	$\pm \Delta S $	d_S	$\pm\Delta d_S$	$ P $	$\pm\Delta P $	d_p	$\pm\Delta d_p$	$ D $	$\pm\Delta D $	d_D	$\pm\Delta d_D$	$ F $	$\pm\Delta F $	d_F	$\pm\Delta d_F$
1.65	0.61	0.07	68.4	8.5	0.41	0.09	31.5	15.7	0.26	0.15	90.0	9.4	0.64	0.03	8.6	0.0
1.67	0.64	0.06	94.7	8.8	0.37	0.11	51.1	21.2	0.23	0.15	90.0	34.1	0.60	0.03	41.3	0.0
1.69	0.60	0.05	92.0	7.8	0.36	0.08	40.7	16.2	0.21	0.12	90.0	15.2	0.678	0.03	35.6	0.0
1.71	0.61	0.07	123.8	9.7	0.35	0.11	69.7	24.3	0.30	0.05	90.0	35.2	0.64	0.03	77.8	0.0
1.73	0.58	0.08	136.3	12.4	0.36	0.08	93.0	30.6	0.33	0.05	90.0	33.5	0.63	0.03	99.0	0.0
1.75	0.54	0.06	129.8	14.2	0.22	0.05	119.4	48.1	0.39	0.06	90.0	23.7	0.663	0.03	102.8	0.0
1.77	0.54	0.11	139.4	20.1	0.26	0.14	89.7	0.8	0.42	0.08	90.0	30.1	0.5	0.04	106.6	0.0
1.79	0.42	0.15	153.7	26.5	0.46	0.15	57.7	47.8	0.35	0.06	90.0	51.9	0.5	0.03	98.2	0.0

Table 16: Data for EM-solution D

M_{III} Gev.	$ s $	$\pm \Delta s $	$d_s \pm \Delta d_s$	$ p $	$\pm \Delta p $	d_p	$\pm \Delta d_p$	$ D $	$\pm \Delta D $	d_D	$\pm d_D$	$ F $	$\pm \Delta F $	d_F	$\pm \Delta d_F$	
1.01	0.63	0.07	140.3	6.8	0.40	0.11	211.7	4.6	0.40	0.05	90.0	0.0	0.03	0.0	78.7	0.0
1.03	0.64	0.06	143.6	6.5	0.32	0.10	207.5	4.2	0.43	0.05	90.0	0.0	0.03	0.0	77.3	0.0
1.05	0.56	0.10	149.3	5.7	0.46	0.10	214.9	4.5	0.43	0.04	90.0	0.0	0.03	0.0	75.8	0.0
1.07	0.71	0.06	140.7	7.1	0.35	0.11	209.1	4.6	0.42	0.05	90.0	0.0	0.04	0.0	73.9	0.0
1.09	0.61	0.09	148.4	5.4	0.45	0.10	214.0	4.6	0.50	0.04	90.0	0.0	0.04	0.0	71.7	0.0
1.11	0.61	0.10	147.2	4.8	0.42	0.11	210.8	5.4	0.65	0.03	90.0	0.0	0.05	0.0	69.0	0.0
1.13	0.45	0.16	141.2	12.8	0.46	0.15	195.0	14.2	0.74	0.03	90.0	0.0	0.05	0.0	65.6	0.0
1.15	0.64	0.10	148.8	4.3	0.29	0.11	197.9	4.1	0.69	0.03	90.0	0.0	0.06	0.0	61.5	0.0
1.17	0.56	0.10	138.2	5.3	0.29	0.08	189.2	3.9	0.87	0.03	90.0	0.0	0.06	0.0	56.4	0.0
1.19	0.73	0.09	141.4	4.7	0.18	0.12	178.7	12.8	0.88	0.04	90.0	0.0	0.07	0.0	49.9	0.0
1.21	0.64	0.14	130.1	10.4	0.19	0.20	159.8	33.5	1.07	0.03	90.0	0.0	0.07	0.0	41.8	0.0
1.23	0.70	0.11	129.8	9.3	0.23	0.22	162.1	27.8	1.11	0.03	90.0	0.0	0.08	0.0	31.9	0.0
1.25	0.75	0.06	121.3	8.7	0.19	0.11	130.1	30.1	1.23	0.03	90.0	0.0	0.09	0.0	20.6	0.0
1.27	0.71	0.10	118.7	11.9	0.16	0.10	97.9	40.1	1.25	0.05	90.0	0.0	0.10	0.0	8.6	0.0
1.29	0.89	0.07	124.7	6.3	0.21	0.10	70.1	40.3	1.10	0.06	90.0	0.0	0.11	0.0	-2.8	0.0
1.31	0.76	0.08	117.7	10.5	0.40	0.16	46.5	17.9	1.13	0.03	90.0	0.0	0.12	0.0	-12.8	0.0

Table 16: Data for EM-solution D

$M_{\pi\pi}$ Gev.	$ S $	$\pm\Delta S $	δ_S	$\pm\Delta\delta_S$	$ P $	$\pm\Delta P $	δ_P	$\pm\Delta\delta_P$	$ D $	$\pm\Delta D $	δ_D	$\pm\Delta\delta_D$	$ F $	$\pm\Delta F $	δ_F	$\pm\Delta\delta_F$
1.33	0.67	0.07	109.1	12.6	0.32	0.11	63.8	27.0	1.11	0.02	90.0	0.0	0.13	0.0	-21.0	0.0
1.35	0.72	0.11	118.7	10.8	0.54	0.19	39.5	13.1	0.84	0.07	90.0	0.0	0.14	0.0	-27.4	0.0
1.37	0.71	0.11	114.1	14.7	0.30	0.26	52.6	30.5	0.86	0.05	90.0	0.0	0.11	0.02	-90.8	70.0
1.39	0.71	0.11	117.8	13.2	0.28	0.29	55.5	40.2	0.79	0.05	90.0	0.0	0.11	0.02	-92.9	82.3
1.41	0.47	0.13	88.8	24.9	0.57	0.14	24.5	11.6	0.73	0.06	90.0	0.0	0.13	0.05	-68.1	38.8
1.43	0.40	0.17	80.7	30.2	0.67	0.15	22.3	18.4	0.62	0.12	90.0	0.0	0.23	0.07	-46.1	12.8
1.45	0.29	0.15	56.1	50.4	0.77	0.12	17.1	16.6	0.43	0.13	90.0	0.0	0.27	0.06	-37.7	7.5
1.47	0.44	0.45	97.4	78.4	0.45	0.41	35.2	56.1	0.51	0.06	90.0	0.0	0.17	0.02	-99.2	30.7
1.49	0.33	0.10	80.9	23.0	0.47	0.04	26.7	7.4	0.55	0.08	90.0	0.0	0.16	0.02	-99.9	19.9
1.51	0.20	0.06	57.8	14.4	0.57	0.06	18.4	11.0	0.41	0.07	90.0	0.0	0.27	0.06	-60.7	12.7
1.53	0.25	0.07	19.8	16.4	0.63	0.06	23.1	5.6	0.27	0.06	90.0	0.0	0.32	0.04	-46.2	4.6
1.55	0.27	0.07	36.4	15.1	0.66	0.06	37.5	4.9	0.26	0.05	90.0	0.0	0.40	0.03	-27.7	4.3
1.57	0.28	0.06	41.7	15.7	0.75	0.05	65.9	6.4	0.11	0.07	90.0	30.6	0.43	0.04	7.4	0.0
1.59	0.11	0.07	107.6	60.5	0.57	0.08	61.4	6.7	0.33	0.15	90.0	7.2	0.45	0.04	-9.0	0.0
1.61	0.36	0.08	20.5	14.3	0.72	0.05	54.0	8.9	0.14	0.05	90.0	14.8	0.43	0.04	-6.7	0.0
1.63	0.42	0.09	83.4	14.2	0.65	0.08	113.1	12.1	0.06	0.07	90.0	80.1	0.57	0.03	58.7	0.0

Table 16(Continued)

$M_{\pi\pi}$ Gev.	$ s $	$\pm\Delta s $	d_s	$\pm\Delta d_s$	$ p $	$\pm\Delta p $	d_p	$\pm d_p$	$ D $	$\pm\Delta D $	d_D	$\pm\Delta d_D$	$ F $	$\pm\Delta F $	d_F	$\pm\Delta d_F$
1.65	0.40	0.13	116.1	14.9	0.67	0.07	142.3	11.7	0.04	0.03	90.0	100.9	0.64	0.03	92.2	0.0
1.67	0.48	0.06	139.3	12.4	0.58	0.07	175.1	8.1	0.19	0.05	90.0	20.0	0.60	0.02	126.2	0.0
1.69	0.42	0.10	146.8	15.2	0.57	0.09	184.6	12.1	0.19	0.14	90.0	42.3	0.58	0.03	135.4	0.0
1.71	0.52	0.06	136.2	14.0	0.42	0.08	168.4	14.7	0.37	0.06	90.0	12.4	0.64	0.03	126.6	0.0
1.73	0.55	0.06	139.4	17.3	0.35	0.09	147.5	31.5	0.39	0.11	90.0	21.0	0.63	0.03	123.3	0.0
1.75	0.54	0.06	129.8	13.9	0.22	0.05	119.1	49.9	0.39	0.06	90.0	23.1	0.56	0.03	102.9	0.0
1.77	0.53	0.09	138.4	25.2	0.22	0.07	124.5	49.5	0.45	0.12	90.0	24.2	0.55	0.03	117.8	0.0
1.79	0.42	0.13	126.8	43.4	0.20	0.25	147.0	106.4	0.53	0.19	90.0	17.7	0.55	1.03	139.8	0.0

Table 17: To test sum-rule inequalities (EM-data: sols. A, B, C & D)

sol.	N_1	R	A	VPK	ANS1	ANS2	FINANS.
A	1	0.38	0.010000	1.00000	-7.0227	1.5159	-5.5068574
	2	0.99	0.010000	1.00000			
		0.99	0.010000	1.00015	-68.6928	26.5347	-42.158070
	3	0.99	0.010000	1.00000			
		0.99	1.188531	1.00000			
		0.99	0.010000	1.00000	-278.892	91.7325	-187.15938
B	1	0.338426	0.010000	1.00000	-6.7689	1.7835	-4.985397
	2	0.99	0.010000	1.00000			
		0.99	0.010000	1.00000	-76.4596	35.8887	-40.570932
	3	0.99	0.010000	1.00007			
		0.99	1.070246	1.00000			
		0.99	0.010000	1.00001	-302.102	144.5777	-157.52438
C	1	0.33861	0.010000	1.00000	-6.0770	1.9279	-4.1491247
	2	0.99	0.010000	1.0000			
		0.99	0.010000	1.00000	-92.8313	38.1776	-54.653739
	3	0.99	0.010000	1.00000			
		0.99	0.912435	1.00000			
		0.99	0.010000	1.00000	-404.825	174.974	-229.85132
D	1	0.407606	0.010000	1.00000	-6.7681	1.9136	-4.8545553
	2	0.99	0.010000	1.00000			
		0.99	0.010000	1.00000	-127.829	35.2693	-92.559633
	3	0.99	0.010000	1.000066			
		0.99	0.669326	1.000000			
		0.99	0.010000	1.000002	-379.59	191.050	-188.54578

Table 18:FP data [68,68a]

M_{II} Gev.	n_{o2}^2 n_o	d_{o2}^2 d_o	n_2^2 n_2	d_2^2 d_2	n_o^o n_o	d_{oo}^o d_o	n_1^1 n_1	d_{11}^1 d_1	n_{2o}^o n_2	d_{2o}^o d_2	n_3^1 n_3	d_{31}^1 d_3	χ^2
1.010	1 o	-23.5 o	1 o	-1.0 o	0.34 +0.26	14.0 21.4	0.97 0.08	-24.1 4.7	0.83 0.07	14.0 2.3	1.00 0.01	0.0 0.3	9.1
1.030	1 o	-23.7 o	1 o	-1.0 o	0.28 0.25	8.8 26.0	0.94 0.08	-22.8 4.9	0.79 0.07	15.6 2.5	1.0 0.01	0.0 0.3	8.8
1.050	1 o	-23.8 o	1 o	-1.1 o	0.12 0.22	52.7 51.7	0.98 0.08	-21.3 4.7	0.86 0.07	16.1 2.2	1.00 0.01	0.0 0.3	3.9
1.070	1 o	-24.0 o	1 o	-1.2 o	0.35 0.22	75.4 17.9	0.97 0.07	-20.6 4.1	0.81 0.07	16.6 2.4	1.00 0.01	0.0 0.3	8.3
1.090	1 o	-24.1 o	1 o	-1.3 o	0.37 0.22	79.8 16.8	0.98 0.07	-19.4 4.1	0.83 0.07	20.3 2.3	1.00 0.01	0.0 0.3	3.0
1.110	1 o	-24.3 o	1 o	-1.4 o	0.48 0.21	82.3 12.7	0.95 0.07	-18.2 4.2	0.83 0.07	26.8 2.4	1.00 0.01	0.0 0.4	3.8
1.130	1 o	-24.4 o	1 o	-1.5 o	0.43 0.21	82.9 14.8	0.89 0.07	-15.9 4.5	0.80 0.07	31.2 2.5	1.00 0.02	0.0 0.4	3.4

Table 18 (Continued)

M_{II} Gev.	n_{o2}^2 n_o	d_o^2 d_o^2	n_2^2 n_2^2	d_2^2 d_2^2	n_{oo}^o n_o	d_{oo}^o d_{oo}^o	n_{11}^1 n_1^1	d_1^1 d_1^1	n_2^o n_2^o	d_2^o d_2^o	n_3^1 n_3^1	d_3^1 d_3^1	χ^2
1.15	1 o	-24.5 o	1 o	-1.6 o	0.51 0.21	-86.6 11.9	0.88 0.07	-14.3 4.5	0.78 0.07	30.8 2.6	1.00 0.02	0.0 0.4	2.5
1.17	1 o	-24.6 o	1 o	-1.7 o	0.49 0.21	89.3 12.1	0.89 0.07	-13.4 4.5	0.77 0.07	39.7 2.7	1.00 0.02	0.0 0.4	2.2
1.19	1 o	-24.7 o	1 o	-1.8 o	0.69 0.21	-83.5 8.6	0.89 0.07	-13.2 4.5	0.72 0.07	43.3 2.9	1.00 0.03	0.0 0.5	2.2
1.21	1 o	-24.8 o	1 o	-1.9 o	0.64 0.21	-83.2 9.4	0.88 0.07	-12.9 4.5	0.71 0.07	55.3 3.0	1.00 0.03	0.0 0.5	1.8
1.23	1 o	+24.8 o	1 o	-2.0 o	0.92 0.19	-76.1 6.0	0.91 0.07	-12.5 4.4	0.65 0.07	61.5 3.1	1.00 0.03	0.0 0.5	1.0
1.25	1 o	-24.9 o	1 o	-2.1 o	1.10 0.19	-72.1 5.5	0.92 0.07	-12.2 4.3	0.67 0.07	76.1 3.0	1.00 0.03	0.0 0.5	1.8
1.27	1 o	-25.0 o	1 o	-2.2 o	1.14 0.20	-63.6 5.6	0.95 0.07	-10.3 4.2	0.64 0.07	89.0 3.2	1.00 0.02	0.0 0.6	2.2

Table 18(continued)

M_{II} Gev	n_o^2 n_o^2	d_o^2 d_o^2	n_2 n_2^2	d_2^2 d_2^2	n_o^o n_o	d_o^o d_o^o	n_{11}^1 n_{11}^1	d_{11}^1 d_{11}^1	n_{2o}^o n_2	d_{2o}^o d_{2o}^o	n_{31}^1 n_{31}^1	d_{31}^1 d_{31}^1	χ^2
1.29	1 o	-25.1 o	1 o	-2.4 o	0.99 0.18	-55.7 5.2	1.01 0.07	-11.3 4.0	0.61 0.07	-76.3 3.3	1.00 0.02	0.0 0.6	8.8
1.31	1 o	-25.1 o	1 o	-2.5 o	1.05 0.18	-49.2 5.2	0.93 0.07	-9.6 4.3	0.75 0.07	-65.2 2.8	1.00 0.02	0.0 0.7	8.6
1.33	1 o	-25.1 o	1 o	-2.6 o	1.08 0.19	-42.0 5.3	0.86 0.07	-8.3 4.8	0.81 0.07	-56.4 2.6	1.00 0.03	0.0 0.7	10.5
1.35	1 o	-25.1 o	1 o	-2.8 o	1.18 0.19	-38.0 5.5	0.83 0.07	-5.3 4.8	0.77 0.08	-46.9 2.9	1.00 0.03	0.7 0.6	21.6
1.37	1 o	-25.1 o	1 o	-2.9 o	1.00 0.22	-38.1 6.4	0.77 0.07	-3.8 5.2	0.76 0.08	-40.6 3.0	1.00 0.03	1.5 0.7	30.3
1.39	1 o	-25.2 o	1 o	-3.1 o	1.00 0.21	-35.1 6.0	0.71 0.07	-3.1 5.6	0.78 0.07	-35.8 2.7	1.00 0.03	1.9 0.8	20.0
1.41	1 o	-25.2 o	1 o	-3.2 o	1.00 0.21	-32.3 6.0	0.65 0.07	-3.6 6.2	0.80 0.08	-32.8 2.7	1.00 0.03	1.2 0.8	11.5

(144)

Table 18(continued)

M_{IIIV} GeV.	n_o^2 n_o^2	d_o^2 d_o^2	n_2^2 n_2^2	d_2^2 d_2^2	n_{oo}^o n_o^o	d_o^o d_o^o	n_1^1 n_1^1	d_1^1 d_1^1	n_2^o n_2^o	d_2^o d_2^o	n_3^1 n_3^1	d_3^1 d_3^1	χ^2
1.43	1 o	-25.2 o	1 o	-3.4 o	1.00 o.21	-30.2 6.0	o.61 o.o7	-4.2 6.6	o.80 o.o8	-30.6 2.7	1.00 o.o3	3.3 o.9	10.8
1.45	1 o	-25.2 o	1 o	-3.6 o	1.00 o.21	-27.0 6.1	o.57 o.o7	-4.5 7.0	o.76 o.o8	-27.4 2.9	1.00 o.o3	3.8 o.9	6.3
1.47	1 o	-25.2 o	1 o	-3.8 o	1.00 o.22	-21.9 6.2	o.56 o.o7	-4.5 7.1	o.74 o.o8	-21.1 3.0	1.00 o.o3	4.0 1.0	5.9
1.49	1 o	-25.2 o	1 o	-3.9 o	1.00 o.22	-18.8 6.2	o.52 o.o7	-4.2 7.7	o.74 o.o8	-20.2 3.0	1.00 o.o3	4.6 1.0	3.7
1.51	1 o	-25.3 o	1 o	-4.1 o	1.00 o.22	-14.5 6.2	o.51 o.o7	-4.0 8.5	o.75 o.o8	-18.8 3.0	1.00 o.o3	5.7 1.0	3.9
1.53	1 o	-25.3 o	1 o	-4.3 o	1.00 o.22	-12.7 6.2	o.47 o.o7	-8.4 8.5	o.69 o.o8	-17.4 3.3	o.95 o.o3	6.2 1.0	1.7
1.55	1 o	-25.3 o	1 o	-4.5 o	1.00 o.22	-10.4 6.2	o.43 o.o7	-12.1 9.3	o.65 o.o8	-17.6 3.4	o.92 o.o3	7.2 1.0	1.7
1.57	1 o	-25.3 o	1 o	-4.7 o	1.00 o.22	-8.2 6.2	o.39 o.o7	-15.0 10.7	o.61 o.o8	-16.7 3.7	o.87 o.o3	7.7 2.2	3.8

Table 18(continued)

M_{III} Gev.	$n_{n_0}^2$	$d_{d_0}^2$	$n_{n_2}^2$	$d_{d_2}^2$	$n_{n_0}^0$	$d_{d_0}^0$	$n_{n_1}^1$	$d_{d_1}^1$	$n_{n_2}^0$	$d_{d_2}^0$	$n_{n_3}^1$	$d_{d_3}^1$	χ^2
1.590	1 0	-25.3 0	1 0	-4.9 0	1.00 0.22	-4.0 6.2	0.40 0.07	-17.4 9.9	0.67 0.08	-15.1 3.3	0.87 0.03	8.6 2.2	3.6
1.610	1 0	-25.3 0	1 0	-5.1 0	1.00 0.22	-0.6 6.2	0.42 0.07	-23.2 9.5	0.64 0.08	-14.4 3.5	0.84 0.03	8.7 2.3	1.1
1.630	1 0	-25.3 0	1 0	-5.4 0	1.00 0.21	4.3 6.1	0.45 0.07	-25.3 8.8	0.63 0.08	-13.4 3.5	0.77 0.03	10.1 2.5	4.3
1.650	1 0	-25.3 0	1 0	-5.6 0	1.00 0.21	8.6 6.1	0.49 0.07	-28.0 8.1	0.69 0.08	-12.3 3.2	0.72 0.03	11.2 2.7	7.7
1.670	1 0	-25.4 0	1 0	-5.8 0	1.00 0.22	13.3 6.2	0.57 0.07	-27.8 7.0	0.62 0.08	-9.2 3.6	0.69 0.03	9.6 2.8	3.9
1.690	1 0	-25.4 0	1 0	-6.1 0	1.00 0.22	18.6 6.3	0.65 0.07	-27.1 6.1	0.68 0.08	-6.6 3.3	0.63 0.03	9.5 3.0	8.2
1.710	1 0	-25.4 0	1 0	-6.3 0	1.00 0.23	23.7 6.4	0.71 0.07	-25.6 5.6	0.52 0.08	-4.7 4.5	0.60 0.04	7.2 3.8	2.5

Table 18(continued)

M_{III} Gev.	n_{o2}^2 n_o	d_{o2}^2 d_o	n_{22}^2 n_2	d_{22}^2 d_2	n_o^o n_o	d_o^o d_o	n_1^1 n_1	d_{11}^1 d_1	n_2^o n_2	d_2^o d_2	n_{31}^1 n_3	d_3^1 d_3	χ^2
1.730	1 o	-25.5 o	1 o	-6.6 o	o.97 o.23	29.5 6.8	o.74 o.o7	-23.6 5.4	o.48 o.o8	-3.7 5.1	o.6o o.o4	5.6 3.8	2.6
1.750	1 o	-25.5 o	1 o	-6.8 o	o.91 o.24	32.8 7.5	o.78 o.o7	-2o.2 5.1	o.45 o.o9	o.o 5.6	o.61 o.o4	4.2 3.8	2.o
1.770	1 o	-25.6 o	1 o	-7.1 o	o.82 o.25	37.7 8.6	o.78 o.o7	--8.3 5.1	o.43 o.o9	1.2 6.1	o.63 o.o4	3.2 3.7	1.3
1.790	1 o	-25.6 o	1 o	-7.4 o	o.76 o.25	42.3 9.6	o.79 o.o7	-16.4 5.1	o.47 o.1o	3.2 5.8	o.65 o.o4	2.6 3.5	5.6

Table 19: Test of sum-rule inequality for FP [68,68a] data

FP'S P.S.	N ₁	R	A	VPK	ANS1	ANS2	FINANS.
FP [68,68a]	1	0.81238	0.0100000	1.0000008	-9.6389	3.1855	-6.4534856
	2	0.99	0.0277000	1.0000001			
		0.99	0.0100000	1.0000001	-97.476	25.983	-71.493202
	3	0.667921	0.0100000	1.0000047			
		0.99	0.0100000	1.0000000			
		0.99	0.0100000	1.0000101	-139.03	98.81	-40.21967

Table 20: Phase-shift analysis of FP 'data [68,68a] for $\Pi^+\Pi^-$ scattering (1.01 GeV to 1.79 GeV)

M $\Pi^+\Pi^-$ GeV	S ₀		D ₀		P ₁		F ₁		S ₂		D ₂		F($\bar{s}, 0$) = FA.		ERROR inFA
	ReS ₀	ImS ₀	ReD ₀	ImD ₀	ReP ₁	ImP ₁	ReF ₁	ImF ₁	ReS ₂	ImS ₂	ReD ₂	ImD ₂	ReFA	ImFA.	
1.01	0.0810	0.3629	0.1978	0.1364	-0.368	0.1757	0.0	0.0	-0.3727	0.1574	-0.0177	0.0003	-0.5463	1.2767	0.345
1.03	0.0429	0.3803	0.2075	0.1654	-0.3416	0.1706	0.0	0.0	-0.3746	0.1597	-0.018	0.0003	-0.4588	1.3705	0.347
1.05	0.0607	0.5321	0.2321	0.1377	-0.3367	0.1379	0.0	0.0	-0.3753	0.1607	-0.0194	0.0004	-0.3533	1.2818	0.340
1.07	0.0990	0.6696	0.2243	0.1634	-0.3237	0.1338	0.0	0.0	-0.3772	0.1630	-0.0211	0.0004	-0.3182	1.4475	0.312
1.09	0.0795	0.6911	0.2733	0.1861	-0.3105	0.1166	0.0	0.0	-0.3779	0.1641	-0.023	0.0005	-0.1318	1.4867	0.312
1.11	0.0835	0.7499	0.3387	0.2538	-0.2846	0.1168	0.0	0.0	-0.3798	0.1665	-0.025	0.0006	0.1634	1.7527	0.313
1.13	0.0704	0.7262	0.3602	0.3144	-0.2363	0.1222	0.0	0.0	-0.3805	0.1676	-0.026	0.0007	0.3680	1.9557	0.320
1.15	-0.0515	0.7730	0.3481	0.3143	-0.2119	0.1144	0.0	0.0	-0.3813	0.1687	-0.028	0.0008	0.3165	1.9637	0.318
1.17	0.0265	0.7656	0.3867	0.4279	-0.2016	0.1034	0.0	0.0	-0.3821	0.1698	-0.029	0.0009	0.5251	2.3047	0.320
1.19	-0.1057	0.8529	0.3684	0.4778	-0.1986	0.1019	0.0	0.0	-0.3828	0.1709	-0.031	0.0010	0.3819	2.5255	0.332
1.21	-0.1012	0.8266	0.3474	0.6248	-0.1920	0.1044	0.0	0.0	-0.3837	0.1721	-0.032	0.0011	0.3315	3.0062	0.331
1.23	-0.2485	0.9148	0.2895	0.6791	-0.1926	0.0877	0.0	0.0	-0.3833	0.1719	-0.035	0.0012	0.0357	3.1961	0.327
1.25	-0.3592	0.9479	0.1808	0.8050	-0.1901	0.0810	0.0	0.0	-0.3841	0.1731	-0.037	0.0013	-0.3962	3.6183	0.326
1.27	-0.4849	0.8382	0.0378	0.8382	-0.1670	0.0552	0.0	0.0	-0.3850	0.1742	-0.038	0.0014	-0.8904	3.5788	0.322
1.29	-0.4807	0.6729	-0.163	0.7787	-0.1938	0.0326	0.0	0.0	-0.3847	0.1741	-0.004	0.0017	-1.6416	3.2030	0.319
1.31	-0.5344	0.5664	-0.306	0.7427	-0.1526	0.0609	0.0	0.0	-0.3855	0.1753	-0.043	0.0018	-2.0363	3.0974	0.323
1.33	-0.5466	0.4327	-0.389	0.6521	-0.1224	0.0890	0.0	0.0	-0.3853	0.1752	-0.045	0.0020	-2.2337	2.7906	0.338
1.35	-0.5796	0.3450	-0.393	0.5203	-0.0760	0.0937	0.0122	0.0001	-0.3850	0.1750	-0.049	0.0023	-2.0497	2.3088	0.341
1.37	-0.4914	0.3718	-0.381	0.4372	-0.0507	0.1207	0.0260	0.0007	-0.3848	0.1749	-0.050	0.0025	-1.7796	2.1344	0.347
1.39	-0.4744	0.3223	-0.373	0.3725	-0.0381	0.1500	0.0329	0.0011	-0.3857	0.1761	-0.054	0.0028	-1.6628	1.9773	0.337

Table 20 (continued)

M _{II} GeV.	S ₀		D ₀		P ₁		F ₁		S ₂		D ₂		F ⁺ (s, 0) = FA.		Error in FA.
	Re S ₀	Im S ₀	Re D ₀	Im D ₀	Re P ₁	Im P ₁	Re F ₁	Im F ₁	Re S ₂	Im S ₂	Re D ₂	Im D ₂			
1.41	-0.454	0.2779	-0.3664	0.3305	-0.0405	0.1810	0.0208	0.0004	-0.3854	0.1760	0.0554	0.0030	-1.7206	1.8965	0.346
1.43	-0.4361	0.2459	-0.3518	0.3034	-0.0443	0.2020	0.0571	0.0032	-0.3852	0.1759	-0.0586	0.0034	-1.4229	1.8680	0.350
1.45	-0.4047	0.2000	-0.3107	0.2785	-0.0443	0.2225	0.0656	0.0042	-0.3850	0.1758	-0.0622	0.0038	-1.2109	1.8236	0.350
1.47	-0.3451	0.1348	-0.2447	0.2253	-0.0435	0.2274	0.0690	0.0047	-0.3848	0.1757	-0.0656	0.0042	-0.9405	1.6214	0.354
1.49	-0.3036	0.1005	-0.2388	0.2177	-0.0377	0.2470	0.0793	0.0062	-0.3846	0.1757	-0.0673	0.0045	-0.7968	1.6431	0.355
1.51	-0.2408	0.0606	-0.2276	0.2025	-0.0352	0.2517	0.0980	0.0095	-0.3856	0.1769	-0.0707	0.0049	-0.5852	1.6042	0.366
1.53	-0.2128	0.0467	-0.1957	0.2172	-0.0673	0.2792	0.1011	0.0361	-0.3854	0.1768	-0.0741	0.0054	-0.5405	1.9136	0.353
1.55	-0.1760	0.0314	-0.1861	0.2353	-0.0874	0.3079	0.1133	0.0546	-0.3852	0.1767	-0.0775	0.0059	-0.4641	2.1801	0.351
1.57	-0.1398	0.0196	-0.1667	0.2568	-0.0967	0.3351	0.1144	0.0811	-0.3851	0.1766	-0.0808	0.0065	-0.4012	2.4783	0.411
1.59	-0.0689	0.0047	-0.1671	0.2114	-0.1133	0.3392	0.1274	0.0848	-0.3849	0.1766	-0.0842	0.0070	-0.3200	2.3896	0.404
1.61	-0.0104	0.0001	-0.1528	0.2209	-0.1513	0.3574	0.1243	0.0997	-0.3848	0.1765	-0.0876	0.0076	-0.3741	2.5783	0.406
1.63	0.0739	0.0054	-0.1407	0.2204	-0.1731	0.3585	0.1316	0.1395	-0.3846	0.1764	-0.0926	0.0085	-0.3006	2.8633	0.403
1.65	0.1462	0.0215	-0.1421	0.1874	-0.2025	0.3631	0.1357	0.1682	-0.3845	0.1764	-0.096	0.0092	-0.3217	2.9797	0.405
1.67	0.2216	0.0510	-0.0967	0.2079	-0.2343	0.3378	0.1122	0.1757	-0.3855	0.1776	-0.0993	0.0098	-0.3864	3.0458	0.401
1.69	0.2996	0.0980	-0.0767	0.1709	-0.2624	0.3077	0.1014	0.2041	-0.3853	0.1776	-0.1044	0.0109	-0.4360	3.0636	0.402
1.71	0.3656	0.1558	-0.0419	0.2466	-0.2757	0.2749	0.0737	0.2118	-0.3852	0.1775	-0.1077	0.0116	-0.5134	3.3112	0.443
1.73	0.4143	0.2423	-0.0305	0.2653	-0.2695	0.2461	0.0575	0.2081	-0.3862	0.1788	-0.1127	0.0127	-0.5481	3.3218	0.446
1.75	0.4138	0.3037	0.000	0.2785	-0.2505	0.2010	0.0440	0.2007	-0.3861	0.1787	-0.1160	0.0135	-0.4899	3.2204	0.456
1.77	0.3979	0.3880	0.008	0.2888	-0.2302	0.1854	0.0346	0.1892	-0.3871	0.1800	-0.1210	0.0147	-0.4839	3.1863	0.460
1.79	0.3813	0.4553	0.0258	0.2697	-0.2116	0.1669	0.0290	0.1784	-0.3870	0.1799	-0.1260	0.0159	-0.4301	3.0385	0.465

(150)

4.6 Discussion of results.

We have derived the constraints of sum-rule inequality (4.5.9) on the basis of unitarity and positivity with phenomenological input of data in the form of EM's solutions A,B,C,D and FP's analysis togetherwith the experimental errors involved therein. If the constraints are satisfied we should get positive values of integral (4.5.9).

(A) Rotated Data:

In case of rotated data for solution A, we find minima of sum-rule inequality (4.5.9) consistently for the set $\{R \approx 0.99\}$, which is almost at the boundary of the unitary circle $\Rightarrow v_p^j = r_p^j e^{i\theta_p^j}$. The minima are found consistently for set of angles in the radian measure $\{\theta \approx 0.01\}$, except in one case of polynomial of order 3. Also, we find the minima very consistently for $\{v_p^k \approx 1.000001\}$, just at the beginning of the cut outside the circle. There is some violation of our sum-rule inequality (4.5.9): the higher is the order of polynomial $P(v)$ the higher is the degree of violation of our sum-rule inequality. The results are very sensitive to input values of v_p^k in polynomial (4.3.3), in general.

There is similar situation with solution B. The minima are found for $\{R \approx 0.545\}$, $\{\theta \approx 0.015\}$ and $\{v_p^k \approx 1.0000006\}$ in case of polynomial $P(v)$ of order 1. The error integral shows less numerical value than that in case A.

In case of solution C, the error integral of sum-rule inequality (4.5.9) shows larger value than that in case of solution B. However, total value of the sum-rule inequality (4.5.9) for solution C is less than that in case B. Consequently, there is less violation of unitarity in case of solution C than in case of solution B for polynomials of order 1 and 2; the reverse is the case with polynomial of order 3.

As the error integrals are concerned, the solution D shows less error than solutions A,B&C for polynomials of order 1 & 2, but the total value of the integral (4.5.9) is more negative for solution D than for solutions A,B and C.

(B) EM'S Unrotated Data:

In case of EM'S solutions A,B,C and D (unrotated), we have less values of error integrals than the corresponding values with rotated data. The minima are found consistently for the set $\{v_p^k=1.0000001\}$, $\{A=0.01\}$ and $\{R=0.99\}$, with a few exceptions in case of polynomials of higher orders.

Solution A shows the least values of error integrals in (4.5.9) followed by solutions B,C&D. However, solution C shows the least violation of our sum-rule inequality for the polynomial of order 1, followed by solutions D,B and A.

(C) FP'S Data:

In case of FP data, the minima are found almost consistently for the set $\{v_p^k=1.000001\}$, $\{A=0.01\}$ and $\{R=0.99\}$, except in one case of polynomial where it is for the set $\{R=0.81 \text{ or } 0.63\}$. The errors in integral (4.5.9) are less in this case than those for EM'S solutions. However, the data show much more smooth behaviour and the violation of our sum-rule inequality (4.5.9) is of the order of experimental errors involved in the data, thereby, we cannot rule out completely the FP-solution.

4.7 CONCLUSIONS.

We have derived the sum-rule inequality (4.5.9) on the basis of unitarity, analyticity of $\Pi^+\Pi^-$ amplitude and positivity of its absorptive part $A(s,0)$ with phenomenological input of experimental data in the inelastic region. Its violation shows either a clear indication of the experimental data at fault or something wrong with our basic properties of the scattering amplitude. The chosen data satisfy the sum-rule inequalities of Common[74]. EM'S figures give the impression of very smooth argand diagrams, but actual solutions are very noisy. However, the problem is not solved by changing and rotating the overall phase. On the other hand, the problem of truncation at $L=3$ introduces spurious uniqueness and there are continuum ambiguities clearly present. On plotting argand diagrams of FP's data, we get smoother curves which agree with the published papers [68,68a].

On the basis of our computational results, after local minimization with respect to the zeros of the parameters, we find that there are clear violations of our sum-rule inequality (4.5.9) in case of EM's solutions A,B,C and D. This violation is found to be less pronounced in the case of unrotated data than in the case of rotated data. However, they are of the order of one to two standard deviations, in most of the cases, which is the order of errors involved in the experimental data. Hence we cannot rule out EM-solutions completely on the basis of violations of our sum-rule inequality.

In case of FP-data, the analysis shows much more smooth behaviour and there is less violation of our sum-rule inequality and we cannot rule out the two solutions. So, the smoother data is more consistent with analyticity properties of the scattering amplitudes.

Appendix

1. Convergence of s:
In order to prove

$$\int_{v_{\infty}}^0 \text{Im } f(v+i\epsilon) P(v) dv \sim \int A(s,0) \left[v(v-v_{\infty}) \right] \frac{dv}{ds} ds \sim \int \frac{A(s,0)}{s^3} ds,$$

we proceed as follows:

$$v = \frac{\sqrt{\frac{1}{s} - \frac{1}{s_2}} - \sqrt{\frac{1}{s} - \frac{1}{s_1}}}{\sqrt{\frac{1}{s} - \frac{1}{s_2}} + \sqrt{\frac{1}{s} - \frac{1}{s_1}}} \quad (\text{A1})$$

$$s \rightarrow \infty, v_{\infty} = \frac{\sqrt{\frac{-1}{s_2}} - \sqrt{\frac{-1}{s_1}}}{\sqrt{-\frac{1}{s_2}} + \sqrt{-\frac{1}{s_1}}} = -0.2786. \quad (\text{A2})$$

$$v = \frac{\sqrt{1 - \frac{s}{s_2}} - \sqrt{1 - \frac{s}{s_1}}}{\sqrt{1 - \frac{s}{s_2}} + \sqrt{1 - \frac{s}{s_1}}} \quad (\text{A3})$$

$$\frac{dv}{ds} = \frac{\frac{1}{s_1} \sqrt{\frac{1}{s} - \frac{1}{s_2}} - \frac{1}{s_2} \sqrt{\frac{1}{s} - \frac{1}{s_1}}}{s \left[\sqrt{\frac{1}{s} - \frac{1}{s_2}} + \sqrt{\frac{1}{s} - \frac{1}{s_1}} \right]^2} \quad (\text{A4})$$

$$\left[v(v-v_{\infty}) \right] \frac{dv}{ds} = \frac{\left(\frac{1}{s} - \frac{1}{s_2} \right)^{1/2} - \left(\frac{1}{s} - \frac{1}{s_1} \right)^{1/2} \quad \left(-\frac{1}{s_2} \right)^{1/2} - \left(-\frac{1}{s_1} \right)^{1/2}}{\left(\frac{1}{s} - \frac{1}{s_2} \right)^{1/2} + \left(\frac{1}{s} - \frac{1}{s_1} \right)^{1/2} \quad \left(-\frac{1}{s_2} \right)^{1/2} + \left(-\frac{1}{s_1} \right)^{1/2}} \cdot \frac{\frac{1}{s_1} \left(\frac{1}{s} - \frac{1}{s_2} \right)^{1/2} - \frac{1}{s_2} \left(\frac{1}{s} - \frac{1}{s_1} \right)^{1/2}}{s \left[\left(\frac{1}{s} - \frac{1}{s_2} \right)^{1/2} + \left(\frac{1}{s} - \frac{1}{s_1} \right)^{1/2} \right]^2}$$

= A.B.C ,

$$\text{where } A = \frac{\left[\left(\frac{1}{s} - \frac{1}{s_2} \right)^{1/2} - \left(\frac{1}{s} - \frac{1}{s_1} \right)^{1/2} \right]^2 - \left[\left(-\frac{1}{s_2} \right)^{1/2} - \left(-\frac{1}{s_1} \right)^{1/2} \right]^2}{\left(\frac{1}{s_1} - \frac{1}{s_2} \right) \left(\frac{1}{s_1} - \frac{1}{s_2} \right)} \quad (\text{A5})$$

$$B = \frac{1}{s} \left[\frac{(1/s - 1/s_2)^{1/2}}{(1/s - 1/s_1)} \right] - \frac{1}{s_2} \left[\frac{(1/s - 1/s_1)^{1/2}}{(1/s - 1/s_2)} \right] \quad (A6)$$

$$C = \frac{1}{s} \left[\frac{1}{\left(\frac{1}{s} - \frac{1}{s_2} \right)^{1/2} + \left(\frac{1}{s} - \frac{1}{s_1} \right)^{1/2}} \right]^2 \quad (A7)$$

Now we consider these factors separately:

$$A = \left[\frac{(1/s - 1/s_2 + 1/s - 1/s_1 - 2(1/s - 1/s_2)^{1/2}(1/s - 1/s_1)^{1/2})}{(1/s_1 - 1/s_2)} \right. \\ \left. \frac{(-1/s_2 - 1/s_1 - 2(-1/s_1 s_2)^{1/2})}{(1/s_1 - 1/s_2)} \right] \\ = \frac{2/s - 2/(s_1 s_2)^{1/2} \left\{ (1 - \frac{1}{2}(s_2/s) - 1/8(s_2/s)^2) (1 - \frac{1}{2}(s_1/s) - 1/8(s_1/s)^2 - 1) \right\}}{(1/s_1 - 1/s_2)} \\ = \frac{2/s - 2/(s_1 s_2)^{1/2} \left\{ -\frac{1}{2}(s_1/s + s_2/s) + O(1/s)^2 \right\}}{(1/s_1 - 1/s_2)}, \text{ neglecting higher order terms.}$$

$$= \frac{2/s + 2/(s_1 s_2)^{1/2} \cdot (1/2s) \cdot (s_1 + s_2)}{(1/s_1 - 1/s_2)} + O(1/s)^2 \\ = A'/s + O(1/s)^2, \text{ where } A' = \left[2 + \frac{s_1 + s_2}{(s_1 s_2)^{1/2}} \right] \quad (A8)$$

$$B = \frac{1}{s_1} \left(\frac{-1/s_2(1-s_2/s)}{-1/s_1(1-s_1/s)} \right)^{1/2} - \frac{1}{s_2} \left(\frac{-1/s_1(1-s_1/s)}{-1/s_2(1-s_2/s)} \right)^{1/2}$$

$$= \frac{1}{s_1 s_2} \left[-1/2s(s_2 - s_1) + 1/2s(s_1 - s_2) + O(1/s)^2 \right], \text{ neglecting}$$

higher order terms.

$$= \frac{1}{s_1 s_2} \frac{(s_1 - s_2)^{1/2}}{s} + O(1/s)^2$$

$$\text{or } B = B'/s + O(1/s)^2, \text{ where } B' = \frac{s_1 - s_2}{(s_1 s_2)^{1/2}} \quad (A9)$$

$$\begin{aligned}
C &= 1/s \cdot \left[\frac{1}{(1/s - 1/s_2)^{\frac{1}{2}} + (1/s - 1/s_1)^{\frac{1}{2}}} \right]^2 \\
&= 1/s \cdot \left[\frac{[(1/s - 1/s_2)^{\frac{1}{2}} - (1/s - 1/s_1)^{\frac{1}{2}}]}{(-1/s_2 + 1/s_1)^2} \right]^2 \\
&= 1/s \cdot \left[\frac{-1/s_2 - 1/s_1 - 2/(s_1 s_2)^{\frac{1}{2}}}{(-1/s_2 + 1/s_1)^2} \right]^2 + O(1/s)^2 \\
&\equiv C'/s + O(1/s)^2, \tag{A10}
\end{aligned}$$

where $C' = \left[\frac{-1/s_2 - 1/s_1 - 2/(s_1 s_2)^{\frac{1}{2}}}{(-1/s_2 + 1/s_1)^2} \right]^2$

Putting the values from (A8), (A9) and (A10) we have

$$\begin{aligned}
A.B.C &\approx (A'/s + O(1/s)^2)(B'/s + O(1/s)^2)(C'/s + O(1/s)^2) \\
&\approx \frac{A'B'C'}{s^3} + O(1/s)^4 \quad \text{as } s \rightarrow \infty \tag{A11}
\end{aligned}$$

$$\text{i.e. for } \sqrt{s_1} = 1.01 \text{ GeV}, s_2 = 1.79 \text{ GeV}, A.B.C \approx 13.7(1/s)^3 + O(1/s)^4 \tag{A12}$$

Putting the result (A12) into (A14), we have

$$v(v - v_\infty) \frac{dv}{ds} \approx 13.7 (1/s)^3 + O(1/s)^4 \tag{A13}$$

$$\text{Hence, } \int_{v_\infty}^0 \text{Im}f(v+i\epsilon)P(v) dv \sim \int A(s,0) \left[v(v - v_\infty) \frac{dv}{ds} \right] ds \sim \int \frac{A(s,0) ds}{s^3} \tag{A14}$$

is true for small negative values of v .

2. Table Captions.

1. The central values and errors used to compute the bounds for the real and imaginary parts of the amplitude on the intermediate energy region $0.45 \text{ GeV} \leq E_{\text{c.m.}} \leq 1.9 \text{ GeV}$. The phase shifts are given in degrees and the inelasticities fulfil [18]

$$\text{Sup} \{0, \eta - \Delta\eta\} \leq \eta \leq \text{Inf} \{1, \eta + \Delta\eta\}.$$

2. Upper bounds on $F_{\Pi^0 + \Pi^0 \rightarrow \Pi^0 + \Pi^0}(s, 4) = 1/3 \cdot (F^0 + 2F^2) = 1/3 \cdot (a_0 + 2a_2)$ for s-wave in the elastic region ($0.45 \text{ GeV} \leq E_{\text{c.m.}} \leq 0.95 \text{ GeV}$).

3. Upper bounds on $F_{\Pi^+ \Pi^0 \rightarrow \Pi^+ \Pi^0}(s, 4) = \frac{1}{2}(F^1 + F^2) = \frac{1}{3}(a_0 - a_2)$ in the elastic region.

4. Upper bounds on $F_{\Pi^0 \Pi^0 \rightarrow \Pi^0 \Pi^0}(s, 4) = 1/3 \cdot (F^0 + 2F^2) = 1/3 \cdot (a_0 + 2a_2)$ for s-wave in the broad energy region ($0.45 \text{ GeV} \leq E_{\text{c.m.}} \leq 1.9 \text{ GeV}$).

5. Upper bounds on $F_{\Pi^+ \Pi^0 \rightarrow \Pi^+ \Pi^0}(s, 4) = \frac{1}{2}(F^1 + F^2) = \frac{1}{3}(a_0 - a_2)$ for s-wave in the broad energy region.

6. Numerical values for different \mathcal{E} -values of the bounds on $a_0, a_2, (2a_0 - 5a_2)$ and $(a_0 + 2a_2)$ obtained by Bonnier [18]. The bounds are approximately linear with \mathcal{E} ($0 \leq \mathcal{E} \leq 1$).

7. Low-energy s-wave parameters calculated for the Saclay and CM-EM1 phase shifts by BFP [30].

8. EM'S data [81] rotated by Common [82] for solution A

9. Do for solution B

10. Do for solution C

11. Do for solution D

12. Test of our sum-rule inequality for EM'S (rotated by Common) solutions: A, B, C & D

13. EM's data [81] for solution A

14. Do B

15. Do C

16. EM'S data [81] for solution D
17. Test of our sum-rule inequality for EM'S solutions:A,B,C&D.
18. FP data [68,68a]: $M_{\pi^+ \pi^-}$ is dipion mass in Gev. For orbital angular momentum l and isospin I , δ_l^I and η_l^I are phase shift in degrees and elasticity coefficients. For $I=2$ numbers represent fixed input into the analysis. The other column is a measure of uncertainty. The last column gives the χ^2 for a fixed energy to 7 Legendre moments of elastic cross-section.
19. Test of our sum-rule inequality for FP data [68,68a]
20. Phase shifts analysis of FP data [68,68a] for $\pi^+ \pi^-$ scattering in the inelastic region.

3. Figure captions.

1. SCATTERING PROCESS: Four lines representing four ingoing free particles.
2. The scattering process: $\pi + \pi \rightarrow \pi + \pi$ in the cms.
3. Mandelstam diagram: Physical regions for s-, t- and u-channels.
4. Mandelstam diagram: t vs u .
5. Singularities of the scattering amplitude in $z = \cos\theta_s$ -plane.
6. Feynman diagram for nucleon-nucleon scattering with pion as an exchange particle.
7. (a) Nucleon-nucleon scattering in c.m. frame.
(b) Feynman diagram for proton-proton scattering with pion as an exchange particle, producing a pion and a nucleon.
8. (a) Argand circle for small inelastic amplitudes: the partial waves lie near the centre of the circle.
(b) Argand circle for elastic processes, where the high partial waves lie near the edge of the circle.
9. Bohnier's Mapping [18] from (a) z-plane to (b) v-plane.
10. Mappings: z-plane to w-plane, and w-plane to v-plane.
11. Complex z-plane: right hand cut and a pole z_0 on the real axis.
12. Complex $h(v)$ -plane: (a) $\theta = \text{Arg } h(v+i\epsilon)$, (b) contour near v_T .
13. Special mapping from complex s-plane to v-plane with contours of integration.

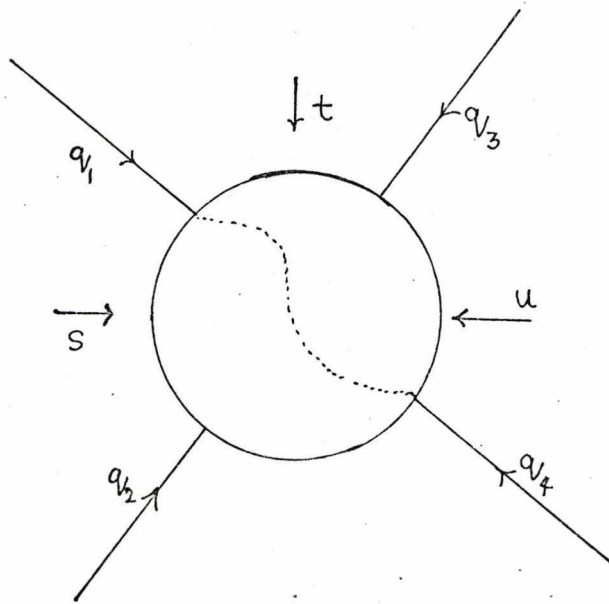


Fig. 1

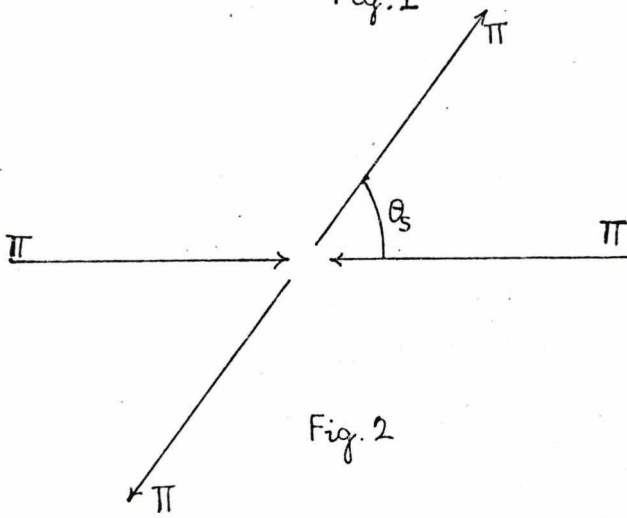


Fig. 2

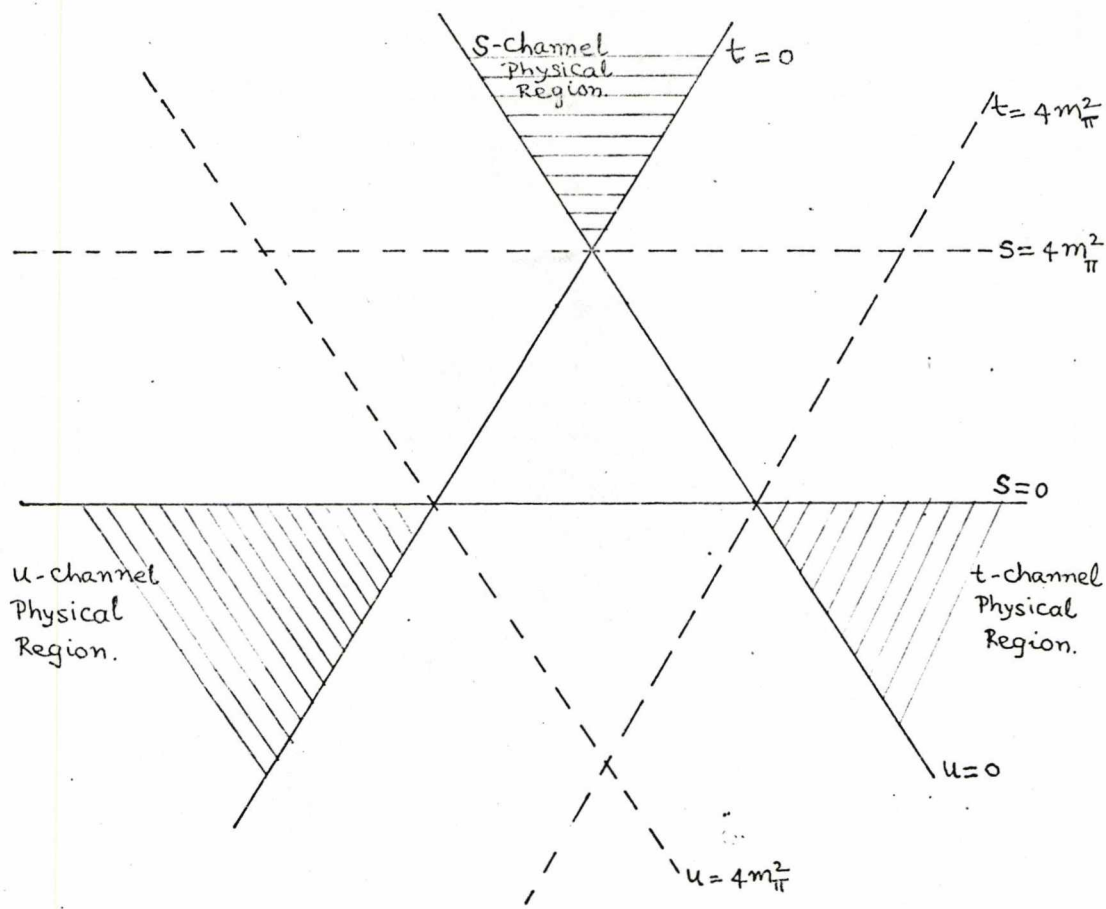


Fig. 3

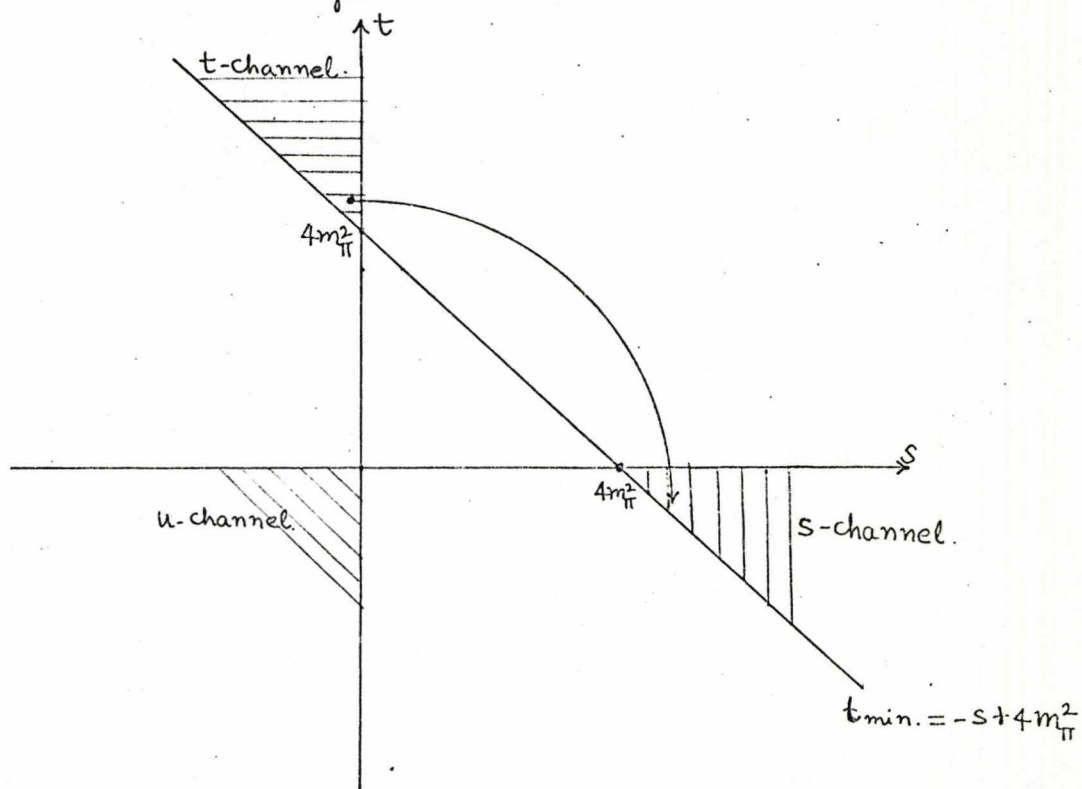
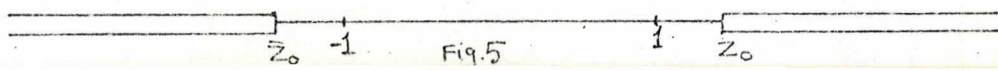


Fig. 4



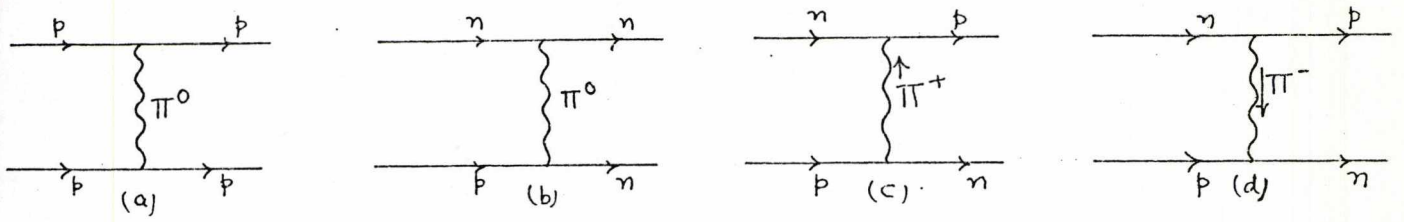


Fig. 6

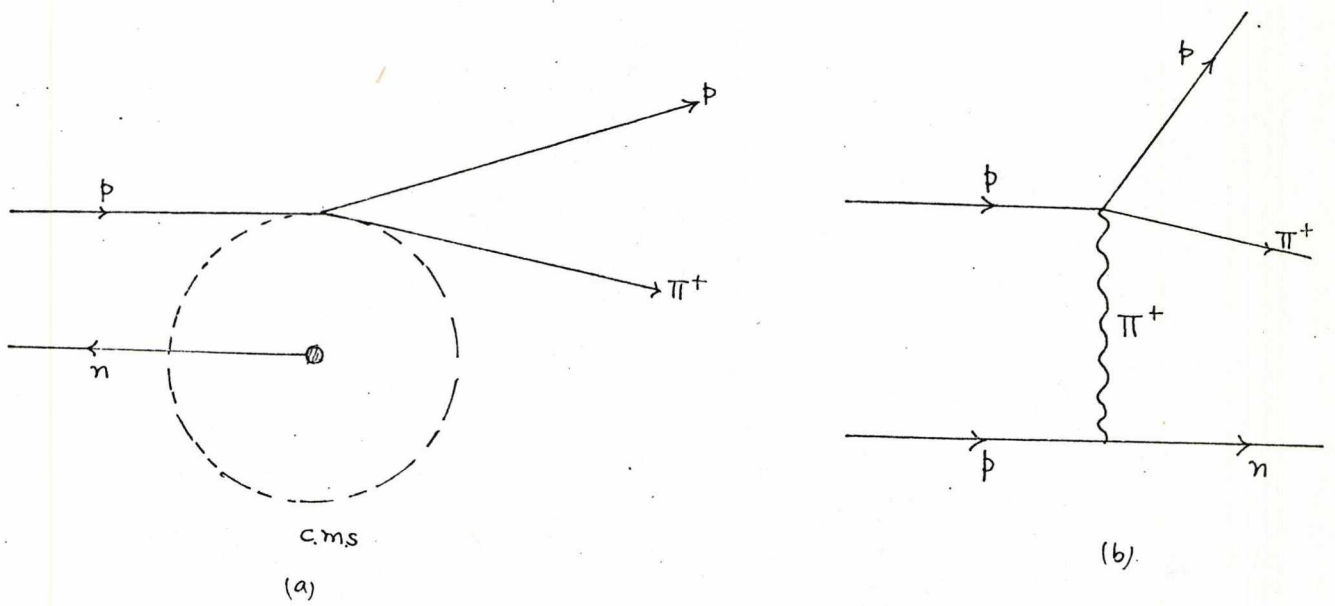


Fig. 7

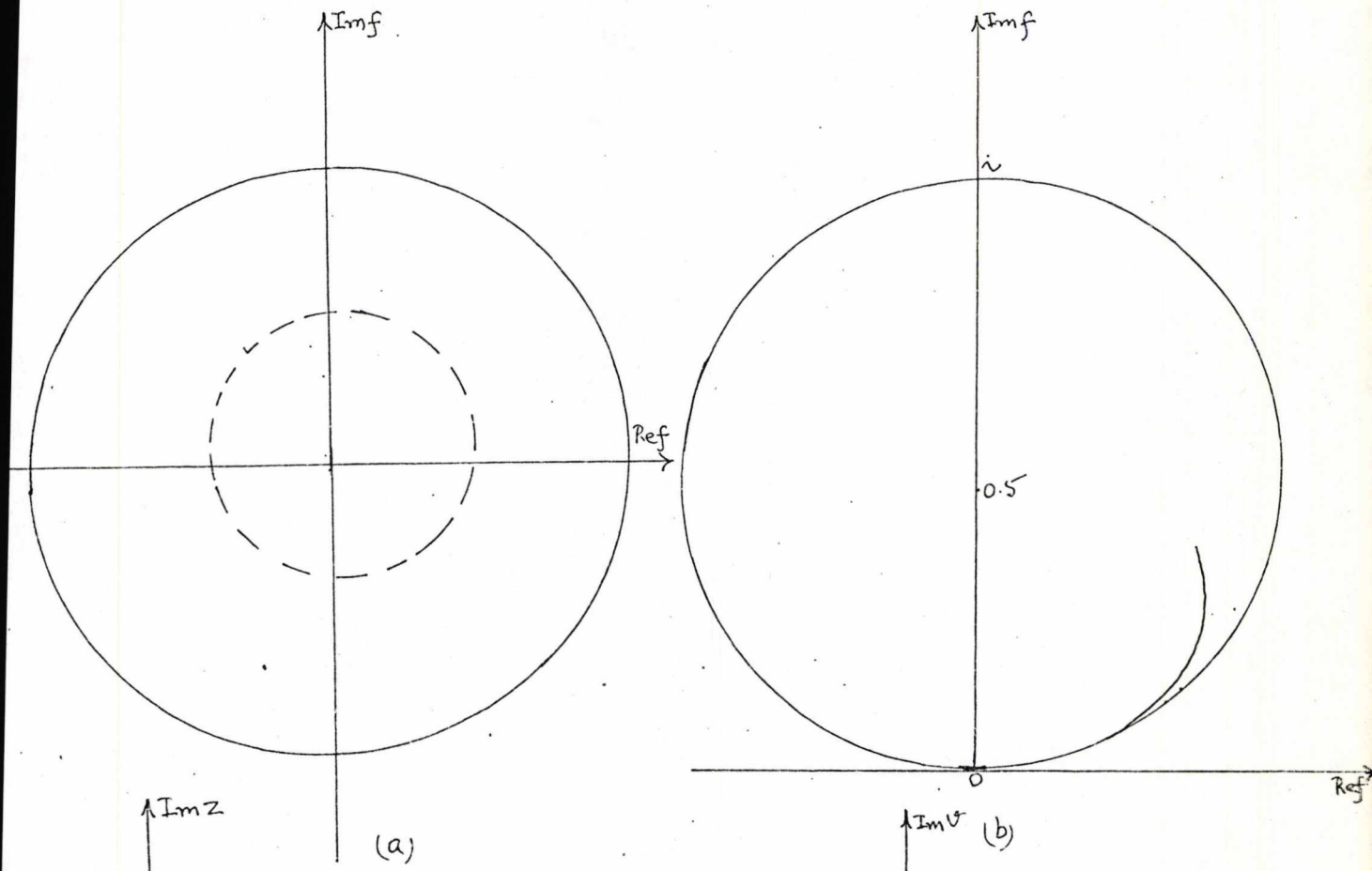


Fig. 8

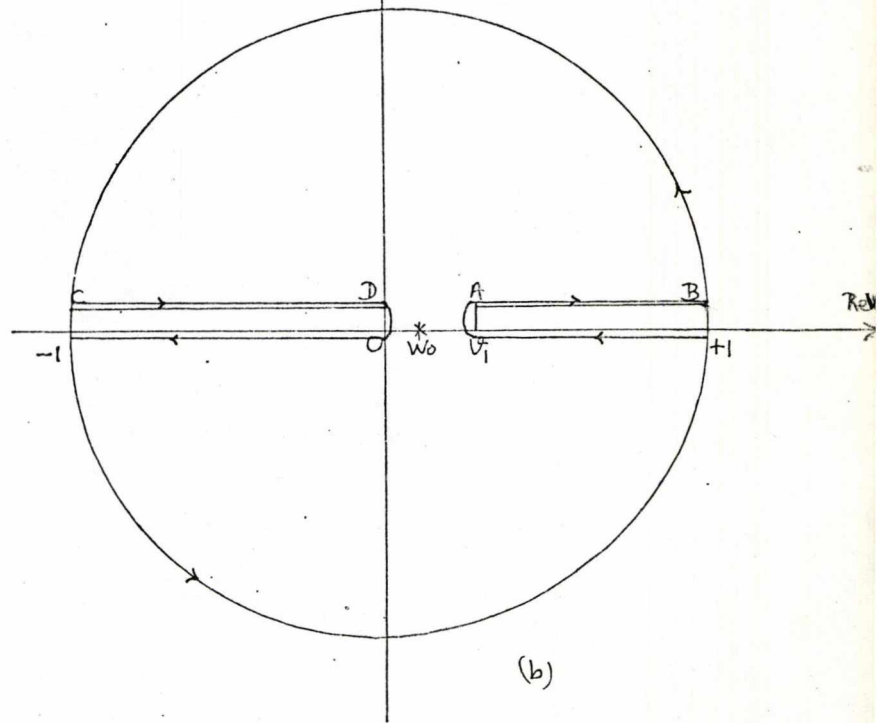
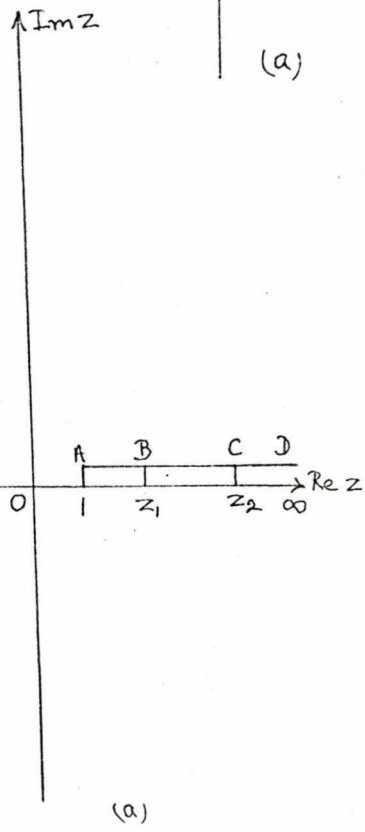


Fig. 9

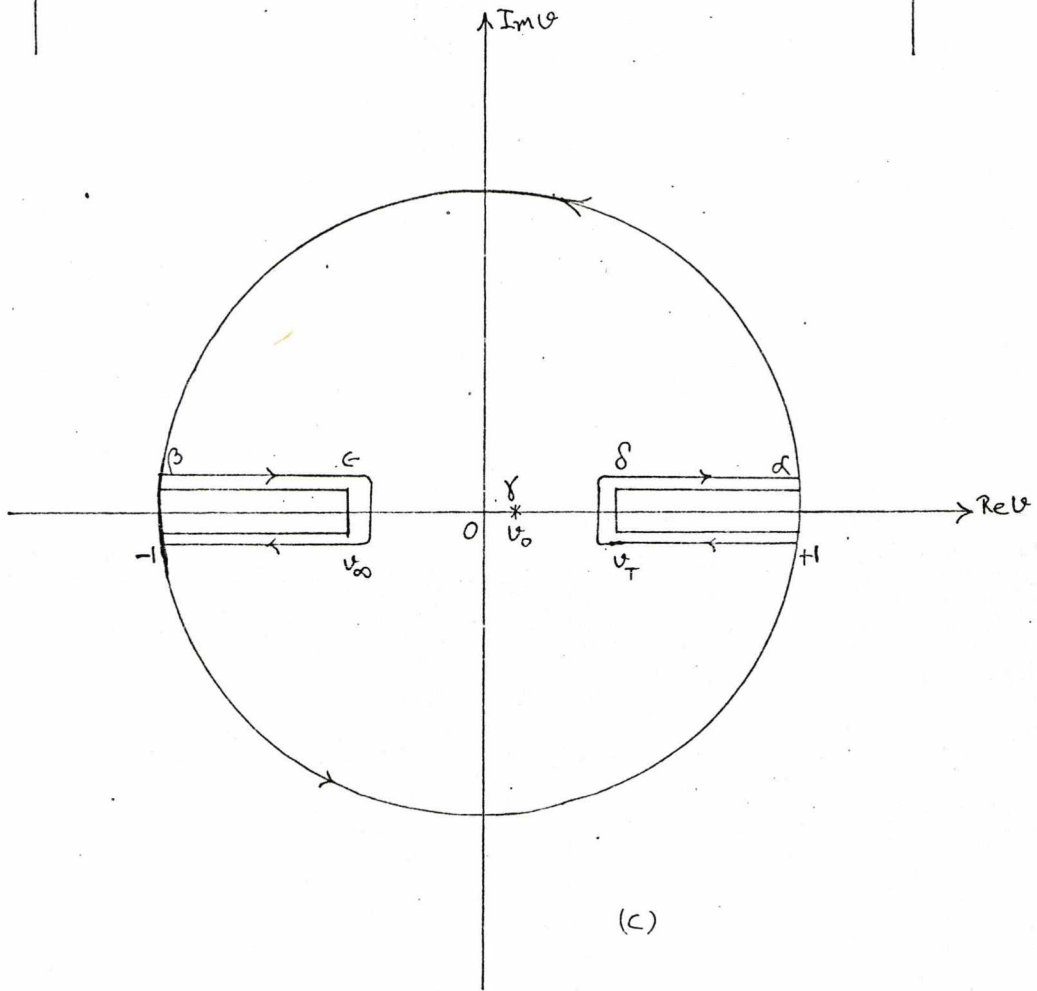
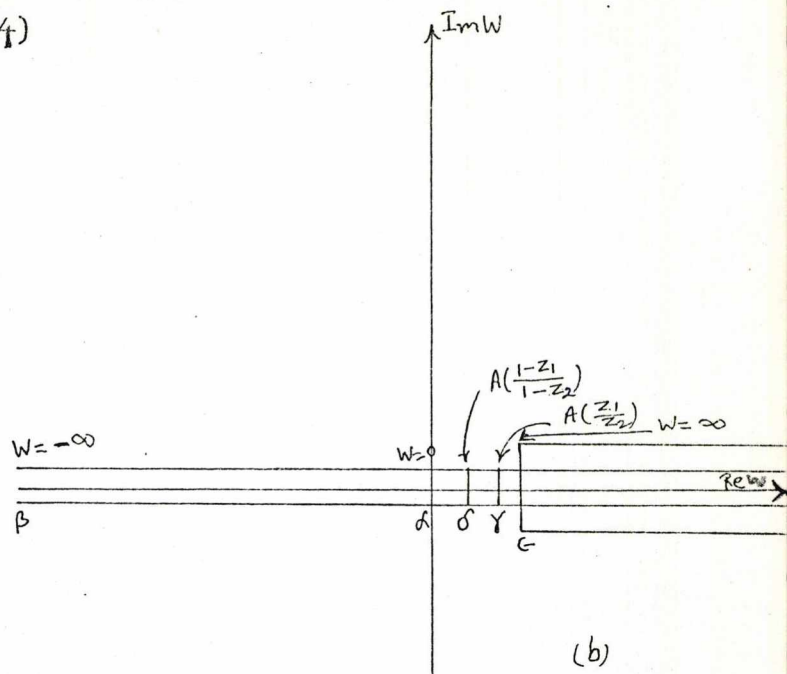
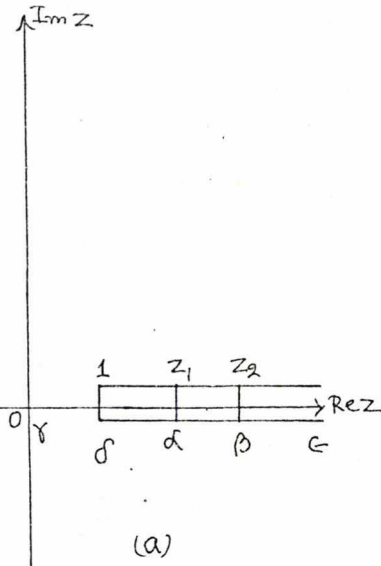
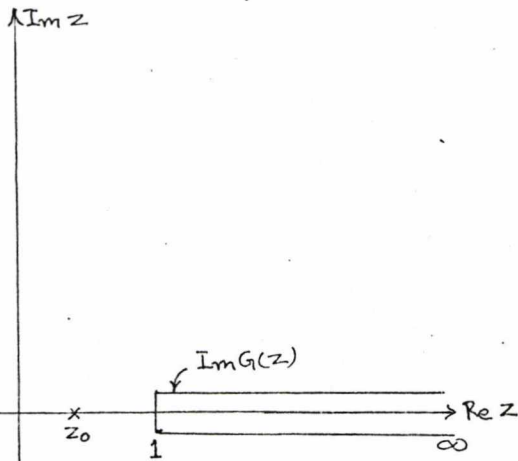
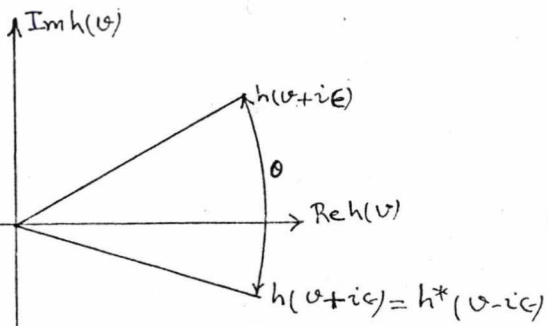


Fig. 10

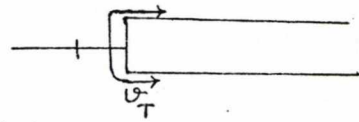


(a)

Fig. 11



(a)



(b)

Fig. 12

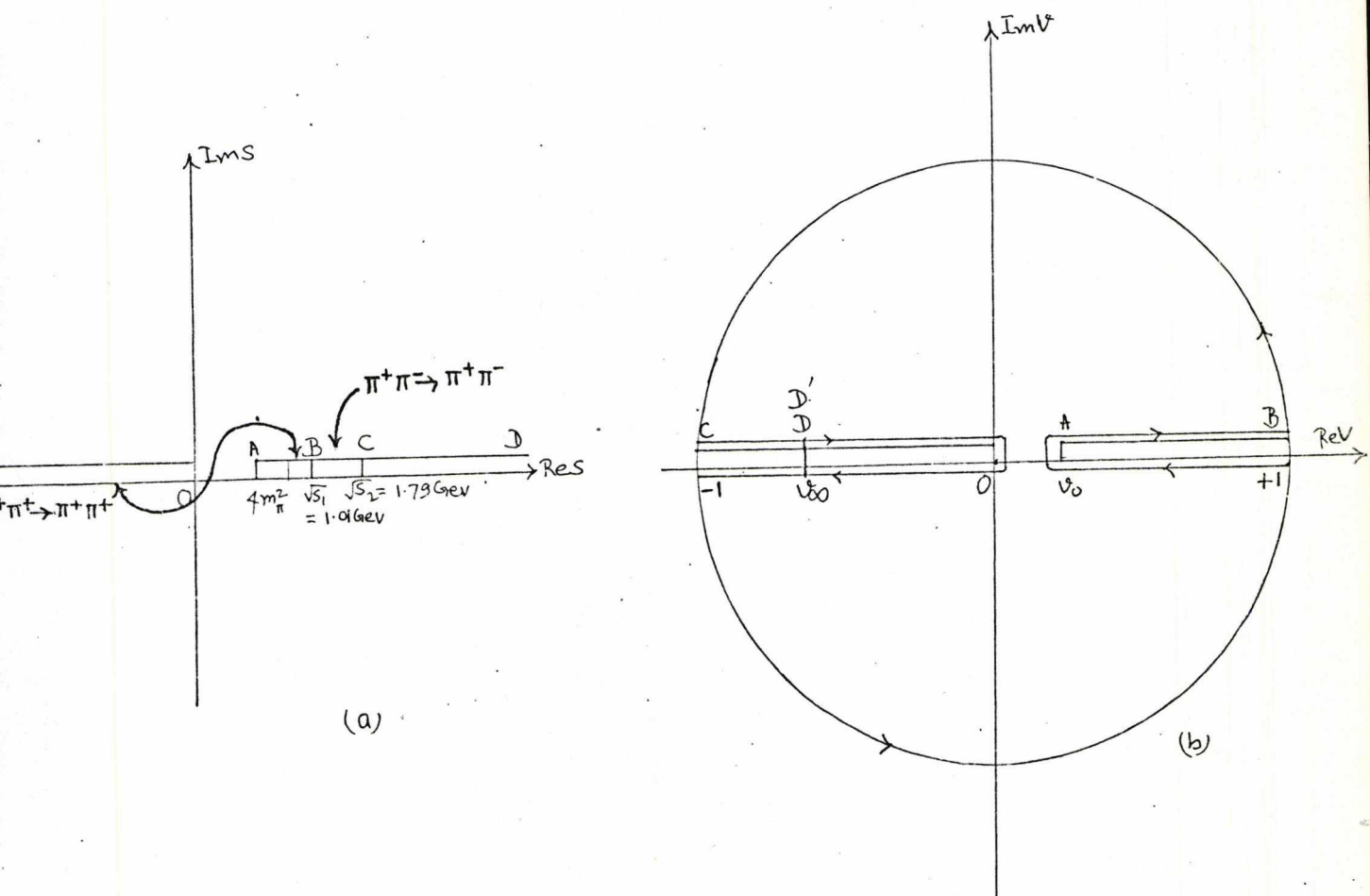


Fig. 13

4. ACKNOWLEDGEMENTS.

The author takes this opportunity of expressing his sincere thanks to Dr. Alan Kenneth Common for his sincere supervision and encouragement during the whole of this work. It is a great pleasure to thank Professor J.S.R. Chisholm for arranging studentship at University of Kent, to the University of Bihar, Muzaffarpur for granting him the leave for study abroad and to the British Council, London for other financial help.

17. Y.S. Jin and A. Martin: Phys. Rev. 135, B1369 (1964)
 B. Bonnier and R. Vinh Mau: Phys. Letters: 24B, 477 (1967)
 Phys. Rev. 165, 1923 (1968)
 C. J. Goebel and G. Shaw: Phys. Letters 27B, 291 (1968)
 L. Lukaszuk and A. Martin, Nuov. Cim. 47A, 265 (1967)
18. B. Bonnier: CERN-TH. 1795 (1974)
 CERN-TH. 2008 (1975)
19. C. Lopez: Nucl. Phys. 88B, 358-364 (1975)
- 19a. C. Lopez; Lettere AL Nuov. Cim. Vol 13 No. 2 (1975)
20. A. K. Common and R. de Wit : Nuov. Cim. 3A, 179 (1971)
 P. Dita: Nuov. Cim. 12A, 442 (1972)
 W. Furmansky: Nucl. Phys. 71B, 119 (1974)
 H. Kuhnelt and P. Grassberger: Nuov. Cim. Letters 9, 59 (1974)
21. B. Bonnier, C. Lopez and G. Mennessier: CERN-TH 2091 (1975)
22. C. Lopez and G. Mennessier: preprint, Laboratoire de Physique
 Theorique' et Hautes energies, Paris (1975).
23. G. Mahoux, S. M. Roy and G. Wanders: Nucl. Phys. B70 (1974)
24. S. M. Roy: Phys. Lett. 36B (1971) 353
25. M. R. Pennington and Protopopescu: Phys. Rev. D7, 1429 (1973)
 and 259
- 25a. D. Morgan and J. Pisut, Springer tracts in Modern Physics 55
26. C. D. Froggatt and J. L. Petersen, NORDITA-75/2 (1975)
- 26a. H. Burkhardt CERN-TH. 1784 (1973).
27. B. Bonnier and P. Gauron: Nucl. Phys. B52, 506 (1973)
28. J. C. LE Guillou and J. L. Basdevant: Ann. Inst. Henri Poincare'
 17, 22 (1972)
29. M. R. Pennington and S. D. Protopopescu: Phys. Rev. D7, 1429, 2591
 (1973)
30. J. L. Basdevant, C. D. Froggatt and J. L. Peterson:
 Nucl. Phys. B72, 413-453 (1974)
31. P. Geniseni: Lett. Nuov. Cim. 8, 171 (1973)
- 32a. J. L. Basdevant, C. D. Froggatt and J. L. Petersen: CERN-TH 1518
 (1972)

- 32b. J.L. Basdevant, C.D. Froggatt: CERN-TH.1519 (1972)
& J.L. Petersen
33. D.Morgan and G.Shaw : Phys.Rev.D2, 520 (1970)
Nucl.Phys.B10, 261 (1969)
34. J.P.Baton et al. Phys.Letters 33B, 525, 528 (1970)
Phys.Letters 38B, 555 (1972)
S.D.Protopopescu et al. L.B.L. 787 (preprint)
35. J.L.Basdevant, B.Bonnier, C. Schomblond, C.D.Froggatt
and J.L.Petersen: IInd Aix-en-Provence International Conference
on Elementary Particles (1973).
36. G.Grayer et al . Nucl.Phys.B75 (1974) 189
37. J.H.Crichton: Nuov.Cim.A45, 256-8 (1966).
38. A.Martin: CERN-TH.2077 (1975)
- 38a. N.P.Klepikov: Sov.Phys.-JETP, 14, 1846 (1960)
39. R.G. Newton: J.Math.Phys. 9, 2050 (1968)
40. A.Martin: Nuov.Cim. A59, 131-52 (1969)
41. D.Atkinson, P.W.Johnson and R.L.Warnock: Commun.Math.Phys. 28,
133-58 (1972)
ibid. 33, 221-42 (1973)
42. D.Atkinson: Nucl.Phys. B55, 125-42 (1973)
43. H.Cornille and J.M.Drouffe: Nuov.Cim.A20, 401-37 (1974)
44. Itzykson and A.Martin: Nuov.Cim. A17, 245-87 (1973)
45. F.A.Berends and S.N.M.Ruysenaars: Nucl.Phys.B56 507-24 (1973)
46. A.Gersten: Nucl.Phys.B12, 537-48 (1969)
47. Kinoshita and A.Martin: Unpublished.
48. H.Cornille and A.Martin: Nucl.Phys.B49, 413 (1972)
49. J.E.Bowcock et al.: Proc. Int. Conf.on Elementary particles,
Amsterdam (1971)
50. E.Pietarinen: Nuov.Cim.B55, 541-50 (1973), Proc.Triangle Seminar (1973)

51. J.E. Bowcock and D.C. Hodgson: Univ. Birmingham report (1972)
52. D. Atkinson: Z. Phys. 266, 373-81 (1974),
Nucl. Phys. B77, 109-33 (1974)
53. D. Atkinson et al.: Univ. Of Groningen, Netherlands (1975)
54. Van. Driel; Univ. of Groningen Report (1975)
55. D. Atkinson, A.C. Herskerk and S.D. Swierstra: Univ. of Groningen
Preprint (1976)
56. G. Grayer et al. CERN preprint
57. S.D. Protopopescu et al.: Phys. Rev. D7, 1279 (1973)
58. S.M. Flatte et al.: Phys. Letters 38B, 232 (1972)
59. V. Alles-Borelli et al.: Nuov. Cim. 30A, 136 (1975)
60. W. Lee: Proc. Int. Symposium on Lepton and Photon Interactions
(1975) Ed. W.T. Kirk p213
61. B. Hyams et al.: Nucl. Phys. B100, 205 (1975)
62. E. Barrelet: Nuov. Cim. 8A, 331 (1972)
63. P. Estabrooks and A.D. Martin: Univ. of Durham, Preprint (1974),
Nucl. Phys. B95, 322 (1975)
64. J.T. Carroll et al.: Phys. Rev. Letters 28, 318 (1972).
65. P. Estabrooks and A.D. Martin: Nucl. Phys. B79, 301 (1974)
66. B. Hyams et al.: Nucl. Phys. B64, 134 (1973)
Phys. Letters 50B, (1974)
67. R.C. Johnson, A.D. Martin and M.R. Pennington: Preprint, Univ. of
Durham, March 1976
68. C.D. Froggatt and J.L. Petersen: Nucl. Phys. B91, 454 (1975)
- 68a. ibid : Nucl. Phys. 186E (1976)
69. E. Pietarinen: Nucl. Phys. B76, 231 (1974)
Nuov. Cim. 12A, 522 (1972)
Nucl. Phys. B65, 541 (1973)
70. A. Martin: Phys. Rev. 129, 1432 (1963)
F. Cerulus and A. Martin: Phys. Lett: 8, 80 (1963)

(172)

71. L. Lukaszuk and A. Martin: Nuov. Cim. 52A, 122 (1967)
72. M. Froissart: Phys. Rev. 123, 1053 (1961)
73. C. Lopez: Nucl. Phys. B88, 358-364 (1975)
74. A. K. Common: Univ. Kent Preprint (1973)
75. C. J. Goebel and G. Shaw: Phys. Lett. 27B, 291 (1968).
76. N. I. Akhiezer: "The classical moment Problem", Oliver and Boyd,
London (1965)
77. P. Baillon et al. : Phys. Letters 38B, 555 (1972)
78. P. Estabrooks et al. : CERN-Th. 1661 (1973)
G. Villet et al: Preprint D. Ph. P. E. CERN, Saclay (1973)
79. P. Grassberger: Bonn. Univ. PIB 2-140, Aug (1973)
80. P. Estabrooks: Proc. Int. Conf. on $\Pi\Pi$ scattering, Tallahassee,
28-30 March (1973)
81. P. Estabrooks and A. D. Martin: Phys. Letters B53 (1974)
82. A. K. Common: Private communication.

